

A novel approach to photon transfer conversion gain estimation

Aaron Hendrickson
ahendr16@jh.edu

March 19, 2022

Abstract

Nonuniformities in the imaging characteristics of modern image sensors are a primary factor in the push to develop a pixel-level generalization of the photon transfer characterization method. In this paper, we seek to develop a body of theoretical results leading toward a comprehensive approach for tackling the biggest obstacle in the way of this goal: a means of pixel-level conversion gain estimation. This is accomplished by developing an estimator for the reciprocal-difference of normal variances and then using this to construct a novel estimator of the conversion gain. The first two moments of this estimator are derived and used to construct exact and approximate confidence intervals for its absolute relative bias and absolute coefficient of variation, respectively. A means of approximating and computing optimal sample sizes are also discussed and used to demonstrate the process of pixel-level conversion gain estimation for a real image sensor.

Keywords: Photon transfer, conversion gain, confidence intervals, summability calculus, hypergeometric function.

2010 Mathematics Subject Classification: Primary 62F10, 62P35 Secondary 40G99, 33C20.

Contents

1	Introduction	4
1.1	Mathematical preliminaries	6
1.2	Previous work	9
2	Estimation of the Reciprocal Difference of Normal Variances	11
2.1	The estimator \mathcal{T}_n	12
2.2	Summability calculus	14
2.2.1	Incomplete geometric series	16
2.2.2	Incomplete Lerch Transcendent	16
2.2.3	Sine-modulated incomplete hypergeometric function	19
2.3	The generalized estimator \mathcal{T}_ν	20
2.3.1	Asymptotic expansion for large α_1 and α_2	23
2.4	Measures of dispersion	26
2.4.1	The functions $g_{n,\omega}$ and $\tilde{g}_{n,\omega}$	27
2.4.2	Variance	37
2.4.3	Coefficient of variation	44
2.5	Confidence intervals	47
3	Photon Transfer Conversion Gain Estimation	52
3.1	A brief review of photon transfer theory	53
3.1.1	Bose-Einstein statistics and the uncertain nature of light	53
3.1.2	Photon transfer $\gamma \rightarrow \text{DN}$ and conversion gain	53
3.2	Noise model	57
3.3	The estimator \mathcal{G}_ν	58
3.4	A demonstration of g -estimation with confidence intervals	62
3.5	Optimal sample sizes	63
3.5.1	Asymptotic properties at low illumination	66
3.5.2	Computation of optimal sample sizes for $\mathcal{T}_{\nu^\dagger}$	73
3.6	Pixel-level conversion gain estimation: An introduction	85
3.6.1	Pixel grouping	87
3.6.2	Experimental setup	88
3.6.3	Design of experiment	89
3.6.4	Data collection	90
3.6.5	Summary of results	92

4	Conclusions	102
5	Appendices	105
A	Definitions and relations	105
B	Limiting properties of \mathcal{T}_ν as $ \nu \rightarrow \infty$	108
C	Proofs of differential operator identities	111
D	Estimate of truncation error for the ACV \mathcal{T}_ν series expansion . . .	113
E	Bounding functions for $ \partial_\beta^n F(\alpha, \alpha; \beta; x) $	115

Chapter 1

Introduction

Photon Transfer (PT) is a methodology initially developed back in the 1970s for the design, characterization, and optimization of solid state image sensors. Since its inception, PT has evolved to become the standard for image sensor characterization, culminating in its use as the basis for the European Machine Vision Association (EMVA) 1288 standard in 2005 [8]. To fully characterize the performance of an image sensor many types of performance metrics are measured including but not limited to conversion gain, read noise, and dynamic range.

Of all performance metrics prescribed by the PT method, the so-called conversion gain, g , is fundamental for two reasons. First, g is a conversion constant that facilitates unit conversion of sensor measurements from arbitrary units of digital numbers (DN) into units of electrons (e^-). For example, the read noise of a pixel is found according to the formula

$$\sigma_{\text{READ}}(e^-) = \sigma_d(\text{DN}) \times g(e^-/\text{DN}),$$

where σ_d is the population standard deviation of the pixel's noise in the absence of illumination, i.e. darkness¹. Since units of DN are physically meaningless it is only after multiplying by g that the measurement of σ_d represent a physical quantity. For this reason, nearly all imaging performance metrics measurable by the PT method at some point require multiplying quantities in DN by g . Second, in actual implementation of PT, g is an estimated quantity; thus, the precision and accuracy of its measurement fundamentally limits the precision and accuracy of the entire PT method. This is easily seen when looking back at the equation for σ_{READ} above, for even if σ_d is measured with perfect certainty, that is, it's a known constant, we still have

$$\text{Bias } \hat{\sigma}_{\text{READ}} = \sigma_d \times \text{Bias } G$$

¹Throughout this work we will consider the characterization of individual pixels via the PT method as not to impose the unnecessary assumption of *sensor uniformity*. If however a sensor is *uniform*, so that it is comprised of an array of identical pixels, we may implement PT in such a manner as to characterize the entire array with global estimates of key population parameters (see Section 3.6).

and

$$\text{Var } \hat{\sigma}_{\text{READ}} = \sigma_{\text{d}}^2 \times \text{Var } G,$$

with G being a random variable representing some estimator of g .

In some cases the pixels comprising the sensor will exhibit a linear *transfer function* so that g can be expressed by the formula [16, Eqs. 5.1,6.1]

$$g = \frac{\mu_{\text{p+d}} - \mu_{\text{d}}}{\sigma_{\text{p+d}}^2 - \sigma_{\text{d}}^2} = \frac{\mu_{\text{p}}}{\sigma_{\text{p}}^2}, \quad (1.1)$$

where $\mu_{\text{p+d}}$ (DN) and $\sigma_{\text{p+d}}^2$ (DN²) are the population mean and variance of a pixel's output when exposed to some amount of incident illumination and μ_{d} (DN) and σ_{d}^2 (DN²) are the corresponding population parameters for the pixel's output under dark conditions. In this way, g is found from the ratio of the photon induced mean, μ_{p} (DN), and photon induced variance σ_{p}^2 (DN²). Linearity of the pixel's transfer function means that despite $\mu_{\text{p+d}}$ and $\sigma_{\text{p+d}}^2$ increasing with increasing illumination, g remains constant and thus can be measured at any illumination level. While linearity makes g easy to compute it tends to be an over idealized assumption for many modern pixel architectures such as CMOS active-pixel sensors. Fortunately, the formula for g in (1.1) can still be used so long as the illumination level is sufficiently low [16].

Assuming all quantities in (1.1) are finite, a natural estimator for g is [13, 16]

$$G = \frac{\bar{X} - \bar{Y}}{\hat{X} - \hat{Y}} = \frac{\bar{P}}{\hat{P}}, \quad (1.2)$$

where $\bar{X} = n_1^{-1} \sum_{k=1}^{n_1} X_i$ and $\hat{X} = (n_1 - 1)^{-1} \sum_{k=1}^{n_1} (X_i - \bar{X})^2$ are the sample mean and variance computed from a sample of n_1 digital observations of a single pixel when exposed to illumination and \bar{Y} and \hat{Y} are the corresponding sample statistics taken from an independent sample of n_2 observations of the same pixel in the dark. It follows that $\bar{P} = \bar{X} - \bar{Y}$ and $\hat{P} = \hat{X} - \hat{Y}$ estimate the unknown photon induced mean and variance, respectively. Apart from its simplicity, what makes this estimator for g attractive is that it is independent of distributional assumptions on the pixel's noise since $T = (\bar{X}, \bar{Y}, \hat{X}, \hat{Y})$ is an unbiased estimator of $\theta = (\mu_{\text{p+d}}, \mu_{\text{d}}, \sigma_{\text{p+d}}^2, \sigma_{\text{d}}^2)$; regardless of the underlying distribution [6, Thm. 5.2.6]. This simplicity and lack of distributional assumptions does however come at the cost of some particularly undesirable statistical properties.

In virtually any conceivable distributional model for the pixel noise, the density of \hat{P} will be nonzero at the origin. As a result, \hat{P}^{-1} and subsequently G fall into the domain of attraction of the Cauchy law and thus have no finite moments [22]. To avoid the Cauchy-like behavior of the estimator (1.2) that results from this lack of well-defined moments experimenters typically measure g under high illumination conditions. By doing this, the probability of \hat{P} being in the neighborhood of zero is negligible, which results in G being quasi well-behaved. However, in the case of nonlinear pixels one is forced to measure g under low illumination where the behavior of G is the most ill-behaved. In this

scenario, one must capture increasingly large samples to force $P(|\hat{P}| < \epsilon) \approx 0$ and produce a well-behaved estimate of \hat{P}^{-1} . This tension between the need to measure g at low-illumination and the large sample sizes it entails ultimately led to the *low-illumination problem* of conversion gain measurement [12].

While convenient, the lack of distributional assumptions on the estimator (1.2) is not all that important. Indeed, many authors have shown that most image sensors produce noise that is accurately modeled as normal [16, 3, 13]. Even in the case where the pixel noise exhibits departures from normality, PT typically requires large sample sizes such that the distributions of the sample statistics $(\bar{X}, \bar{Y}, \hat{X}, \hat{Y})$ show excellent agreement with what is predicted by a normal model. As such, this paper seeks an improved estimator for g under the normal model of pixel noise which does not have the undesirable properties of the estimator (1.2). Since the normal model implies (\bar{X}, \bar{Y}) is independent of (\hat{X}, \hat{Y}) , this task amounts to deriving an estimator for $(\sigma_{p+d}^2 - \sigma_d^2)^{-1}$ to replace \hat{P}^{-1} .

With the task at hand, this paper is organized as follows. We will begin by closing out this chapter with sections 1.1-1.2, which introduce some of the most important functions in the subsequent analysis and provide a brief background on the progression of estimators for g . Chapter 2 then tackles the problem of finding an improved estimator, denoted \mathcal{T}_ν , for the reciprocal difference of variance $\tau = (\sigma_{p+d}^2 - \sigma_d^2)^{-1}$ under the normal model. Several important results pertaining to \mathcal{T}_ν will be established including: (1) a proof of its first moment (Section 2.3), an asymptotic expansion for large sample sizes (Section 2.3.1), its second moment (Section 2.4.2), and exact confidence intervals for its absolute relative bias and absolute coefficient of variation (Section 2.5).

Chapter 3 will then apply the results of Chapter 2 to construct a novel estimator, \mathcal{G}_ν , for the conversion gain based on \mathcal{T}_ν . Section 3.4 will utilize this new estimator as well as the theoretical results of the previous sections in a Monte Carlo experiment to demonstrate the process of estimating g with \mathcal{G}_ν . Since reducing sample sizes is an important consideration, Section 3.5 investigates the behavior of optimal sample sizes for both \mathcal{T}_ν and \mathcal{G}_ν . In particular, a close look at the behavior of the optimal sample sizes in low illumination will be conducted (Section 3.5.1) followed by a detailed discussion on the approximation and computation of the optimal sample sizes (Section 3.5.2). Finally, Section 3.6 will apply all of the preceding results to present the design and control of experiment for pixel-level conversion gain estimation using a real image sensor; opening the door to a comprehensive approach of pixel-level PT characterization.

1.1 Mathematical preliminaries

This work will make extensive use of gamma, Pochhammer, hypergeometric, and related functions. The purpose of this section is to introduce some notation and present key properties of these functions. It is recommended the reader also briefly familiarize themselves with the additional list of definitions and relations in Appendix A.

For $\Re s > 0$ the gamma function can be expressed in the form of the integral

$$\Gamma(s) = \int_0^\infty t^{s-1} e^{-t} dt$$

and is defined by analytic continuation of this integral to a meromorphic function in the complex plane via the reflection formula $\Gamma(s)\Gamma(1-s) = \pi \csc \pi s$. Directly tied to the gamma function are three additional functions that are of great importance, namely, the beta function

$$B(s, z) := \frac{\Gamma(s)\Gamma(z)}{\Gamma(s+z)},$$

Pochhammer symbol (rising factorial)

$$(s)_n := \frac{\Gamma(s+n)}{\Gamma(s)} = \begin{cases} 1, & n = 0 \\ \prod_{k=0}^{n-1} (s+k), & n \in \mathbb{N}, \end{cases}$$

and factorial power (falling factorial)

$$(s)^{(n)} := \frac{\Gamma(s+1)}{\Gamma(s-n+1)} = \begin{cases} 1, & n = 0 \\ \prod_{k=0}^{n-1} (s-k), & n \in \mathbb{N}, \end{cases}$$

of which the latter two are related by $(s)^{(n)} = (-1)^n (-s)_n$ when $n \in \mathbb{Z}$. Through application of the gamma reflection formula we can also easily derive for $n \in \mathbb{Z}$ the following transformations

$$(s)_n = (-1)^n (1-s-n)_n = \frac{(-1)^n}{(1-s)_{-n}}.$$

Additionally, the Pochhammer symbol is related to the Stirling numbers by

$$\begin{aligned} s^n &= \sum_{k=0}^n (-1)^k {}_2\mathcal{S}_n^{(k)} (-s)_k, \\ (s)_n &= \sum_{k=0}^n (-1)^{n-k} \mathcal{S}_n^{(k)} s^k, \end{aligned}$$

where $\mathcal{S}_n^{(k)}$ and ${}_2\mathcal{S}_n^{(k)}$ represent Stirling numbers of the 1st-kind and 2nd-kinds as well as the binomial coefficient via

$$\binom{n}{k} = \frac{(-1)^k (-n)_k}{k!}.$$

Of perhaps greater significance is the use of the Pochhammer symbol in defining generalized hypergeometric functions which may be formally represented through the generalized hypergeometric series

$${}_pF_q \left(\begin{matrix} a_1, \dots, a_p \\ b_1, \dots, b_q \end{matrix}; z \right) = \sum_{k=0}^{\infty} \frac{(a_1)_k \cdots (a_p)_k}{(b_1)_k \cdots (b_q)_k} \frac{z^k}{k!}.$$

If any of the top parameters a_j is a nonpositive integer then this series reduces to a polynomial in z since $n \in \mathbb{N}_0 \implies (-n)_k = 0$ for all $k = n+1, n+2, \dots$. For the specific case $p = q+1$ the generalized hypergeometric series has a radius of convergence of one and is defined by analytic continuation in z for $|z| > 1$. On the unit disk $|z| = 1$ the series representation for ${}_{q+1}F_q(z)$ is absolutely convergent if $\Re \gamma_q > 0$, convergent except at $z = 1$ if $-1 < \Re \gamma_q \leq 0$, and divergent if $\Re \gamma_q \leq -1$ where [7, §16.2(iii)]

$$\gamma_q = b_1 + \dots + b_q - (a_1 + \dots + a_{q+1}).$$

For convenience, we will use several differing notations for generalized hypergeometric functions when appropriate. These include ${}_pF_q(\mathbf{a}; \mathbf{b}; z)$ as well as the regularized version

$${}_p\mathbf{F}_q \left(\begin{matrix} a_1, \dots, a_p \\ b_1, \dots, b_q \end{matrix}; z \right) := \frac{1}{\prod_{k=1}^q \Gamma(b_k)} {}_pF_q \left(\begin{matrix} a_1, \dots, a_p \\ b_1, \dots, b_q \end{matrix}; z \right),$$

which is an entire function of the parameters $a_1, \dots, a_p, b_1, \dots, b_q$. Of particular importance here is “the” hypergeometric function ${}_2F_1(a, b; c; z)$, which due to its prolific use in the literature is commonly denoted simply as $F(a, b; c; z)$. There are several properties of the hypergeometric function that will be heavily used here including the transformations [7, Eq. 15.8.1]

$$\mathbf{F} \left(\begin{matrix} a, b \\ c \end{matrix}; z \right) = \begin{cases} (1-z)^{-a} \mathbf{F} \left(\begin{matrix} a, c-b \\ c \end{matrix}; \frac{z}{z-1} \right) & \text{(i)} \\ (1-z)^{-b} \mathbf{F} \left(\begin{matrix} c-a, b \\ c \end{matrix}; \frac{z}{z-1} \right) & \text{(ii)} \\ (1-z)^{c-a-b} \mathbf{F} \left(\begin{matrix} c-a, c-b \\ c \end{matrix}; z \right) & \text{(iii)}, \end{cases} \quad (1.3)$$

which hold for $|\text{ph}(1-z)| < \pi$ as well as the integral form

$$\mathbf{F}(a, b; c; z) = \int_0^1 \frac{t^{b-1} (1-t)^{c-b-1} (1-zt)^{-a}}{\Gamma(b)\Gamma(c-b)} dt,$$

when $|\text{ph}(1-z)| < \pi$ and $\Re c > \Re b > 0$. Additionally, we note the special cases

$$F(a, b; c; 1) = \frac{\Gamma(c)\Gamma(c-a-b)}{\Gamma(c-a)\Gamma(c-b)}, \quad \Re\{c-a-b\} > 0$$

and

$$F(1, b; c; z) = (c-1)z^{1-c}(1-z)^{-(b-c+1)} \mathbf{B}_z(c-1, b-c+1),$$

where $\mathbf{B}_z(\alpha, \beta)$ denotes the incomplete beta function of Definition 32. Lastly, for clarity we will use the following notation to denote various sets of numbers.

\mathbb{N}	$= \{1, 2, \dots\}$	natural numbers
\mathbb{N}_0	$= \mathbb{N} \cup \{0\}$	nonnegative integers
\mathbb{Z}	$= -\mathbb{N} \cup \mathbb{N}_0$	integers
\mathbb{R}	$= (-\infty, \infty)$	real numbers
\mathbb{R}^+	$= (0, \infty)$	positive real numbers
\mathbb{R}_0^+	$= \mathbb{R}^+ \cup \{0\}$	nonnegative real numbers

1.2 Previous work

Statistical analysis of estimators for the conversion gain date back to the work of Beecken and Fossum [3]. For sensors that are able to achieve a *shot noise limited response*, illuminating the sensor with a sufficiently high illumination implies $\mu_{p+d} \gg \mu_d$ and $\sigma_{p+d}^2 \gg \sigma_d^2$ such that $g \approx \mu_{p+d}/\sigma_{p+d}^2$. Consequently, the gain can be estimated with [3]

$$G = \frac{\bar{X}}{\hat{X}}, \quad (1.4)$$

where the normal model dictates $\bar{X} \sim \mathcal{N}(\mu_{p+d}, \sigma_{p+d}^2/n_1)$ and $\hat{X} \sim \mathcal{G}(\alpha_1, \beta_1)$ with $\alpha_1 = (n_1 - 1)/2$ and $\beta_1 = \alpha_1/\sigma_{p+d}^2$ are independent normal and gamma random variables, respectively. One of the important conclusions in this work was that under sufficiently high illumination the variance of G is dominated by the variance of \hat{X}^{-1} , that is,

$$\text{Var}G \approx \bar{X}^2 \text{Var}\hat{X}^{-1}.$$

Hence, confidence intervals for G can be approximated by scaling confidence intervals for \hat{X}^{-1} by \bar{X}^2 .

For sensors that cannot achieve a shot noise limited response one cannot ignore the noise produced by the pixel in the absence of illumination. As such, Hendrickson studied the estimator [13]

$$G = \frac{\bar{X} - \bar{Y}}{\hat{X} - \hat{Y}} = \frac{\bar{P}}{\hat{P}}, \quad (1.5)$$

where $\bar{Y} \sim \mathcal{N}(\mu_d, \sigma_d^2/n_2)$ and $\hat{Y} \sim \mathcal{G}(\alpha_2, \beta_2)$ with $\alpha_2 = (n_2 - 1)/2$ and $\beta_2 = \alpha_2/\sigma_d^2$. The distribution of this estimator was derived in the form of the centralized inverse-Fano distribution and it was noted that this distribution had no finite moments due the density of \hat{P} being nonzero at the origin. In an effort to gain some insight about this estimator, further investigations were carried out in [12] to derive the first moment in the sense of the Cauchy principal value

$$\text{PVEG} = \lim_{R \rightarrow \infty} \int_{-R}^R g f_G(g) dg = (E\bar{P})(\text{PVE}\hat{P}^{-1}).$$

An expression for PVEG opened the door to discussing the bias of G in experimental settings and thus was useful from both theoretical and practical viewpoints. In particular, knowing G is an estimator for g one could define its principal-valued absolute relative bias as $\text{ARB}G = |\text{PVEG}/g - 1|$ so that

$$\text{ARB}G = \text{ARB}\hat{P}^{-1} = |\text{RB}\hat{P}^{-1} - 1|,$$

where

$$\begin{aligned} \text{RB}\hat{P}^{-1} = & \frac{\alpha_1 (1 - \zeta) \left(\frac{\alpha_2}{\alpha_1} \zeta^{-1}\right)^{\alpha_2} \left(1 + \frac{\alpha_2}{\alpha_1} \zeta^{-1}\right)^{1-\alpha_1-\alpha_2}}{(\alpha_1 + \alpha_2 - 1) \text{B}(\alpha_1, \alpha_2)} \left(\psi(\alpha_1) - \psi(\alpha_2) \right. \\ & - \log \left(\frac{\alpha_1}{\alpha_2} \zeta \right) - \frac{\alpha_2 - 1}{\alpha_2} \zeta {}_3F_2 \left(\begin{matrix} 1, 1, 2 - \alpha_2 \\ 2, \alpha_1 + 1 \end{matrix}; -\frac{\alpha_1}{\alpha_2} \zeta \right) \\ & \left. + \frac{\alpha_1 - 1}{\alpha_1} \zeta^{-1} {}_3F_2 \left(\begin{matrix} 1, 1, 2 - \alpha_1 \\ 2, \alpha_2 + 1 \end{matrix}; -\frac{\alpha_2}{\alpha_1} \zeta^{-1} \right) \right), \end{aligned}$$

$\zeta = \sigma_d^2 / \sigma_{p+d}^2$, $\psi(z) := \partial_z \log \Gamma(z)$ is the digamma function, and $\log z$ is the natural logarithm. This shows that the absolute relative bias of G is equal to that of \hat{P}^{-1} , which is a function of only the sample sizes and variance ratio ζ . To expound on the findings by Beecken and Fossum it was further demonstrated in a simulation that $\hat{P}^{-1} / \text{PVE}\hat{P}^{-1}$ converges in distribution to $G / \text{PVE}G$ as illumination increases. In other words, the dispersion of G is dominated by that of \hat{P}^{-1} at sufficiently high illumination. While these results led to increased theoretical understanding, the estimator (1.5) still presented major challenges for the purpose of low illumination conversion gain measurement and thus motivated further work².

²Although it does not fit in with the natural progression of estimators discussed here, recent work into conversion gain estimation for more exotic technologies like deep sub-electron read noise image sensors have also been studied [24].

Chapter 2

Estimation of the Reciprocal Difference of Normal Variances

We are now ready to turn to deriving an estimator for $(\sigma_{\text{p+d}}^2 - \sigma_{\text{d}}^2)^{-1}$. Under the normal model of pixel noise recall that $\hat{X} \sim \mathcal{G}(\alpha_1, \beta_1)$ and $\hat{Y} \sim \mathcal{G}(\alpha_2, \beta_2)$ are independent gamma random variables with shape $\alpha_i = (n_i - 1)/2$ and $\beta_1 = \alpha_1/\sigma_{\text{p+d}}^2$, $\beta_2 = \alpha_2/\sigma_{\text{d}}^2$. For the sake of brevity, we will modify our notation by considering the independent gamma random variables Y_1 and Y_2 where $Y_i \sim \mathcal{G}(\alpha_i, \beta_i)$, α_i is known, and $\beta_i = \alpha_i/\kappa_i$ with the understanding that these random variables have the same distributional form as that of \hat{X} and \hat{Y} . Our first result establishes a key statistical property of these random variables.

Lemma 1. *Let $Y_1 \sim \mathcal{G}(\alpha_1, \beta_1)$ and $Y_2 \sim \mathcal{G}(\alpha_2, \beta_2)$ be independent gamma random variables parameterized in terms of known shape α_i and unknown rate $\beta_i = \alpha_i/\kappa_i$, $i = 1, 2$. Then, $T(Y_1, Y_2) = (Y_1, Y_2)$ is a complete-sufficient statistic for $\theta = (\kappa_1, \kappa_2)$.*

Proof. We only need to establish the proof for a single gamma variable with the extension to two independent gamma variables being trivial. For known α , the gamma density $f(y|\beta) = h(y)c(\beta)\exp(w(\beta)T(y))$ with $h(y) = \mathbb{1}_{(0,\infty)}(y)y^{\alpha-1}$, $c(\beta) = \beta^\alpha/\Gamma(\alpha)$, $w(\beta) = -\beta$, and $T(y) = y$ is a member of the exponential family. It follows that that $T(Y) = Y$ is a sufficient statistic for β [6, Thm. 6.2.10]. Furthermore, the parameter space $\beta \in (0, \infty)$ is an open subset of \mathbb{R} which implies that $T(Y)$ must also be complete [6, Thm. 6.2.25]. Since $\kappa = \alpha/\beta$ is a one-to-one function of β any complete-sufficient statistic for β must also be complete-sufficient for κ . The proof is now complete. \square

2.1 The estimator \mathcal{T}_n

In light of Lemma 1, to find an unbiased estimator $\mathcal{T}(Y_1, Y_2)$ of the estimand $\tau = (\kappa_1 - \kappa_2)^{-1}$ one would need to solve the integral equation

$$\int_{\mathbb{R}^+ \times \mathbb{R}^+} \mathcal{T}(y_1, y_2) f_{Y_1}(y_1) f_{Y_2}(y_2) d(y_1, y_2) = \frac{1}{\kappa_1 - \kappa_2}. \quad (2.1)$$

Taking into account the form of the gamma densities at hand, namely,

$$f_{Y_i}(y_i) = \frac{\beta_i^{\alpha_i}}{\Gamma(\alpha_i)} y_i^{\alpha_i-1} e^{-\beta_i y_i}, \quad i = 1, 2,$$

and noting $\kappa_i = \alpha_i/\beta_i$, the l.h.s. of (2.1) can be interpreted as an iterated Laplace transform of two variables to produce the equivalent expression

$$\mathcal{L}\{y_2^{\alpha_2-1} \mathcal{L}\{y_1^{\alpha_1-1} \mathcal{T}(y_1, y_2)\}(\beta_1)\}(\beta_2) = \Gamma(\alpha_1) \Gamma(\alpha_2) \frac{\beta_1^{-\alpha_1} \beta_2^{-\alpha_2}}{\alpha_1/\beta_1 - \alpha_2/\beta_2}. \quad (2.2)$$

Recovering \mathcal{T} is subsequently achieved by successively inverting the r.h.s. of (2.2). Given the rich theory of Laplace transforms one might hope that published tables of transform pairs will provide the necessary result to invert this equation. Indeed, inversion w.r.t. β_2 is achieved via [19, Eq. 5.4.9] yielding an unbiased estimator for τ when κ_1 is known (see Appendix B). However, the final inversion w.r.t. β_1 leads to an intractable problem; suggesting the possibility that the estimator \mathcal{T} does not exist.

Conjecture 1. *There is no estimator \mathcal{T} satisfying (2.1) for unknown κ_1 and κ_2 .*

Even if \mathcal{T} does exist there is no guarantee that it will have desirable properties outside of unbiasedness. As the following theorem shows, if \mathcal{T} exists, it must have infinite variance for at least certain values of the parameters κ_1 and κ_2 .

Theorem 1. *Let Y_1 and Y_2 be as in Lemma 1. If an estimator \mathcal{T} satisfying (2.1) exists, then $\text{Var} \mathcal{T} = \infty$ for at least $1/2 < \kappa_2/\kappa_1 < 2$.*

Proof. Read Lemma 3 and Lemma 20. Then see Appendix B. \square

Theorem 1 is significant because even if \mathcal{T} exists and has finite variance outside $1/2 < \kappa_2/\kappa_1 < 2$ there would be no way to know if any given estimate $\hat{\tau} = \mathcal{T}(y_1, y_2)$ has finite variance due to the unknown nature of κ_1 and κ_2 . To overcome these challenges we appeal to the statistical principle of bias-variance tradeoff and expand our search to include biased estimators of τ . Upon inspection, note that $\tau = \kappa_1^{-1}(1 - \kappa_2/\kappa_1)^{-1}$. Letting $\zeta = \kappa_2/\kappa_1$, if we assume $\zeta < 1$ it follows that the r.h.s. of (2.1) can be approximated by the incomplete geometric series

$$\tau_n = \kappa_1^{-1}(1 + \zeta + \dots + \zeta^{n-1}) = \frac{1 - \zeta^n}{\kappa_1 - \kappa_2},$$

where the magnitude of the approximation error $E_n = -\tau \times \zeta^n$ can be made arbitrarily small with increasing n . In addition to the ability to achieve arbitrarily small error, this approximation is attractive since it is a finite sum of simple terms; thus, rendering it compatible with term-wise inversion to find a biased estimator \mathcal{T}_n . Here we state a simple but useful result and then proceed with the deriving the estimator \mathcal{T}_n .

Lemma 2. For $Y \sim \mathcal{G}(\alpha, \beta)$ and $s \in \mathbb{C}$ with $\alpha + \Re s > 0$, $\mathbb{E}Y^s = \beta^{-s}(\alpha)_s$.

Lemma 3. Let Y_1 and Y_2 be as in Lemma 1. If $n \in \mathbb{N}_0 : 0 \leq n < \alpha_1$ then

$$\mathcal{T}_n = \frac{1}{\alpha_1 Y_1} \sum_{k=0}^{n-1} \frac{1}{(\alpha_1)_{-k-1} (\alpha_2)_k} \left(\frac{\alpha_2 Y_2}{\alpha_1 Y_1} \right)^k,$$

is an unbiased estimator of τ_n where $\mathcal{T}_0 := 0$ is the empty sum.

Proof. Assume $n \in \mathbb{N}$. We seek an estimator \mathcal{T}_n with the property

$$\mathbb{E} \mathcal{T}_n = \tau_n = \sum_{k=0}^{n-1} \kappa_2^k \kappa_1^{-(k+1)}.$$

From Lemma 2 we know $\alpha_2^k / (\alpha_2)_k Y_2^k$ and $\alpha_1^{-k-1} / (\alpha_1)_{-k-1} Y_1^{-k-1}$ are unbiased estimators of κ_2^k and $\kappa_1^{-(k+1)}$ with the latter having finite expected value if $n < \alpha_1$. Since Y_1 and Y_2 are independent, the desired expression for \mathcal{T}_n immediately follows. Now writing $\mathcal{T}_n = \sum_{k=0}^{n-1} g(k)$ we have $\mathcal{T}_n = \mathcal{T}_{n-1} + g(n-1)$. Substituting $n = 1$ into this recurrence formula and noting $\mathcal{T}_1 = g(0)$ implies $\mathcal{T}_0 = 0$. The proof is now complete. \square

Remark 1. Lemma 3 makes no mention of the restriction $\kappa_1 > \kappa_2$. However, if one is to use \mathcal{T}_n as an estimator for τ this is required for the absolute bias $|\text{Bias} \mathcal{T}_n| = \zeta^n |\tau|$ to be less than $|\tau|$.

The discrete nature of the parameter n leads to a simple derivation of the estimator \mathcal{T}_n , however, this simplicity comes at the cost of flexibility. This is easily seen by noting that for fixed α_i and κ_i the moments $\mathbb{E} \mathcal{T}_n^m$ can only take on a countable set of values which prohibits arbitrary choices of key statistical properties such as bias. To illustrate why this is problematic, suppose there exists a generalized estimator \mathcal{T}_ν , continuous in ν , that interpolates \mathcal{T}_n and its moments, that is, $\mathcal{T}_\nu = \mathcal{T}_n$ and $\mathbb{E} \mathcal{T}_\nu^m = \mathbb{E} \mathcal{T}_n^m$ when $\nu = n$. Then again fixing α_i and κ_i , if one wishes to minimize mean-squared-error we know it must be the case that $\min_{\nu \in \mathbb{R}_0^+} \text{MSE} \mathcal{T}_\nu \leq \min_{n \in \mathbb{N}_0} \text{MSE} \mathcal{T}_n$; rendering \mathcal{T}_ν the superior estimator in terms of mean-squared-error. Figure 2.1 plots $\text{MSE} \mathcal{T}_n$ for some sample parameters along with one possible continuous generalization showing a discrepancy between their minimum values. Since the additional degree of freedom afforded by a continuous generalization of \mathcal{T}_n can improve performance the question arises: How do we go about seeking such a generalization? In a rather remarkable fashion we will see how this can be achieved through the methods of *summability calculus*.

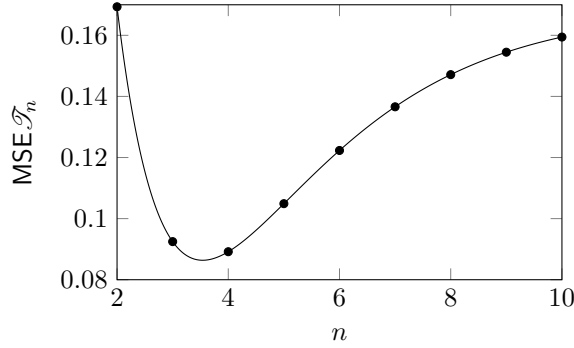


Figure 2.1: Plot of $\text{MSE}_{\mathcal{T}_n}$ versus n (points) with one possible continuous interpolation (line).

2.2 Summability calculus

Summability calculus is in essence a theoretical framework for generalizing finite sums $f(n) = \sum_{k=0}^{n-1} s_k g(k, n)$ for a periodic sequence s_k and analytic function $g(k, n)$ to complex-valued n and performing infinitesimal calculus on these generalized sums. A key point of the theory of summability calculus is that $f(n)$ is itself an analytic form leading to the ability to perform infinitesimal calculus on the generalized sum even if the explicit form of the generalized sum is not known. To see how such a generalization is obtained, we will limit the discussion to so-called *simple finite sums* of the form $f(n) = \sum_{k=0}^{n-1} g(k)$. By definition, the simple finite sum $f(n)$ satisfies the recurrence relation $f(n) = f(n-1) + g(n-1)$ and upon substituting $n = 1$ we find $f(1) = g(0) + f(0) \implies f(0) = 0$. Consequently, one can fully characterize $f(n)$ by the recurrence relation and initial condition

$$f(n) = g(n-1) + f(n-1), \quad f(0) = 0.$$

With this information we can then construct a generalized *fractional finite sum* $f_G(\nu) : \mathbb{C} \rightarrow \mathbb{C}$ via an iterative polynomial approximation scheme. At the r th iteration we approximate generalized sum with

$$f_{G,r}(\nu) = \begin{cases} p_r(\nu) & \nu \in [0, 1] \\ g(\nu-1) + f_{G,r}(\nu-1) & \text{otherwise,} \end{cases}$$

where $p_r(\nu) = a_1\nu + \dots + a_r\nu^r$ is a polynomial of degree r . If for each iteration we require $f_{G,r}(\nu)$ to be $(r-1)$ -times continuously differentiable on $\nu \in (0, 2)$ then the coefficients of $p_r(\nu)$ are unique and so is the limiting function $f_G(\nu) = \lim_{r \rightarrow \infty} f_{G,r}(\nu)$.

Theorem 2 (Statement of uniqueness: [1, Thm. 2.1]). *Given a simple finite sum $f(n) = \sum_{k=0}^{n-1} g(k)$ where $g : \mathbb{C} \rightarrow \mathbb{C}$ is analytic at the origin, let $p_r(\nu)$ be a*

polynomial in ν of degree r and define

$$f_{G,r}(\nu) = \begin{cases} p_r(\nu) & \nu \in [0, 1] \\ g(\nu - 1) + f_{G,r}(\nu - 1) & \text{otherwise.} \end{cases}$$

If we require $f_{G,r}(\nu)$ to be $(r - 1)$ -times differentiable on $\nu \in (0, 2)$, then the limiting function $f_G(\nu) = \lim_{r \rightarrow \infty} f_{G,r}(\nu)$ is unique, satisfies the recurrence identity $f_G(\nu) = g(\nu - 1) + f_G(\nu - 1)$, and the initial condition $f_G(0) = 0$.

Using this iterative polynomial approximation procedure one subsequently obtains the generalized sum $f_G(\nu)$ formally given by the Taylor series

$$f_G(\nu) = \sum_{k=1}^{\infty} \frac{\nu^k}{k!} \sum_{\ell=0}^{\infty} \frac{B_{\ell}}{\ell!} g^{(k+\ell-1)}(0), \quad (2.3)$$

where $B_n = \{1, -\frac{1}{2}, \frac{1}{6}, 0, \dots\}$ are the Bernoulli numbers¹. This formal series expansion for $f_G(\nu)$ may or may not converge and so explicit methods for evaluating fractional sums are desired. The following presents a summability method and theorem that will be used extensively for evaluating fractional finite sums in this work.

Definition 1 (\mathfrak{T} -summation: [1, Def. 4.1]). *Let $h(s)$ be the function whose Taylor series about the origin is given by*

$$h(s) = \sum_{k=0}^{\infty} g(k)s^k.$$

If $h(s)$ is analytic on $s \in [0, 1]$ then we define the \mathfrak{T} -sum of $\sum_{k=0}^{\infty} g(k)$ by

$$\sum_{k=0}^{\infty} g(k) \stackrel{\mathfrak{T}}{=} h(1).$$

Lemma 4 (Properties of \mathfrak{T} [1, Prop. 4.2]). *The summability method \mathfrak{T} is regular, linear, and stable.*

Theorem 3 (Evaluating simple finite sums: [1, Thm. 5.5]). *Given a simple finite sum $f(n) = \sum_{k=0}^{n-1} g(k)$, if $\sum_{k=0}^{\infty} g(k)$ is \mathfrak{T} -summable then the unique generalization of $f(n)$ consistent with Theorem 2 is given by*

$$f_G(\nu) \stackrel{\mathfrak{T}}{=} \sum_{k=0}^{\infty} g(k) - \sum_{k=0}^{\infty} g(k + \nu).$$

With these results at hand, we will take the next few sections to present three fractional finite sums for later use in deriving the generalized estimator \mathcal{T}_{ν} and its associated properties.

¹It is interesting to note that if we interchange the order of summation in (2.3) we find

$$f_G(\nu) = \sum_{\ell=0}^{\infty} \frac{B_{\ell}}{\ell!} \left(g^{(\ell-1)}(\nu) - g^{(\ell-1)}(0) \right),$$

which is precisely the Euler-Maclaurin formula for $\sum_{k=0}^{\nu-1} g(k)$.

2.2.1 Incomplete geometric series

The first fractional sum we study is the incomplete geometric series which is foundational to the evaluation of many other fractional sums.

Definition 2 (Incomplete geometric series). *The incomplete geometric series ${}_1F_0(1, -; z)_\nu$ is given by*

$${}_1F_0(1, -; z)_\nu := \nu F(1, 1 - \nu; 2; 1 - z).$$

Lemma 5. ${}_1F_0(1, -; z)_\nu$ is the unique generalization of $f(n) = \sum_{k=0}^{n-1} z^k$ consistent with Theorem 2.

Proof. Defining $h(s) := (1 - zs)^{-1}$ we see that $h(s)$ is analytic on $s \in [0, 1]$ if $z \notin [1, \infty)$; thus

$$\sum_{k=0}^{\infty} z^k \stackrel{\mathfrak{T}}{=} h(1) = \frac{1}{1 - z}, \quad z \in \mathbb{C} \setminus [1, \infty).$$

Taking regularity, linearity, and stability as axioms we then extend this results to include all $z \in \mathbb{C} \setminus \{1\}$. In accordance with Theorem 3 it then follows that the fractional generalization of $f(n)$ is

$$f_G(\nu) = (1 - z^\nu) \sum_{k=0}^{\infty} z^k \stackrel{\mathfrak{T}}{=} \frac{1 - z^\nu}{1 - z}, \quad z \in \mathbb{C} \setminus \{1\}.$$

To derive the form in Definition 2 we use the generalized binomial theorem to obtain the formal expression

$$(1 - z)f_G(\nu) = 1 - (1 - (1 - z))^\nu = 1 - \sum_{k=0}^{\infty} \binom{\nu}{k} (-1)^k (1 - z)^k.$$

The first term in the series expansion is one, therefore after some algebraic manipulations we arrive at

$$(1 - z)f_G(\nu) = (1 - z)\nu \sum_{k=0}^{\infty} \frac{(1)_k (1 - \nu)_k}{(2)_k k!} (1 - z)^k,$$

which upon dividing both sides by $(1 - z)$ yields the desired result. \square

2.2.2 Incomplete Lerch Transcendent

We now present our second fractional finite sum in the form of the incomplete Lerch Transcendent. This fractional finite sum will be used in deriving a series expansion for E_ν^2 in Section 2.4.2 as well as an asymptotic expansion of \mathcal{T}_ν in Section 2.3.1. We first begin with the definition of the (complete) Lerch Transcendent.

Definition 3 (Lerch transcendent). *The Lerch transcendent $\Phi(z, s, \omega)$ is defined as the analytic continuation of the series*

$$\Phi(z, s, \omega) := \sum_{k=0}^{\infty} (k + \omega)^{-s} z^k,$$

with $\Phi(z, 0, \omega) := {}_1F_0(1; -; z)$.

Definition 4 (Incomplete Lerch transcendent). *The incomplete Lerch transcendent $\Phi(z, s, \omega)_\nu$ is given by*

$$\Phi(z, s, \omega)_\nu := \Phi(z, s, \omega) - z^\nu \Phi(z, s, \omega + \nu),$$

with $\Phi(z, 0, \omega)_\nu := {}_1F_0(1, -; z)_\nu$.

Lemma 6. $\Phi(z, s, \omega)_\nu$ is the unique generalization of $f(n) = \sum_{k=0}^{n-1} (k + \omega)^{-s} z^k$ consistent with Theorem 2.

Proof. This follows from the fact that

$$h(s) := \Phi(sz, t, \omega) \stackrel{\mathfrak{T}}{=} \sum_{k=0}^{\infty} (k + \omega)^{-t} (sz)^k$$

is analytic for $s \in [0, 1]$ when $|z| < 1$. Therefore, by Theorem 3 the unique generalization is

$$f_G(\nu) \stackrel{\mathfrak{T}}{=} \sum_{k=0}^{\infty} (k + \omega)^{-s} z^k - \sum_{k=0}^{\infty} (k + \omega + \nu)^{-s} z^{k+\nu},$$

which is extended to $z \in \mathbb{C}$ via analytic continuation of $\Phi(z, s, \omega)$. \square

To obtain a deeper understanding of the incomplete Lerch Transcendent we now introduce three differential operators and present many identities relating them. These identities will then allow us to derive properties of $\Phi(z, s, \omega)_\nu$; including its relationship to the incomplete geometric series for use in Section 2.4.1.

Definition 5 (Theta operator). $\vartheta := z \partial_z$

Definition 6 (Lowering operator). $\Lambda_\omega := \omega + \vartheta$

Definition 7 (Factorial operator). *Let \mathcal{D} be a differential operator, then*

$$(\mathcal{D})^{(n)} := \begin{cases} 1, & n = 0 \\ \prod_{k=0}^{n-1} (\mathcal{D} - k), & n \in \mathbb{N}. \end{cases}$$

Lemma 7 (Operator identities). *For $n \in \mathbb{N}_0$ and $\omega \in \mathbb{Z}$,*

$$\begin{aligned}
(i) \quad & \Lambda_\omega z^s = z^s \Lambda_{\omega+s} \\
(ii) \quad & (\vartheta z)^n = z^n \partial_z^n z^n, \\
(iii) \quad & (z\vartheta)^n = z^{n+1} \partial_z^n z^{n-1}, \\
(iv) \quad & \Lambda_\omega^n = z^{-\omega} \vartheta^n z^\omega, \\
(v) \quad & (\vartheta)^{(n)} = z^n \partial_z^n, \\
(vi) \quad & (\Lambda_\omega)^{(n)} = z^{n-\omega} \partial_z^n z^\omega, \\
(vii) \quad & \vartheta^n = \sum_{k=0}^n {}_2\mathcal{S}_n^{(k)} z^k \partial_z^k.
\end{aligned}$$

Proof. See Appendix C. □

Lemma 8. *For $n \in \mathbb{N}_0$, the Lerch Transcendent satisfies*

$$\Lambda_\omega^n \Phi(z, s, \omega) = \Phi(z, s - n, \omega).$$

We can now establish the properties of the incomplete Lerch transcendent that are needed in the following sections.

Lemma 9. *For $n \in \mathbb{N}_0$, the incomplete Lerch Transcendent satisfies the same differential relation as that of Lemma 8, namely,*

$$\Lambda_\omega^n \Phi(z, s, \omega)_\nu = \Phi(z, s - n, \omega)_\nu.$$

Proof. Defining $P(n) : \Lambda_\omega^n \Phi(z, s, \omega)_\nu = \Phi(z, s - n, \omega)_\nu$ we observe that $P(0)$ trivially holds. Now assuming $P(n)$ and using Lemma 7 (i) and Lemma 8 we have

$$\begin{aligned}
\Lambda_\omega^{n+1} \Phi(z, s, \omega)_\nu &= \Lambda_\omega \Phi(z, s - n, \omega)_\nu \\
&= \Lambda_\omega \Phi(z, s - n, \omega) - \Lambda_\omega z^\nu \Phi(z, s - n, \omega + \nu) \\
&= \Lambda_\omega \Phi(z, s - n, \omega) - z^\nu \Lambda_{\omega+\nu} \Phi(z, s - n, \omega + \nu) \\
&= \Phi(z, s - (n+1), \omega) - z^\nu \Phi(z, s - (n+1), \omega + \nu) \\
&= \Phi(z, s - (n+1), \omega)_\nu.
\end{aligned}$$

Thus, $P(n) \implies P(n+1)$ which completes the proof. □

Corollary 1. *Setting $s = 0$ in Lemma 9 yields the formula,*

$$\Phi(z, -n, \omega)_\nu = \Lambda_{\omega 1}^n F_0(1; -; z)_\nu.$$

If in addition $\omega = 0$ one finds

$$\Phi(z, -n, 0)_\nu = \vartheta^n {}_1F_0(1; -; z)_\nu.$$

Corollary 2. *For $n \in \mathbb{N}_0$ and $|\text{ph } z| < \pi$*

$$\Phi(z, -n, 0)_\nu = \frac{1}{z} \sum_{k=0}^n \frac{{}_2\mathcal{S}_n^{(k)}(\nu)^{(k+1)}}{k+1} F\left(\begin{matrix} 1+k, 1+\nu \\ 2+k \end{matrix}; 1 - \frac{1}{z}\right).$$

Proof. With Lemma 7 (vii) and [7, Eq. 15.5.2], we have

$$\Phi(z, -n, 0)_\nu = \sum_{k=0}^n \frac{(1)_k}{(2)_k} {}_2S_n^{(k)} (-1)^k \nu (1-\nu)_k z^k F\left(\begin{matrix} 1+k, 1-\nu+k \\ 2+k \end{matrix}; 1-z\right).$$

Using $(1)_k/(2)_k = 1/(k+1)$, $(-1)^k \nu (1-\nu)_k = (\nu)^{(k+1)}$, and applying the transformation [7, Eq. 15.8.1(i)] to the hypergeometric term yields the desired result. \square

2.2.3 Sine-modulated incomplete hypergeometric function

We now introduce our last fractional finite sum: the sine-modulated incomplete hypergeometric function. This fractional finite sum will serve as the cornerstone for defining the generalized estimator \mathcal{T}_ν .

Definition 8 (Sine-modulated incomplete hypergeometric function). *For $-\gamma \notin \mathbb{N}_0$, the sine-modulated incomplete hypergeometric functions is given by*

$$\mathcal{F}(\alpha, \beta; \gamma; z)_\nu := F\left(\begin{matrix} \alpha, \beta \\ \gamma \end{matrix}; z\right) - \frac{(\alpha)_\nu (-z)^\nu}{(1)_\nu (1-\beta)_{-\nu} (\gamma)_\nu} {}_3F_2\left(\begin{matrix} 1, \alpha+\nu, \beta+\nu \\ 1+\nu, \gamma+\nu \end{matrix}; z\right).$$

Lemma 10. $\mathcal{F}(\alpha, \beta; \gamma; -z)_\nu$ is the unique generalization of

$$f(n) = \sum_{k=0}^{n-1} \frac{\sin(\pi(\beta+k))}{\sin \pi \beta} \frac{(\alpha)_k (\beta)_k}{(\gamma)_k} \frac{z^k}{k!}$$

consistent with Theorem 2.

Proof. Again with the help of Theorem 1 we define

$$h(s) := F\left(\begin{matrix} \alpha, \beta \\ \gamma \end{matrix}; -sz\right) \stackrel{\mathfrak{T}}{=} \sum_{k=0}^{\infty} \frac{\sin(\pi(\beta+k))}{\sin \pi \beta} \frac{(\alpha)_k (\beta)_k}{(\gamma)_k} \frac{(sz)^k}{k!},$$

which is analytic on $s \in [0, 1]$ for all $|z| < 1$; thus, by Theorem 3 the fractional generalization of $f(n)$ is

$$f_G(\nu) \stackrel{\mathfrak{T}}{=} \sum_{k=0}^{\infty} \frac{(\alpha)_k (\beta)_k}{(\gamma)_k} \frac{(-z)^k}{k!} - \frac{\sin(\pi(\beta+\nu))}{\sin \pi \beta} \sum_{k=0}^{\infty} (-1)^k \frac{(\alpha)_{k+\nu} (\beta)_{k+\nu}}{(\gamma)_{k+\nu} \Gamma(1+\nu+k)} z^{k+\nu},$$

for $|z| < 1$. Then using the identity $(s)_{z+r} = (s)_z (s+z)_r$ produces

$$\begin{aligned} f_G(\nu) &\stackrel{\mathfrak{T}}{=} \sum_{k=0}^{\infty} \frac{(\alpha)_k (\beta)_k}{(\gamma)_k} \frac{(-z)^k}{k!} \\ &\quad - \frac{\sin(\pi(\beta+\nu))}{\sin \pi \beta} \frac{(\alpha)_\nu (\beta)_\nu}{(1)_\nu (\gamma)_\nu} z^\nu \sum_{k=0}^{\infty} \frac{(1)_k (\alpha+\nu)_k (\beta+\nu)_k}{(1+\nu)_k (\gamma+\nu)_k} \frac{(-z)^k}{k!}, \end{aligned}$$

where each series is now identified as being generalized hypergeometric series. Finally, from the gamma reflection formula we have

$$\frac{\sin(\pi(\beta + \nu))}{\sin \pi \beta} (\beta)_\nu = \frac{1}{(1 - \beta)_{-\nu}}.$$

Substituting this result into $f_G(\nu)$ yields the desired form of $\mathcal{F}(\alpha, \beta; \gamma; -z)_\nu$, which is extended to $z \in \mathbb{C}$ via analytic continuation of the generalized hypergeometric function. The proof is now complete. \square

Corollary 3 (Special case for $\alpha = 1$).

$$\mathcal{F}(1, \beta; \gamma; -z)_\nu = F\left(\begin{matrix} 1, \beta \\ \gamma \end{matrix}; -z\right) - \frac{z^\nu}{(1 - \beta)_{-\nu}(\gamma)_\nu} F\left(\begin{matrix} 1, \beta + \nu \\ \gamma + \nu \end{matrix}; -z\right)$$

Corollary 4. For $n \in \{n \in \mathbb{N}_0 : 0 \leq n < \alpha_1\}$

$$\mathcal{T}_n = \frac{\alpha_1 - 1}{\alpha_1 Y_1} \mathcal{F}\left(\begin{matrix} 1, 2 - \alpha_1 \\ \alpha_2 \end{matrix}; -\frac{\alpha_2 Y_2}{\alpha_1 Y_1}\right)_n.$$

Proof. Recalling the expression for \mathcal{T}_n , application of the gamma reflection formula gives

$$\mathcal{T}_n = \frac{\alpha_1 - 1}{\alpha_1 Y_1} \sum_{k=0}^{n-1} \frac{\sin(\pi(\alpha_1 - k))}{\sin \pi \alpha_1} \frac{(1)_k (2 - \alpha_1)_k}{(\alpha_2)_k k!} \left(\frac{\alpha_2 Y_2}{\alpha_1 Y_1}\right)^k.$$

By the properties of the sine function we can write

$$\frac{\sin(\pi(\alpha_1 - k))}{\sin \pi \alpha_1} = \frac{\sin(\pi(2 - \alpha_1 + k))}{\sin(\pi(2 - \alpha_1))},$$

which upon substitution into the expression for \mathcal{T}_n yields the form of $f(n)$ in Lemma 10 for $\alpha = 1$, $\beta = 2 - \alpha_1$, $\gamma = \alpha_2$, and $z = \alpha_2 Y_2 (\alpha_1 Y_1)^{-1}$. \square

2.3 The generalized estimator \mathcal{T}_ν

This section introduces the unique fractional generalization of the estimator \mathcal{T}_n and its properties. In light of Corollary 4, we may now suspect that the sine-modulated incomplete hypergeometric function can be used to extend the domain of \mathcal{T}_n beyond integer valued n while preserving statistical properties. The following theorem proves this conjecture to be true. We will first present the estimator \mathcal{T}_ν with complex parameter ν in its full generality and then show how *a priori* knowledge of κ_1 and κ_2 can be incorporated to produce a useful estimator for $\tau = (\kappa_1 - \kappa_2)^{-1}$.

Theorem 4. Let Y_1 and Y_2 be as in Lemma 1. If $\nu \in \mathbb{C} : -\alpha_2 < \Re \nu < \alpha_1$, then

$$\mathcal{T}_\nu = \frac{\alpha_1 - 1}{\alpha_1 Y_1} \mathcal{F}\left(\begin{matrix} 1, 2 - \alpha_1 \\ \alpha_2 \end{matrix}; -\frac{\alpha_2 Y_2}{\alpha_1 Y_1}\right)_\nu,$$

is an unbiased estimator of $\tau_\nu = (1 - \zeta^\nu)/(\kappa_1 - \kappa_2)$.

Proof. We simply need to show that \mathcal{T}_ν yields the correct expected value. Given $Y_i \sim \mathcal{G}(\alpha_i, \alpha_i/\kappa_i)$ one has $\alpha_i Y_i \sim \kappa_i Y_i^*$ where $Y_i^* \sim \mathcal{G}(\alpha_i, 1)$. Let $U = Y_1^*$, $V = Y_2^*/Y_1^*$, $\zeta = \kappa_2/\kappa_1$, and $\mathcal{F}(-\zeta V)_\nu = \mathcal{F}(1, 2 - \alpha_1; \alpha_2; -\zeta V)_\nu$, then

$$\mathcal{T}_\nu = \frac{\alpha_1 - 1}{\kappa_1} U^{-1} \mathcal{F}(-\zeta V)_\nu.$$

Given $Y_1 \perp Y_2$ we use change of variables to write the joint density

$$f_{UV}(u, v) = \frac{(1+v)^{\alpha_1+\alpha_2}}{\Gamma(\alpha_1+\alpha_2)} u^{\alpha_1+\alpha_2-1} e^{-(1+v)u} \frac{v^{\alpha_2-1} (1+v)^{-\alpha_1-\alpha_2}}{B(\alpha_1, \alpha_2)},$$

which upon inspection has the form $f_{UV}(u, v) = f_{U|V}(u, v) f_V(v)$ where $U|V \sim \mathcal{G}(\alpha_1 + \alpha_2, 1 + V)$ and $V \sim \beta'(\alpha_2, \alpha_1)$, which is a *beta prime* random variable. Now making use of Lemma 2 we write

$$\mathbb{E} \mathcal{T}_\nu = \mathbb{E} \mathbb{E}(\mathcal{T}_\nu | V) = \frac{1}{\kappa_1} \frac{\alpha_1 - 1}{\alpha_1 + \alpha_2 - 1} \mathbb{E}[(1 + V) \mathcal{F}(-\zeta V)_\nu] = \frac{1}{\kappa_1} \mathbb{E} \mathcal{F}(-\zeta W)_\nu,$$

where $W \sim \beta'(\alpha_2, \alpha_1 - 1)^2$. Reintroducing the expression for $\mathcal{F}(-\zeta W)_\nu$ we arrive at

$$\kappa_1 \mathbb{E} \mathcal{T}_\nu = \mathbb{E} F\left(\begin{matrix} 1, 2 - \alpha_1 \\ \alpha_2 \end{matrix}; -\zeta W\right) - \zeta^\nu \frac{\mathbb{E} W^\nu F\left(\begin{matrix} 1, 2 - \alpha_1 + \nu \\ \alpha_2 + \nu \end{matrix}; -\zeta W\right)}{(\alpha_1 - 1)_{-\nu} (\alpha_2)_\nu}.$$

The expected value of each term can be evaluated via [11, Eq. 7.512.10] to find

$$\kappa_1 \zeta^{1-\alpha_1} \mathbb{E} \mathcal{T}_\nu = -(1-\alpha_1) F\left(\begin{matrix} 1, \alpha_1 \\ 2 \end{matrix}; 1 - \zeta\right) + (1-\alpha_1+\nu) F\left(\begin{matrix} 1, \alpha_1 - \nu \\ 2 \end{matrix}; 1 - \zeta\right),$$

where the second term is finite if only if $-\alpha_2 < \Re \nu < \alpha_1$. Now, upon inspection of Definition 2 we see that this result is equivalent to

$$\kappa_1 \zeta^{1-\alpha_1} \mathbb{E} \mathcal{T}_\nu = {}_1F_0(1; -; \zeta)_{1-\alpha_1+\nu} - {}_1F_0(1; -; \zeta)_{1-\alpha_1}.$$

Therefore, given the identity ${}_1F_0(1; -; z)_\nu = (1 - z^\nu)(1 - z)^{-1}$ we have

$$\mathbb{E} \mathcal{T}_\nu = \frac{1 - \zeta^{\alpha_1-1}}{\kappa_1 - \kappa_2} - \frac{\zeta^\nu - \zeta^{\alpha_1-1}}{\kappa_1 - \kappa_2},$$

which upon simplifying yields the desired result. \square

Corollary 5 (Minimum variance estimation). *\mathcal{T}_ν is the uniformly minimum variance unbiased estimator of τ_ν .*

Proof. From Lemma 1 we know that $T = (Y_1, Y_2)$ is a complete-sufficient statistic of (κ_1, κ_2) . Since $\mathcal{T}_\nu(Y_1, Y_2)$ is a function of T it follows from the Lehmann-Scheffé theorem that \mathcal{T}_ν is the unique uniformly minimum variance unbiased estimator of its expected value τ_ν . \square

²The last equality can be easily reach upon multiplying the density f_V with $\frac{(\alpha_1-1)(1+v)}{\alpha_1+\alpha_2-1}$.

Corollary 6. $\mathcal{T}_0 \sim \delta_0$ is a degenerate random variable with $\mathbf{E}\mathcal{T}_0 = 0$.

Proof. This follows directly from the fundamental property of fractional finite sums: $f_G(0) = 0$. \square

At this point we have established \mathcal{T}_ν to be the unique generalization of \mathcal{T}_n and presented a couple of its properties. We now proceed to show that \mathcal{T}_ν satisfies a reflection formula, which will be used many times in later sections.

Theorem 5 (Reflection formula).

$$\mathcal{T}_\nu(Y_1, Y_2, \alpha_1, \alpha_2) = -\mathcal{T}_{-\nu}(Y_2, Y_1, \alpha_2, \alpha_1)$$

Proof. We begin with the general expression for \mathcal{T}_ν , namely,

$$\begin{aligned} \mathcal{T}_\nu(Y_1, Y_2, \alpha_1, \alpha_2) &= \frac{\alpha_1 - 1}{\alpha_1 Y_1} \left(F \left(\begin{matrix} 1, 2 - \alpha_1 \\ \alpha_2 \end{matrix}; -\frac{\alpha_2 Y_2}{\alpha_1 Y_1} \right) \right. \\ &\quad \left. - \frac{\left(\frac{\alpha_2 Y_2}{\alpha_1 Y_1} \right)^\nu}{(\alpha_1 - 1)_{-\nu} (\alpha_2)_\nu} F \left(\begin{matrix} 1, 2 - \alpha_1 + \nu \\ \alpha_2 + \nu \end{matrix}; -\frac{\alpha_2 Y_2}{\alpha_1 Y_1} \right) \right). \end{aligned}$$

Then, [7, Eq. 15.8.2] provides the necessary result to derive the transformation formula

$$F \left(\begin{matrix} 1, \beta \\ \gamma \end{matrix}; -z \right) = \frac{\Gamma(1 - \beta) z^{1 - \gamma}}{(\gamma)_{-\beta} (1 + z)^{\beta - \gamma + 1}} - \frac{\gamma - 1}{z(1 - \beta)} F \left(\begin{matrix} 1, 2 - \gamma \\ 2 - \beta \end{matrix}; -\frac{1}{z} \right),$$

which is subject to the constraint $|\text{ph } z| < \pi$. Applying this transformation to each hypergeometric term in \mathcal{T}_ν and simplifying yields

$$\begin{aligned} \mathcal{T}_\nu(Y_1, Y_2, \alpha_1, \alpha_2) &= -\frac{\alpha_2 - 1}{\alpha_2 Y_2} \left(F \left(\begin{matrix} 1, 2 - \alpha_2 \\ \alpha_1 \end{matrix}; -\frac{\alpha_1 Y_1}{\alpha_2 Y_2} \right) \right. \\ &\quad \left. - \frac{\left(\frac{\alpha_1 Y_1}{\alpha_2 Y_2} \right)^{-\nu}}{(\alpha_2 - 1)_\nu (\alpha_1)_{-\nu}} F \left(\begin{matrix} 1, 2 - \alpha_2 - \nu \\ \alpha_1 - \nu \end{matrix}; -\frac{\alpha_1 Y_1}{\alpha_2 Y_2} \right) \right) \\ &= -\mathcal{T}_{-\nu}(Y_2, Y_1, \alpha_2, \alpha_1), \end{aligned}$$

which completes the proof. \square

Corollary 7. $(\mathbf{E}\mathcal{T}_\nu^n)(\kappa_1, \kappa_2, \alpha_1, \alpha_2) = (-1)^n (\mathbf{E}\mathcal{T}_{-\nu}^n)(\kappa_2, \kappa_1, \alpha_2, \alpha_1)$.

Proof. The proof follows immediately from the reflection formula of Corollary 5 and $Y_i \sim \kappa_i / \alpha_i Y_i^*$ with $Y_i^* \sim \mathcal{G}(\alpha_i, 1)$. In other words, interchanging Y_1 and Y_2 interchanges κ_1 and κ_2 in the expected value. \square

Proposition 1. As an estimator for $\tau = (\kappa_1 - \kappa_2)^{-1}$, \mathcal{T}_ν is biased with bias equal to

$$\text{Bias}\mathcal{T}_\nu := \mathbf{E}\mathcal{T}_\nu - \tau = -\frac{\zeta^\nu}{\kappa_1 - \kappa_2}$$

and absolute relative bias equal to

$$\text{ARB}\mathcal{T}_\nu := \left| \frac{\mathbf{E}\mathcal{T}_\nu - \tau}{\tau} \right| = \zeta^\nu.$$

Corollary 6, Theorem 5, and Proposition 1 all hint at the significance of the parameter ν in controlling the bias, dispersion, and sign of \mathcal{T}_ν . To gain a better intuition for these relationships it would be informative to plot the density of \mathcal{T}_ν for several values ν . Deriving explicit forms of this density is likely impossible so we shall turn to estimating it with Monte Carlo methods. Estimating the density was done by first generating a total of 10^6 i.i.d. pseudo-random observations of Y_1 and Y_2 using the parameters $\alpha_1 = 20$, $\alpha_2 = 15$, $\kappa_1 = 2$, and $\kappa_2 = 1$, which correspond to $\tau = 1$. These pseudo-random observations and parameters were then used to generate equally sized samples of $\mathcal{T}_\nu(Y_1, Y_2, 20, 15)$ for the eight selected values of ν in Table 2.1³.

Symbol	Name/Expression	Decimal Expansion
$\zeta'(2)$	$\frac{1}{6}\pi^2(\gamma + \log 2\pi - 12 \log A)$	$-0.9375482543 \dots$
δ_1	Hall–Montgomery constant	$-0.6569990137 \dots$
$m_{1,4}$	Meissel–Mertens constant	$-0.2867420562 \dots$
i^i	$\exp(-\pi/2)$	$0.2078795764 \dots$
K	Landau–Ramanujan constant	$0.7642236535 \dots$
x_Γ	Minimizer of $\Gamma(x)$ on \mathbb{R}^+	$1.4616321449 \dots$
L	Lévy constant, $\exp(\pi^2/\log 64)$	$10.7310157948 \dots$
ζ_0	First non-trivial zero of $\zeta(s)$	$1/2 + 14.1347251417i$

Table 2.1: Special constants (see [9] for details). Here, γ is the Euler–Mascheroni constant and A denotes the Glaisher–Kinkelin constant.

Kernel density estimates were computed for all eight samples corresponding to each value of ν as plotted in Figure 2.2. Looking in particular at the plots of the kernel density estimates for the real-valued ν we see that $\text{sign}(\mathcal{T}_\nu) = \text{sign}(\nu)$ and that the dispersion of the density increases with increasing $|\nu|$. Notice also that only the estimates generated with values of $\nu > 0$ serve as useful estimates for τ ; showing that one must incorporate a priori information into \mathcal{T}_ν by requiring $\text{sign}(\nu) = \text{sign}(\tau)$ in order to render it a useful estimator of τ .

Remark 2 (Incorporating *a priori* knowledge of κ_1 and κ_2). *As in Lemma 3, Theorem 4 makes no mention of a restriction on the relative magnitudes of κ_1 and κ_2 , i.e. $\kappa_1 > \kappa_2$ or $\kappa_1 < \kappa_2$. By permitting $\nu \in \mathbb{R}$, \mathcal{T}_ν can be used as an estimator for $\tau = (\kappa_1 - \kappa_2)^{-1}$ in both cases whereby one imposes the rule $\nu > 0$ when $\kappa_1 > \kappa_2$ or $\nu < 0$ when $\kappa_1 < \kappa_2$ to ensure that $\text{ARB} \mathcal{T}_\nu < 1$.*

2.3.1 Asymptotic expansion for large α_1 and α_2

As α_1 and α_2 become large, the estimator \mathcal{T}_ν becomes increasingly difficult to evaluate; rendering it incompatible with practical applications involving large

³Since \mathcal{T}_ν estimates τ_ν for any $\nu \in \mathbb{C}$ along the strip $-\alpha_2 < \Re \nu < \alpha_1$, it seemed proper to choose interesting values of ν for this demonstration.

shape parameters. Here we derive a few preliminary results and then proceed to present an asymptotic expansion of \mathcal{T}_ν in Theorem 6.

Lemma 11 ([25]). *As $z \rightarrow \infty$ in the sector $|\text{ph } z| < \pi$*

$$\frac{\Gamma(z + \alpha)}{\Gamma(z + \beta)} \sim z^{\alpha - \beta} \sum_{k=0}^{\infty} \binom{\alpha - \beta}{k} B_k^{(\alpha - \beta + 1)}(\alpha) \frac{1}{z^k},$$

where $B_n^{(\ell)}(x)$ is the generalized Nørlund polynomial given by Definition 24.

Corollary 8. *As $z \rightarrow \infty$ in the sector $|\text{ph } z| < \pi$*

$$\frac{z^\alpha}{(z)_\alpha} \sim \sum_{k=0}^{\infty} \binom{-\alpha}{k} B_k^{(1-\alpha)} \frac{1}{z^k},$$

where $B_n^{(\ell)} = B_n^{(\ell)}(0)$.

Lemma 12. *For $\alpha = n \in \mathbb{Z}$, the asymptotic series in Corollary 8 converges absolutely for all $z > \max\{0, n - 1\}$.*

Proof. If $n \leq 0$ then

$$\frac{z^n}{(z)_n} \sim \sum_{k=0}^{-n} \binom{-n}{k} B_k^{(1-n)} \frac{1}{z^k},$$

which is a sum of a finite number of terms and thus converges absolutely for all $z > 0$. We now prove absolute convergence for all remaining $n \geq 1$ by induction. Beginning with the relationship between Nørlund's polynomial and the Stirling number of the second-kind we write [5, Eq. 3]

$$\frac{z^n}{(z)_n} \sim \sum_{k=0}^{\infty} (-1)^k {}_2\mathcal{S}_{k+n-1}^{(n-1)} \frac{1}{z^k} =: S_n.$$

Substituting $n = 1$ gives

$$S_1 = \sum_{k=0}^{\infty} (-1)^k \delta_k \frac{1}{z^k} = 1 + 0 + 0 + \dots,$$

which clearly converges absolutely for all $z > 0$. Assuming S_n converges absolutely for all $z > n - 1$ we write with the help of [27, Eq. 04.15.17.0002.01]

$$S_{n+1} = \sum_{k=0}^{\infty} \sum_{\ell=0}^k (-n)^{k-\ell} (-1)^\ell {}_2\mathcal{S}_{\ell+n-1}^{(n-1)} \frac{1}{z^k} = S_n \sum_{k=0}^{\infty} (-n)^k \frac{1}{z^k}.$$

But $\sum_{k=0}^{\infty} (-n)^k \frac{1}{z^k} = (1 + n/z)^{-1}$ converges absolutely if $z > n$; hence, if $z > n$ then S_{n+1} is the product of absolutely convergent series, which is itself absolutely convergent. The proof is now complete. \square

Theorem 6. As $\alpha_1, \alpha_2 \rightarrow \infty$

$$\mathcal{T}_\nu \sim \frac{1}{Y_1} \sum_{k=0}^{\infty} \sum_{\ell=0}^{2k} p_{k,\ell}(\alpha_1, \alpha_2) \Phi(Y_2/Y_1, -\ell, 0)_\nu,$$

where $p_{k,\ell}(\alpha_1, \alpha_2) = \partial_x^\ell P_{2k}(0)/\ell!$,

$$P_{2k}(x) = \sum_{m=0}^k \frac{1}{\alpha_1^m \alpha_2^{k-m}} \binom{x+1}{m} \binom{-x}{k-m} B_m^{(2+x)} B_{k-m}^{(1-x)},$$

and $B_n^{(s)}$ is the Nørlund polynomial defined by the generating function in Definitions 24-25.

Proof. Beginning with the expression for \mathcal{T}_n we have

$$\mathcal{T}_n = \frac{1}{Y_1} \sum_{k=0}^{n-1} \frac{\alpha_1^{-k-1} \alpha_2^k}{(\alpha_1)_{-k-1} (\alpha_2)_k} \left(\frac{Y_2}{Y_1} \right)^k.$$

Now consider the result of Corollary 8, which states $z^s/(z)_s \sim \sum_{\ell=0}^{\infty} G_\ell(s) z^{-\ell}$ as $z \rightarrow \infty$ where [25, 7, Eq. 5.11.13]

$$G_\ell(s) = \binom{-s}{\ell} B_\ell^{(1-s)}.$$

Substituting in appropriate values, we obtain two separate asymptotic series in α_1 and α_2 for which the product yields

$$\frac{\alpha_1^{-k-1} \alpha_2^k}{(\alpha_1)_{-k-1} (\alpha_2)_k} \sim \sum_{\ell=0}^{\infty} \sum_{m=0}^{\ell} G_m(-k-1) G_{\ell-m}(k) \alpha_1^{-m} \alpha_2^{\ell-m}. \quad (2.4)$$

Substituting this asymptotic expansion in \mathcal{T}_ν and rearranging the order of summation then gives

$$\mathcal{T}_n \sim \frac{1}{Y_1} \sum_{\ell=0}^{\infty} \sum_{k=0}^{n-1} \left(\sum_{m=0}^{\ell} \frac{G_m(-k-1) G_{\ell-m}(k)}{\alpha_1^m \alpha_2^{\ell-m}} \right) \left(\frac{Y_2}{Y_1} \right)^k. \quad (2.5)$$

With the help of Definition 23 and [17, Thm. 1] the quantity $G_m(-k-1) G_{\ell-m}(k)$ can be easily shown to be a polynomial in k of degree 2ℓ ; thus, the entire sum inside the parentheses of (2.5) must also be a polynomial in k of degree 2ℓ . Let,

$$\begin{aligned} P_{2\ell}(k) &:= \sum_{m=0}^{\ell} \frac{G_m(-k-1) G_{\ell-m}(k)}{\alpha_1^m \alpha_2^{\ell-m}} \\ &= p_{\ell,0}(\alpha_1, \alpha_2) + p_{\ell,1}(\alpha_1, \alpha_2)k + \cdots + p_{\ell,2\ell}(\alpha_1, \alpha_2)k^{2\ell}. \end{aligned}$$

We can then write

$$\mathcal{T}_n \sim \frac{1}{Y_1} \sum_{\ell=0}^{\infty} \sum_{m=0}^{2\ell} p_{\ell,m}(\alpha_1, \alpha_2) \sum_{k=0}^{n-1} k^m \left(\frac{Y_2}{Y_1} \right)^k.$$

The interior sum over k can now be expressed by $\Phi(Y_2/Y_1, -m, 0)_n$ which is uniquely extended to $n \in \mathbb{C}$ via Lemma 6. \square

Corollary 9 (Zeroth order approximation). *Truncating the asymptotic expansion for \mathcal{T}_ν at $k = 0$ yields*

$$\mathcal{T}_{\nu,0} = \frac{1 - (Y_2/Y_1)^\nu}{Y_1 - Y_2} = \tau_\nu(Y_1, Y_2).$$

Proposition 2 (Asymptotic expansion convergence). *For the special case $\nu = n$ with $n \in \mathbb{N}$, the asymptotic expansion for \mathcal{T}_ν given in Theorem 6 converges absolutely whenever $\alpha_2 > n - 2$.*

Proof. According to Lemma 8, the asymptotic expansion for $\alpha_1^{-k-1}/(\alpha_1)_{-k-1}$ consists of a finite number of terms while the asymptotic expansion for $\alpha_2^k/(\alpha_2)_k$ converges absolutely for all $\alpha_2 > n - 2$. Hence, the product of these expansions must also be absolutely convergent, which leads to the desired conclusion. \square

From a numerical standpoint, using the form of the asymptotic expansion for \mathcal{T}_ν in Theorem 6 is problematic since $\Phi(z, -n, 0)_\nu$ has a removable singularity at $z = 1$. As such, to construct an asymptotic approximation for practical applications, Corollary 2 leads to the more convenient form

$$\mathcal{T}_{\nu,K} = \frac{1}{Y_2} \sum_{m=0}^{2K} c_{m,K}(\alpha_1, \alpha_2)(\nu)^{(m+1)} F\left(\begin{matrix} m+1, 1+\nu \\ m+2 \end{matrix}; 1 - \frac{Y_1}{Y_2}\right), \quad (2.6)$$

where

$$c_{m,K}(\alpha_1, \alpha_2) = \frac{1}{m+1} \sum_{\ell=m}^{2K} \sum_{k=0}^K {}_2\mathcal{S}_\ell^{(m)} p_{k,\ell}(\alpha_1, \alpha_2).$$

2.4 Measures of dispersion

In this section we derive absolutely convergent series expansions and integrals on the unit square for the variance and absolute coefficient of variation of \mathcal{T}_ν . Deriving these expressions directly by integrating powers of \mathcal{T}_ν w.r.t. the joint density of (Y_1, Y_2) prove to be intractable. As such, the following derivations rely on deriving the appropriate quantities for the integer-valued estimator \mathcal{T}_n and then using the uniqueness of the fractional finite sum to generalize to noninteger ν . Central to the following derivations are the functions $g_{n,\omega}(z, \nu)$ and $\tilde{g}_{n,\omega}(z, \nu)$ presented in section 2.4.1. While somewhat extensive, section 2.4.1 provides many useful results for characterizing the behavior of $\text{Var}\mathcal{T}_\nu$ and $\text{ACV}\mathcal{T}_\nu$ and in particular for establishing the monotonicity of $\text{ACV}\mathcal{T}_\nu$ used in Section 2.5 on confidence intervals.

2.4.1 The functions $g_{n,\omega}$ and $\tilde{g}_{n,\omega}$

Definition 9. Let $\mathcal{N} = \{(n, \omega) : (n, \omega) \in \mathbb{N}_0^2 \wedge \omega \leq n\}$. Then for $(n, \omega) \in \mathcal{N}$, $z \in \mathbb{R}_0^+$, and $\nu \in \mathbb{R}$

$$g_{n,\omega}(z, \nu) := (\Lambda_\omega)^{(n)} {}_1F_0(1; -; z)_\nu$$

and

$$\tilde{g}_{n,\omega}(z, \nu) := \frac{g_{n,\omega}(z, \nu)}{{}_1F_0(1; -; z)_\nu},$$

where Λ_ω and $(\mathcal{D})^{(n)}$ are the lowering operator of Definition 6 and factorial operator of Definition 7, respectively.

It is important to note that Definition 9 explicitly defines $g_{n,\omega}$ and its regularized counterpart $\tilde{g}_{n,\omega}$ only for natural n and ω on the set \mathcal{N} . As such, from here on out we will assume $(n, \omega) \in \mathcal{N}$ whenever discussing these functions unless specified otherwise. In the following Theorem we will derive two explicit forms for $g_{n,\omega}$. The expression given by form (ii) possesses a natural extension to noninteger values of n and ω via the gamma function and so form (ii) can be viewed as a more general, continuous extension of form (i). This property will come in handy when we get to Lemma 19 where the ability to differentiate these functions w.r.t n and ω greatly simplifies the proof. Furthermore, the incomplete Lerch transcendent functions $\Phi(\cdot)_\nu$ in form (i) have removable singularities at $z = 1$ whereas form (ii) does not and so form (ii) is also more desirable for numerical computation in the neighborhood of $z = 1$.

Theorem 7.

$$g_{n,\omega}(z, \nu) = \begin{cases} \sum_{k=0}^n \mathcal{S}_n^{(k)} \Phi(z, -k, \omega)_\nu & \text{(i)} \\ n! (\omega + \nu)^{(n+1)} z^\nu \mathbf{F}(1, \omega + \nu + 1; n + 2; 1 - z) & \text{(ii)} \end{cases}$$

Proof. With Relation 3 and Definition 23 we expand the factorial operator yielding

$$g_{n,\omega}(z, \nu) = \left(\sum_{k=0}^n \mathcal{S}_n^{(k)} \Lambda_\omega^k \right) {}_1F_0(1; -; z)_\nu.$$

Upon inspection of Corollary 1 we write $\Lambda_\omega^k {}_1F_0(1; -; z)_\nu = \Phi(z, -k, \omega)_\nu$; hence, form (i) is obtained.

To derive form (ii) begin by using Lemma 7 (vi) and the incomplete geometric series in Definition 2 to write

$$\begin{aligned} g_{n,\omega}(z, \nu) &= \nu z^{n-\omega} \partial_z^n z^\omega F(1, 1 - \nu; 2; 1 - z) \\ &= \nu z^{n-\omega} \partial_z^{n-\omega} z^{-\omega} [(z \partial_z z)^\omega F(1, 1 - \nu; 2; 1 - z)], \end{aligned}$$

where the last equality is a consequence of Lemma 7 (ii). Now consider the term in square brackets and substitute $t = 1 - z$. Noting that $\partial_{1-t} = -\partial_t$ we have

$$(z \partial_z z)^\omega F(1, 1 - \nu; 2; 1 - z) \mapsto (-1)^\omega ((1 - t) \partial_t (1 - t))^\omega F(1, 1 - \nu; 2; t).$$

The resulting differential formula in t is the same form as that of [7, Eq. 15.5.7] giving

$$(-1)^\omega ((1-t)\partial_t(1-t))^\omega F(1, 1-\nu; 2; t) = \frac{(\nu+1)_\omega}{\omega+1} (1-t)^\omega F(\omega+1, 1-\nu; \omega+2; t).$$

Reintroducing $z = 1 - t$ and substituting the result back into $g_{n,\omega}$ then gives

$$g_{n,\omega}(z, \nu) = \nu \frac{(\nu+1)_\omega}{\omega+1} z^{n-\omega} \partial_z^{n-\omega} F(\omega+1, 1-\nu; \omega+2; 1-z).$$

Evaluating the remaining derivative with [7, Eq. 15.5.2] and simplifying we have

$$g_{n,\omega}(z, \nu) = n! (\omega + \nu)^{(n+1)} z^{n-\omega} \mathbf{F}(n+1, 1-\nu+n-\omega; n+2; 1-z),$$

which upon applying the linear transformation in [7, Eq. 15.8.1 (iii)] at last produces form (ii). \square

Corollary 10 (Explicit forms for $\tilde{g}_{n,\omega}$).

$$\tilde{g}_{n,\omega}(z, \nu) = \begin{cases} n! \frac{(\omega+\nu)^{(n+1)}}{\nu} \frac{\mathbf{F}(1, \omega+\nu+1; n+2; 1-z)}{\mathbf{F}(1, \nu+1; 2; 1-z)} & \text{(i)} \\ n! \frac{z^{n-\omega} \mathbf{I}_{1-z}(n+1, \omega+\nu-n)}{(1-z)^n (1-z^\nu)} & \text{(ii)} \\ n! \frac{z^{n-\omega} - z^\nu \sum_{k=0}^n \frac{(\omega+\nu-n)_k}{k!} (1-z)^k}{(1-z)^n (1-z^\nu)} & \text{(iii)} \end{cases}$$

Proof. The proof for form (i) follows from the definition of $\tilde{g}_{n,\omega}$ and the hypergeometric transformation [7, Eq. 15.8.1(iii)] to write ${}_1F_0(1; -; z)_\nu = \nu z^\nu \mathbf{F}(1, \nu+1; 2; 1-z)$. Form (ii) is derived with the aid of Relation 6 and Definition 33. Form (iii) is then found using [27, Eqs. 06.19.03.0003.01] on form (ii). \square

Lemma 13 (Recurrence relation). *Both $g_{n,\omega}$ and $\tilde{g}_{n,\omega}$ satisfy*

$$g_{n+1,\omega+1} = g_{n+1,\omega} + (n+1)g_{n,\omega}.$$

Proof. Denoting $f(z) = {}_1F_0(1; -; z)_\nu$ we have

$$\begin{aligned} g_{n+1,\omega+1} &= z^{n-\omega} \partial_z^{n+1} z^{\omega+1} f \\ &= z^{n-\omega} \sum_{k=0}^{n+1} \binom{n+1}{k} (\partial_z^k z) (\partial_z^{n+1-k} z^\omega f) \\ &= z^{n+1-\omega} \partial_z^{n+1} z^\omega f + (n+1) z^{n-\omega} \partial_z^n z^\omega f, \end{aligned}$$

which is the desired result. Dividing sides of the last equality by f gives the corresponding result for $\tilde{g}_{n,\omega}$. \square

Lemma 14 (Reflection formula).

$$\tilde{g}_{n,\omega}(z, \nu) = (-1)^n \tilde{g}_{n,n-\omega}(1/z, -\nu)$$

Proof. Applying the linear transformation in [7, Eq. 15.8.1(i)] to each hypergeometric term in Corollary 10 and defining $\omega' = n - \omega$ and $\nu' = -\nu$ yields

$$\begin{aligned}\tilde{g}_{n,\omega}(z, \nu) &= \frac{n!(n - \omega' - \nu')^{(n+1)}}{-\nu'} \frac{\mathbf{F}(1, \omega' + \nu' + 1; n + 2; 1 - 1/z)}{\mathbf{F}(1, \nu' + 1, 2, 1 - 1/z)} \\ &= -\frac{n!(-1)^{n+1}(\omega' + \nu')^{(n+1)}}{\nu'} \frac{\mathbf{F}(1, \omega' + \nu' + 1; n + 2; 1 - 1/z)}{\mathbf{F}(1, \nu' + 1, 2, 1 - 1/z)} \\ &= (-1)^n \tilde{g}_{n,\omega'}(1/z, \nu'),\end{aligned}$$

which completes the proof. \square

Lemma 15.

$$\begin{aligned}\lim_{z \rightarrow 0} \tilde{g}_{n,\omega}(z, \nu) &= (\omega + \nu \mathbb{1}_{\nu < 0})^{(n)} \\ \lim_{z \rightarrow \infty} \tilde{g}_{n,\omega}(z, \nu) &= (\omega + \nu \mathbb{1}_{\nu > 0} - 1)^{(n)}.\end{aligned}$$

Proof. Assume $\nu > 0$ and consider the limit approaching zero. As $z \rightarrow 0$, $I_{1-z}(\alpha, \beta) \sim 1 + \mathcal{O}(z^\beta)$ [27, Eq. 06.21.06.0044.01]. Applying this result to Corollary 10 form (ii) then gives

$$\tilde{g}_{n,\omega}(z, \nu) \sim n! (1 + \mathcal{O}(z))(1 + \mathcal{O}(z^\nu)) (z^{n-\omega} + \mathcal{O}(z^\nu)), \quad (2.7)$$

which upon passing to the limit yields

$$\lim_{z \rightarrow 0} \tilde{g}_{n,\omega}(z, \nu) = n! \mathbb{1}_{n=\omega} = (\omega)^{(n)}.$$

Now considering the limit $z \rightarrow \infty$ we use the transformation [7, Eq. 15.8.1(i)] to write

$$\tilde{g}_{n,\omega}(z, \nu) = \frac{n!(\omega + \nu)^{(n+1)}}{\nu \Gamma(n+2)} \frac{F(1, n - \omega + 1 - \nu; n + 2; 1 - 1/z)}{F(1, 1 - \nu, 2, 1 - 1/z)}.$$

According to Relation 12, the limits of the numerator and denominator are finite if $\omega + \nu > 0$ and $\nu > 0$, respectively; thus,

$$\lim_{z \rightarrow \infty} \tilde{g}_{n,\omega}(z, \nu) = \frac{(\omega + \nu)^{(n+1)}}{\nu} \frac{\Gamma(\omega + \nu) \Gamma(\nu + 1)}{\Gamma(\omega + \nu + 1) \Gamma(\nu)} = (\omega + \nu - 1)^{(n)}.$$

Still assuming $\nu > 0$ we may now use the reflection formula in Lemma 14 to deduce

$$\begin{aligned}\lim_{z \rightarrow 0} \tilde{g}_{n,\omega}(z, -\nu) &= (-1)^n \lim_{z \rightarrow \infty} \tilde{g}_{n,n-\omega}(z, \nu) \\ \lim_{z \rightarrow \infty} \tilde{g}_{n,\omega}(z, -\nu) &= (-1)^n \lim_{z \rightarrow 0} \tilde{g}_{n,n-\omega}(z, \nu).\end{aligned}$$

But notice that the limit on the r.h.s. of each equality can be found from our previous results by substituting $\omega \mapsto n - \omega$ and then scaling by $(-1)^n$. It then follows after some simplification that

$$\begin{aligned}\lim_{z \rightarrow 0} \tilde{g}_{n,\omega}(z, -\nu) &= (\omega + \nu)^{(n)} \\ \lim_{z \rightarrow \infty} \tilde{g}_{n,\omega}(z, -\nu) &= (\omega - 1)^{(n)}.\end{aligned}$$

Combining all four result then produces the desired solution. \square

The following definition and relation will be used extensively in the rest of this section.

Definition 10 (Gauss-Hypergeometric distribution). *For $\alpha, \beta > 0$, $\gamma \in \mathbb{R}$, and $\xi > -1$, the Gauss Hypergeometric random variable $X \sim \mathcal{GH}(\alpha, \beta, \gamma, \xi)$ admits a distribution and density function on $x \in (0, 1)$ of the form*

$$\begin{aligned} F_X(x; \alpha, \beta, \gamma, \xi) &= \frac{x^\alpha F_1(\alpha; 1 - \beta, \gamma; \alpha + 1; x, -\xi x)}{\alpha B(\alpha, \beta) F(\alpha, \gamma; \alpha + \beta; -\xi)}, \\ f_X(x; \alpha, \beta, \gamma, \xi) &= \frac{x^{\alpha-1} (1-x)^{\beta-1} (1+\xi x)^{-\gamma}}{B(\alpha, \beta) F(\alpha, \gamma; \alpha + \beta; -\xi)}, \end{aligned}$$

where $F_1(a; b, b'; c; s, z)$ is Appell's 1st hypergeometric function of two variables (see Definition 30).

Relation 1. For $|\text{ph}(1-z)| < \pi$ and $\Re c > \Re d > 0$

$$\mathbf{F}(a, b; c; z) = \int_0^1 F(a, b; d; zt) \frac{t^{d-1} (1-t)^{c-d-1}}{\Gamma(d) \Gamma(c-d)} dt.$$

In particular if $\Re c > \Re b > 0$ then substituting $d = b$ gives

$$\mathbf{F}(a, b; c; z) = \int_0^1 (1-zt)^{-a} \frac{t^{b-1} (1-t)^{c-b-1}}{\Gamma(b) \Gamma(c-b)} dt.$$

An important result needed for obtaining a better understanding of ACV \mathcal{T}_ν are the zeros of $\tilde{g}_{n,\omega}$. The following lemma will serve as a preliminary result needed to find these zeros.

Lemma 16. *Let $\nu \in \mathbb{R}$, $z \in \mathbb{R}_0^+$, and $X \sim \mathcal{GH}(1, 1, 1 + \nu, z - 1)$. Then $\mathbb{E}X = 1 \iff \nu \in \mathbb{R}_0^+ \wedge z = 0$.*

Proof. With the help of Definition 10 we write the density of X as

$$f_X(x|z) = \frac{(1 - (1-z)x)^{-1-\nu}}{F(1, 1 + \nu; 2; 1-z)} \mathbf{1}_{x \in [0,1]}.$$

Consider the family of density functions $f_z = \{f_X(x|z) : z \in \mathbb{R}_0^+\}$ and let $\delta > 0$. We have for the likelihood ratio

$$L(x) := \frac{f_{z+\delta}}{f_z}(x) = C \left(\frac{1 - (1-z)x}{1 - (1-z-\delta)x} \right)^{1+\nu},$$

where C is a positive constant. Differentiating L gives

$$\partial_x L(x) = -\delta C(1+\nu) \frac{(1 - (1-z)x)^\nu}{(1 - (1-z-\delta)x)^{2+\nu}}.$$

For fixed ν , $\text{sign}(\partial_x L(x))$ is constant on the interior of $\text{supp}(X) = [0, 1]$. Consequently, the family of density functions f_z admits a monotone likelihood ratio and

$$\text{sign}(\partial_z EX) = \text{sign}(\partial_x L(x)) = \begin{cases} -1, & \nu > -1 \\ 0, & \nu = -1 \\ 1, & \nu < -1. \end{cases} \quad (2.8)$$

We now want to show that $z > 0 \implies EX < 1$. Evaluating the expected value yields

$$EX = \frac{1 - (1 - z)\nu - z^\nu}{(1 - \nu)(1 - z)(1 - z^\nu)}.$$

Letting $EX(\nu)$ denote the expected value as a function of ν and $EX_a(\nu) := \lim_{z \rightarrow a} EX(\nu)$ we find $EX_0(\nu) = \frac{1}{1 - \nu \mathbb{1}_{\nu < 0}}$, $EX_\infty(\nu) = \frac{\nu}{\nu - 1} \mathbb{1}_{\nu < 0}$, and

$$\max\{EX_0, EX_\infty\}(\nu) = \frac{\mathbb{1}_{\nu \geq -1} - \nu \mathbb{1}_{\nu < -1}}{1 - \nu \mathbb{1}_{\nu < 0}}.$$

Utilizing the monotonicity of EX in (2.8) we have $EX(-1) = \max\{EX_0, EX_\infty\}(-1) = 1/2$ and $EX(\nu) < \max\{EX_0, EX_\infty\}(\nu) \leq 1$ for all $\nu \in \mathbb{R} \setminus \{-1\}$; thus, $z > 0 \implies EX < 1$. Furthermore, when $z = 0$

$$EX = EX_0(\nu) \begin{cases} < 1, & \nu < 0 \\ = 1, & \nu \geq 0 \end{cases}$$

hence, $EX = 1 \iff \nu \in \mathbb{R}_0^+ \wedge z = 0$. The proof is now complete. \square

Many of the proofs that follow will utilize a probabilistic interpretation of $\tilde{g}_{n,\omega}$ to derive some of its most useful properties. The following proposition presents a representation of $\tilde{g}_{n,\omega}$ in terms of an expected value, which will prove to be immensely helpful.

Proposition 3 ($\tilde{g}_{n,\omega}$ expected value representation). *Let $C_{n,\omega}(\nu) = \nu^{-1}(\omega + \nu)^{(n+1)}$, $h_{n,\omega}(x, z) = (1 - x)^n(1 - (1 - z)x)^{-\omega}$, and $X \sim \mathcal{GH}(1, 1, 1 + \nu, z - 1)$. Then,*

$$\tilde{g}_{n,\omega}(z, \nu) = C_{n,\omega}(\nu) \mathbb{E}h_{n,\omega}(X, z).$$

Lemma 17 (Zeros of $\tilde{g}_{n,\omega}$). *For all permissible values of the parameters n , ω , z , and ν in Definition 9*

$$\tilde{g}_{n,\omega}(z, \nu) = 0 \iff (n - \omega - \nu \in \mathbb{N}_0 \wedge \nu \neq 0) \vee (n \in \mathbb{N} \wedge n > \omega \wedge \nu \in \mathbb{R}_0^+ \wedge z = 0).$$

Proof. We begin with the expression for $\tilde{g}_{n,\omega}$ in Proposition 3, namely,

$$\tilde{g}_{n,\omega}(z, \nu) = C_{n,\omega}(\nu) \mathbb{E}h_{n,\omega}(X, z),$$

where $C_{n,\omega}(\nu) = \nu^{-1}(\omega + \nu)^{(n+1)}$, $h_{n,\omega}(x, z) = (1 - x)^n(1 - (1 - z)x)^{-\omega}$ and $X \sim \mathcal{GH}(1, 1, \nu + 1, z - 1)$. If both terms are bounded then

$$\tilde{g}_{n,\omega}(z, \nu) = 0 \iff C_{n,\omega}(\nu) = 0 \vee \mathbb{E}h_{n,\omega}(X, z) = 0.$$

As such, our approach will be to show that $C_{n,\omega}$ and $Eh_{n,\omega}$ are bounded and then determine the location of their zeros. Combining the zeros of each term will subsequently give the zeros of $\tilde{g}_{n,\omega}$.

From Relation 5 we can easily show that $(\omega+\nu)^{(n+1)}$ is a polynomial in $(\omega+\nu)$ of degree no more than $n+1$. Therefore, the only point of concern for verifying that $C_{n,\omega}(\nu)$ is bounded is at $\nu = 0$. With the help of [27, Eq. 06.05.06.0026.01] we have as $\nu \rightarrow 0$

$$C_{n,\omega}(\nu) \sim (-1)^{n-\omega} \Gamma(\omega + \nu + 1)(n - \omega)!(1 + \mathcal{O}(\nu)),$$

which upon passing to the limit yields,

$$\lim_{\nu \rightarrow 0} C_{n,\omega}(\nu) = (-1)^{n-\omega} \omega!(n - \omega)!.$$

From this result it follows that $|C_{n,\omega}(\nu)| < \infty$ for all permissible values of the parameters n , ω , and ν . Now, the zeros of the factorial power term can be easily identified upon writing

$$(\omega + \nu)^{(n+1)} = \frac{\Gamma(\omega + \nu + 1)}{\Gamma(\omega + \nu - n)} = 0 \iff n - \omega - \nu \in \mathbb{N}_0.$$

Noting that $C_{n,\omega}(0) \neq 0$ then gives the result

$$C_{n,\omega}(\nu) = 0 \iff n - \omega - \nu \in \mathbb{N}_0 \wedge \nu \neq 0.$$

Next we turn our attention to the quantity $Eh_{n,\omega}(X, z)$. As a function of x , $h_{n,\omega}(x, z) = (1 - x)^n(1 - (1 - z)x)^{-\omega}$ is nonnegative on $x \in [0, 1]$ for all permissible parameters n , ω , and z . Since, $\text{supp}(X) = [0, 1]$ it follows that $0 \leq Eh_{n,\omega}(X, z)$. Additionally, note that

$$\partial_x h_{n,\omega}(x, z) = - \underbrace{\frac{(1 - x)^{n-1}}{(1 - (1 - z)x)^{\omega+1}}}_{\geq 0} \underbrace{((n - \omega)(1 - x) + (n - \omega)zx + \omega z)}_{\geq 0} \leq 0.$$

By continuity of $h_{n,\omega}$ we have $h_{n,\omega}(x, z) \leq h_{n,\omega}(0, z) = 1 \implies Eh_{n,\omega}(X, z) \leq Eh_{n,\omega}(0, z) = 1$ with the last inequality again being a consequence of $\text{supp}(X) = [0, 1]$. Bringing both results together we have shown for all permissible parameters that $0 \leq Eh_{n,\omega}(X, z) \leq 1$. With boundedness established we turn to locating the zeros of $Eh_{n,\omega}(X, z)$. Observe that both $h_{n,\omega}(x, z)$ and the support of X are both nonnegative; thus, the only way for $Eh_{n,\omega}(X, z) = 0$ is if $X \sim \delta_{x_0}$ where $h_{n,\omega}(x_0, z) = 0$ and δ_μ is the degenerate density function centered at μ . Combing the facts $0 \leq h_{n,\omega}(x, z)$ and $0 \geq \partial_x h_{n,\omega}(x, z)$ shows that all zeros of $h_{n,\omega}$ must reside at $x = 1$. Upon further inspection we determine

$$h_{n,\omega}(1, z) = 0 \iff n \in \mathbb{N} \wedge (z > 0 \vee (z = 0 \wedge n > \omega)). \quad (2.9)$$

Next, we need to determine the parameters for which $X \sim \delta_1$. Since $\text{supp}(X) = [0, 1]$ this is equivalent to finding the parameters for which $EX = 1$, which are

given by Lemma 16. Combining the conditions given in Lemma 16 with (2.9) subsequently shows

$$\text{E}h_{n,\omega}(X, z) = 0 \iff n \in \mathbb{N} \wedge n > \omega \wedge \nu \in \mathbb{R}_0^+ \wedge z = 0.$$

Combining these zeros with those of $C_{n,\omega}$ then yields the desired result. \square

The next two results establish properties about the expected value $\text{E}h_{n,\omega}(X, z)$. In particular, Lemma 19 establishes the conditions under which this expected value is a monotone function of the parameter z . This will then be used in Theorem 8 to establish analogous conditions for when $|\tilde{g}_{n,\omega}|$ is monotone in z .

Lemma 18. *For fixed z and ν , $\text{E}h_{n,\omega}(X, z)$ is decreasing in n , increasing in ω if $z \in [0, 1]$, and decreasing in ω if $z \in [1, \infty)$. Furthermore, $\text{E}h_{n+t,\omega+t}(X, z)$ is decreasing in t .*

Proof. Recall from Lemma 17 that $h_{n,\omega}(x, z)$ is nonnegative for all permissible values of z , ν , n , and ω on $\text{supp}(X) = [0, 1]$. Furthermore, the following results hold everywhere on $\text{supp}(X)$: $\partial_t h_{t,\omega} \leq 0$, $\partial_t h_{n,t} \geq 0$ if $z \in [0, 1]$, $\partial_t h_{n,t} \leq 0$ if $z \in [1, \infty)$, and $\partial_t h_{n+t,\omega+t} \leq 0$. Since, $h_{n,\omega}$ and $\text{supp}(X)$ are nonnegative, the sign of these derivatives will be equal to the sign of their corresponding expected values. The proof is now complete. \square

Lemma 19. *Let \mathcal{N} be given by Definition 9. Then, $\nu > 1 \implies \text{E}h_{n,\omega}(X, z)$ is strictly increasing in z on $z \in \mathbb{R}^+$ for all $(n, \omega) \in \mathcal{N} \setminus \{(0, 0)\}$.*

Proof. We begin with the explicit form

$$\text{E}h_{n,\omega}(X, z) = n! \frac{\mathbf{F}(1, \omega + \nu + 1; n + 2; 1 - z)}{\mathbf{F}(1, \nu + 1; 2; 1 - z)}. \quad (2.10)$$

According to Lemma 17, $z \in \mathbb{R}^+ \implies 0 < \text{E}h_{n,\omega}(X, z)$ for all n , ω , and ν permissible by Definition 9. As such, we will proceed to establish $\text{E}h_{n,\omega}(X, z)$ is strictly increasing in z by showing it has a strictly positive logarithmic derivative. Using Definition 10 and Relation 1 gives

$$\partial_z \log \text{E}h_{n,\omega}(X, z) = r_{0,0}(z, \nu) - r_{n,\omega}(z, \nu),$$

where

$$r_{n,\omega}(z, \nu) = \gamma \frac{\mathbf{F}(2, \gamma + 1; \beta + 2; 1 - z)}{\mathbf{F}(1, \gamma; \beta + 1; 1 - z)} = \frac{\gamma}{z} \text{E}W,$$

$\beta = n + 1$, $\gamma = \omega + \nu + 1$, $W = zX(1 - (1 - z)X)^{-1}$, and $X \sim \mathcal{GH}(1, \beta, \gamma, z - 1)$. Consequently, $\partial_z \log \text{E}h_{n,\omega}(X, z)$ is strictly positive for all $(n, \omega) \in \mathcal{N} \setminus \{(0, 0)\}$ if $r_{n,\omega} < r_{0,0}$. We will prove this by successively maximizing $r_{n,\omega}$ in n and ω , respectively.

$$(1) \quad r_{n,\omega}(z, \nu) \leq r_{\omega,\omega}(z, \nu) \quad \forall (n, \omega) \in \mathcal{N}.$$

Proof. The random variable W is a monotone increasing transformation of X for all $z > 0$; thus,

$$F_W(w) = \mathbb{P}(X \leq (z(w^{-1} - 1) + 1)^{-1}).$$

After a bit of work we find

$$F_W(w) = 1 - \frac{B_{(1-z)(1-w)}(\beta, \gamma - \beta)}{B_{1-z}(\beta, \gamma - \beta)},$$

where $B_s(\alpha, \beta)$ is the incomplete beta function of definition 32 and $\text{supp}(W) = [0, 1]$. Evaluating $\partial_w F_W$ then provides the density

$$f_W(w) = \frac{(1-w)^{\beta-1}(1-(1-z)(1-w))^{\gamma-\beta-1}}{(1-z)^{-\beta} B_{1-z}(\beta, \gamma - \beta)} \mathbf{1}_{w \in [0, 1]}.$$

Consider the family of density functions $f_\beta = \{f_W(w|\beta) : \beta \geq 1\}$ and let $\delta > 0$. We have for the likelihood ratio

$$L(w) := \frac{f_{\beta+\delta}}{f_\beta}(w) = C \left(\frac{1-w}{1-(1-z)(1-w)} \right)^\delta,$$

where C is a positive constant. Differentiating L yields

$$\partial_w L(w) = -\delta C \frac{(1-w)^{\delta-1}}{(1-(1-z)(1-w))^{\delta+1}}.$$

Observe that $\text{sign}(\partial_w L(w)) = -1$ on the interior of $\text{supp}(W)$. Consequently, the family of density functions f_β admits a monotone likelihood ratio and

$$\text{sign}(\partial_\beta \mathbb{E}W) = \text{sign}(\partial_x L(x)) = -1.$$

But now recall that $\beta = n + 1$ which shows that $\partial_n \mathbb{E}W < 0$; hence,

$$\frac{\gamma}{z} \mathbb{E}W \leq \frac{\gamma}{z} \mathbb{E}W|_{n=\omega} \implies r_{n,\omega}(z, \nu) \leq r_{\omega,\omega}(z, \nu).$$

■

$$(2) \quad \nu > 1 \implies r_{\omega,\omega}(z, \nu) < r_{0,0}(z, \nu) \quad \forall \omega > 0$$

Proof. We will establish this claim by showing that $r_{\omega,\omega}(z, \nu)$ is strictly decreasing in ω . To aid in the following calculations we introduce the operators

$$\begin{aligned} \mathcal{A}_1^k F(a_1, a_2; a_3; s) &= F(a_1 + k, a_2; a_3; s), \\ \mathcal{A}_2^k F(a_1, a_2; a_3; s) &= F(a_1, a_2 + k; a_3; s), \\ \mathcal{A}_3^k F(a_1, a_2; a_3; s) &= F(a_1, a_2; a_3 + k; s), \end{aligned}$$

for which $\mathcal{A}_i^0 = \mathcal{I}$ is the identity. In terms of these operators we have

$$r_{\omega,\omega}(z, \nu) = \frac{\frac{\omega+\nu+1}{\omega+2} \mathcal{A}_1 \mathcal{A}_2 \mathcal{A}_3 F(1, \omega + \nu + 1; \omega + 2; 1 - z)}{F(1, \omega + \nu + 1; \omega + 2; 1 - z)}.$$

Now combining the identities [14, Eqs. 10, 13]

$$\begin{aligned} \mathcal{A}_1 &= \mathcal{I} + \frac{a_2}{a_3} s \mathcal{A}_1 \mathcal{A}_2 \mathcal{A}_3, \\ \mathcal{A}_1^{-1} &= \frac{a_1(s-1)}{a_1 - a_3} \mathcal{A}_1 + \frac{2a_1 + (a_2 - a_1)s - a_3}{a_1 - a_3} \mathcal{I}, \end{aligned}$$

we deduce for $a_1 = 1$, $a_2 = \omega + \nu + 1$, $a_3 = \omega + 2$, and $s = 1 - z$

$$\frac{\omega + \nu + 1}{\omega + 2} \mathcal{A}_1 \mathcal{A}_2 \mathcal{A}_3 = \frac{1}{1 - z} \left(\frac{\omega + 1}{z} \mathcal{A}_1^{-1} + \frac{1}{z} ((\omega + \nu)(1 - z) - \omega) \mathcal{I} \right),$$

which permits us to write

$$\begin{aligned} r_{\omega,\omega}(z, \nu) &= \frac{1}{1 - z} \left(\frac{\omega + 1}{z F(1, \omega + \nu + 1; \omega + 2; 1 - z)} \right. \\ &\quad \left. + \frac{1}{z} ((\omega + \nu)(1 - z) - \omega) \right). \end{aligned} \quad (2.11)$$

Now using Relation 6 we obtain the form

$$F(1, \omega + \nu + 1; \omega + 2; 1 - z) = (\omega + 1)(1 - z)^{-(\omega+1)} z^{-\nu} B_{1-z}(\omega + 1, \nu).$$

Substituting this expression into (2.11) and applying the differential formula [27, Eq. 06.19.20.0003.01]

$$\partial_\alpha B_s(\alpha, \beta) = B_s(\alpha, \beta) \log s - \frac{s^\alpha}{\alpha^2} {}_3F_2(1 - \beta, \alpha, \alpha; \alpha + 1, \alpha + 1; s)$$

gives

$$\partial_\omega r_{\omega,\omega}(z, \nu) = \frac{1}{1 - z} \left(\frac{{}_3F_2(1 - \nu, \omega + 1, \omega + 1; \omega + 2, \omega + 2; 1 - z)}{z^{\nu+1} F(1, \omega + \nu + 1; \omega + 2; 1 - z)^2} - 1 \right). \quad (2.12)$$

But in accordance with the integral representation [7, Eq. 16.5.2]

$${}_3F_2 \left(\begin{matrix} a_0, a_1, a_2 \\ b_0, b_1 \end{matrix}; z \right) = \int_0^1 \frac{t^{a_0-1} (1-t)^{b_0-a_0-1}}{B(a_0, b_0 - a_0)} F \left(\begin{matrix} a_1, a_2 \\ b_1 \end{matrix}; zt \right) dt,$$

which holds for $\Re b_0 > \Re a_0 > 0$, the result in (2.12) equivalent to the expected value

$$\partial_\omega r_{\omega,\omega}(z, \nu) = E \mathcal{H}_\omega(X, z, \nu), \quad (2.13)$$

where

$$\mathcal{H}_\omega(x, z, \nu) = \left(\frac{h_\omega(x, z, \nu)/h_\omega(1, z, \nu) - 1}{1 - z} \right),$$

$$h_\omega(x, z, \nu) = (1 - (1 - z)x)F(1, \omega + \nu + 1; \omega + 2; (1 - z)x),$$

and $X \sim \mathcal{GH}(\omega + 1, 1, 1 - \nu, z - 1)$. To establish the conditions for when (2.13) is negative we use [7, Eq. 15.5.7] to write

$$\partial_x \mathcal{H}_\omega(x, z, \nu) = (\nu - 1) \frac{\mathbf{F}(2, \omega + \nu + 1; \omega + 3; (1 - z)x)}{z \mathbf{F}(1, \omega + \nu + 1; \omega + 2; 1 - z)}.$$

For $z > 0$, the ratio of hypergeometric terms is positive resulting in $\text{sign}(\partial_x \mathcal{H}_\omega(x, z, \nu)) = \text{sign}(\nu - 1)$. Therefore, if $\nu > 1$ then $\mathcal{H}_\omega(x, z, \nu) < \mathcal{H}_\omega(1, z, \nu) = 0$ on the interior of $\text{supp}(X) = [0, 1]$. Furthermore, by an argument very similar to that of Lemma 16, we can show that $z > 0 \implies \mathbb{E}X < 1$; thus, guaranteeing the density of X is not degenerate at $x = 1$. Combining these facts leads to the conclusion that $\partial_\omega r_{\omega, \omega}(z, \nu) < 0$ and so⁴

$$\nu > 1 \implies r_{\omega, \omega}(z, \nu) < r_{0, 0}(z, \nu) \quad \forall \omega > 0,$$

which is the desired result. ■

Combining claims (1) and (2) we have shown $\nu > 1 \implies r_{n, \omega}(z, \nu) < r_{0, 0}(z, \nu)$ for all $(n, \omega) \in \mathcal{N} \setminus \{(0, 0)\}$ which completes the proof. □

We are finally able to now establish the conditions for which $|\tilde{g}_{n, \omega}|$ is a monotone function of z . This result will serve as the foundation for establishing exact confidence intervals of ACV \mathcal{T}_ν .

Theorem 8 (Monotony of $|\tilde{g}_{n, \omega}|$ in z). *If $\nu > 1$ then*

- (i) $|\tilde{g}_{n, \omega}(z, \nu)|$ *is increasing in z for all $(n, \omega) \in \mathcal{N}$,*
- (ii) $\exists (n, \omega) \in \mathcal{N}$ *such that $|\tilde{g}_{n, \omega}(z, \nu)|$ is strictly increasing in z .*

If instead $\nu < -1$ replace increasing with decreasing.

Proof. First consider the special case $(n, \omega) = (0, 0) \implies |\tilde{g}_{n, \omega}(z, \nu)| = 1$ which is trivially increasing. Next assume $\nu > 1$ and consider the general case $(n, \omega) \in \mathcal{N} \setminus \{(0, 0)\}$. Using the notation of Lemma 17 we write

$$\partial_z |\tilde{g}_{n, \omega}(z, \nu)| = |C_{n, \omega}(\nu)| \partial_z \mathbb{E} h_{n, \omega}(X, z). \quad (2.14)$$

From Lemma 19 we know $\nu > 1 \implies \partial_z \mathbb{E} h_{n, \omega}(X, z) > 0$ and since $|C_{n, \omega}(\nu)| \geq 0$ we can conclude that $\partial_z |\tilde{g}_{n, \omega}(z, \nu)| \geq 0$ for all $(n, \omega) \in \mathcal{N} \setminus \{(0, 0)\}$; thus, criteria (i) is satisfied. To satisfy criteria (ii) all we need to show is that there is some (n, ω) for which $C_{n, \omega}(\nu) \neq 0$. To accomplish this, consider the image of $f(n, \omega) = n - \omega - \nu$ under $\mathcal{N} \setminus \{(0, 0)\}$:

$$f[\mathcal{N} \setminus \{(0, 0)\}] = \{-\nu, 1 - \nu, 2 - \nu, \dots\}.$$

⁴If the density of X was degenerate at the point $x = 1$ then we would have $\mathbb{E} \mathcal{H}_\omega(X, z, \nu) = \int \mathcal{H}_\omega(x, z, \nu) \delta(x - 1) dx = \mathcal{H}_\omega(1, z, \nu) = 0$.

Since $\nu > 1$ it follows that $f[\mathcal{N} \setminus \{(0, 0)\}]$ always contains at least one element not in \mathbb{N}_0 which according to Lemma 17 implies that $C_{n,\omega}(\nu) \neq 0$. Hence, $\nu > 1 \implies \exists(n, \omega) \in \mathcal{N} \setminus \{(0, 0)\} : C_{n,\omega}(\nu) \neq 0$ and the proof for $\nu > 1$ is complete.

To obtain the proof for $\nu < -1$ observe that if $|\tilde{g}_{n,\omega}(z, \nu)|$ is increasing (strictly increasing) in z then $|\tilde{g}_{n,\omega}(1/z, \nu)|$ must be decreasing (strictly decreasing) in z . With this observation assume $\nu > 1$ and use the reflection formula in Lemma 14 to write

$$|\tilde{g}_{n,\omega}(1/z, \nu)| = |\tilde{g}_{n,\omega'}(z, -\nu)|, \quad (2.15)$$

where $\omega' = n - \omega$. Since the l.h.s. side of (2.15) is decreasing in z and $(n, \omega) \in \mathcal{N} \implies (n, \omega') \in \mathcal{N}$ the proof for $\nu < -1$ immediately follows. \square

2.4.2 Variance

We are now at last ready to begin deriving expressions for the variance. To accomplish this task we will derive the second moment for the integer-valued estimator \mathcal{T}_n and then rely on the uniqueness of the fractional finite sum to obtain the desired result for real-valued ν .

Lemma 20. For $n \in \mathbb{N}_0 : 0 \leq 2n < \alpha_1$,

$$\mathbb{E} \mathcal{T}_n^2 = \frac{1}{\kappa_1^2} \sum_{k,\ell=0}^{n-1} F\left(\begin{matrix} k+1, \ell+1 \\ \alpha_1 \end{matrix}; 1\right) F\left(\begin{matrix} -k, -\ell \\ \alpha_2 \end{matrix}; 1\right) \zeta^{k+\ell}.$$

Proof. We begin by squaring \mathcal{T}_n to find

$$\mathcal{T}_n^2 = \sum_{k,\ell=0}^{n-1} \frac{(\alpha_1 Y_1)^{-k-\ell-2} (\alpha_2 Y_2)^{k+\ell}}{(\alpha_1)_{-k-1} (\alpha_1)_{-\ell-1} (\alpha_2)_k (\alpha_2)_\ell}.$$

Now using the result of Lemma 2 we evaluate the expected value term-wise yielding

$$\mathbb{E} \mathcal{T}_n^2 = \frac{1}{\kappa_1^2} \sum_{k,\ell=0}^{n-1} \frac{\Gamma(\alpha_1) \Gamma(\alpha_1 - k - \ell - 2) \Gamma(\alpha_2) \Gamma(\alpha_2 + k + \ell)}{\Gamma(\alpha_1 - k - 1) \Gamma(\alpha_1 - \ell - 1) \Gamma(\alpha_2 + k) \Gamma(\alpha_2 + \ell)} \zeta^{k+\ell},$$

which requires $2n < \alpha_1$ to guarantee each term is finite. Relation 12 provides the necessary result to write the summand as the product of hypergeometric functions of unity argument; hence, the desired result is obtained. \square

As will be seen in Theorem 9, the second moment of the generalized estimator \mathcal{T}_ν is rather complicated. To determine the convergence criteria for $\mathbb{E} \mathcal{T}_\nu^2$ we will derive an integral representation $\mathbb{E} \mathcal{T}_\nu^2 = \int_{\mathcal{S}} f \, dA$ on the unit square $\mathcal{S} = [0, 1]^2$ and bound the integrand f with a simpler function, Υ , that still captures essential characteristics of f such as its behavior near singular points. Since these singular points ultimately dictate the convergence of the integral representation of $\mathbb{E} \mathcal{T}_\nu^2$, studying the convergence of $\int_{\mathcal{S}} \Upsilon \, dA$ will subsequently

reveal the parameters which which $\mathbb{E} \mathcal{T}_\nu^2 < \infty$. However, even the integral of Υ is complicated and in most cases cannot be evaluated in closed-form. As such, Lemmas 21 and 22 study the convergence properties of various double integrals that will be used to aid in determining the convergence of $\int_{\mathcal{S}} \Upsilon \, dA$.

Relation 2 (Integral representation of harmonic numbers).

$$H_z = \int_0^1 \frac{1-t^{z-1}}{1-t} \, dt, \quad \Re z > -1.$$

Lemma 21. Let $n \in \mathbb{N}_0$, $f(x, y) = 1 - (1-x)(1-y)$, and

$$I_n = \int_0^1 \int_0^1 f^{s-2}(x, y) (\log \circ f)^n(x, y) \, dx dy.$$

Then, I_n converges for all $s > 0$.

Proof. We will first evaluate I_0 . Noting that $|I_n| = (-1)^n I_n$ we perform the change of variables $(t, v) = ((1-x)(1-y), x)$ and integrate over v yielding

$$|I_n| = \int_0^1 (-1)^n \log^n(1-t) (-\log t) (1-t)^{s-2} \, dt.$$

Substituting $n = 0$, we again change variables via $x = 1-t$ and then integrate by parts with $u = -\log(1-x)$ and $dv = x^{s-2} \, dx$ to find

$$I_0 = \frac{1}{s-1} \int_0^1 \frac{1-x^{s-1}}{1-x} \, dx + \log(1-x) \frac{1-x^{s-1}}{s-1} \Big|_{x=0}^1.$$

If $s > 0$ the limit term vanishes and upon inspection of the integral representation for the harmonic numbers in Relation 2

$$I_0 = \frac{H_{s-1}}{s-1}.$$

Now consider the general case I_n . Without loss of generality assume $n \geq 1$ and perform integration by parts with $u = (-1)^n \log^n(1-t)$ and $dv = -\log t (1-t)^{s-2} \, dt$. Expanding the logarithm in dv as a power series in $(1-t)$ and integrating termwise we find

$$v = - \sum_{k=0}^{\infty} \frac{(1-t)^{s+k}}{(s+k)(1+k)}.$$

In this form, it becomes clear that the limit term $uv|_{t=0}^1$ vanishes if $n \geq 1$ so that $|I_n| = \int_0^1 (-v) \, du$. Furthermore, we observe for $s > 0$:

$$-v = \frac{1}{s} (1-t)^{s-1} \sum_{k=0}^{\infty} \frac{s(1-t)^{k+1}}{(s+k)(1+k)} \leq \frac{1}{s} (-\log t) (1-t)^{s-1}.$$

Hence,

$$|I_n| \leq \frac{n}{s} \int_0^1 (-1)^{n-1} \log^{n-1}(1-t)(-\log t)(1-t)^{s-2} du = \frac{n}{s} |I_{n-1}|.$$

Solving the recurrence relation and calling on the result for I_0 we find for $s > 0$:

$$|I_n| \leq \frac{n!}{s^n} \frac{H_{s-1}}{s-1} < \infty,$$

which completes the proof. \square

Lemma 22. Let $z \in \mathbb{R}^+$, $m, n \in \mathbb{N}_0$, $a, b \in (-\infty, 2]$,

$$f(x, y, z) = 1 - \frac{(1-x)(1-y)}{(1-(1-z)x)(1-(1-z)y)},$$

$$F(x, y, z, l, s) = (\log \circ f)^l(x, y, z) f^{s-2}(x, y, z),$$

and

$$I = \int_0^1 \int_0^1 F(x, y, z, n, a) F(x, y, 1, m, b) dx dy.$$

Then I converges when $a + b > 2$ ⁵.

Proof. For convenience we will introduce the auxillary function

$$J(x, y, z) = \frac{z^2}{(z + (1-z)x)^2 (z + (1-z)y)^2}$$

as well as the following properties:

- (FI) For $l \in \mathbb{N}_0$, $z \in \mathbb{R}^+$, and $(x, y) \in [0, 1]^2$: $|F| = (-1)^l F$.
- (FII) $f(\cdot, z)$ is increasing on $z \in \mathbb{R}^+$ from $f(\cdot, 0) = 0$ to $f(\cdot, \infty) = 1$.
- (J) For all $z \in \mathbb{R}^+$ and $(x, y) \in [0, 1]^2$: $0 \leq J(x, y, z) \leq z^{2 \operatorname{sign}(z-1)}$.

Upon inspection of property (FI) we see that $|I| = (-1)^{m+n}$ and so

$$|I| = \int_0^1 \int_0^1 |F(x, y, z, n, a)| |F(x, y, 1, m, b)| dx dy.$$

Furthermore, since $n \in \mathbb{N}_0$ and $a \leq 2$ we are able to deduce from property (FII) that $|F(x, y, z, n, a)|$ is nonnegative and a decreasing function of z for all $z \in \mathbb{R}^+$. Denoting $z^* = \min\{1, z\}$, it follows for all $z \in \mathbb{R}^+$

$$|I| \leq \int_0^1 \int_0^1 |F(x, y, z^*, m+n, a+b-2)| dx dy.$$

⁵One can easily extend this result to other values of a and b using similar methods to those used here and noting that for $s \geq 2$, $0 \leq f^{s-2}(z, y, x) \leq 1$.

Performing the change of variables $(1-u, 1-v) = ((1-x)/(1-(1-z^*)x), (1-y), (1-(1-z^*)y))$ and then using property (J) subsequently gives

$$|I| \leq \max\{1, z^{-2}\} \int_0^1 \int_0^1 |F(u, v, 1, m+n, a+b-2)| \, du dv,$$

which according to Lemma 21 converges if $a+b > 2$. The proof is now complete. \square

Now that we have the preliminary results needed to study the integral of Υ we derive one last result that will be used to construct Υ . The following lemma describes a function $v(\alpha, \beta, x)$ that bounds a particular case of the hypergeometric function $F(\alpha, \alpha; \beta; x)$ on the interval $x \in [0, 1]$. Comparing v with the asymptotic properties of the hypergeometric function in [7, §15.4(ii)] will reveal that it not only bounds our special case of the hypergeometric function but also has the critical property

$$F(\alpha, \alpha; \beta; x) \sim v(\alpha, \beta, x), \quad \text{as } x \searrow 1.$$

Lemma 23. *For $\alpha \in \mathbb{R}$, $\beta \in \mathbb{R}^+$, and $x \in [0, 1]$:*

$$F(\alpha, \alpha; \beta; x) \leq v(\alpha, \beta, x),$$

where

$$v(\alpha, \beta, x) = \begin{cases} \frac{\Gamma(\beta)\Gamma(\beta-2\alpha)}{\Gamma(\beta-\alpha)\Gamma(\beta-\alpha)}, & \beta > 2\alpha \\ 1 - \frac{\Gamma(2\alpha)}{\Gamma(\alpha)\Gamma(\alpha)} \log(1-x), & \beta = 2\alpha \\ \frac{\Gamma(\beta)\Gamma(2\alpha-\beta)}{\Gamma(\alpha)\Gamma(\alpha)} (1-x)^{\beta-2\alpha}, & \beta < 2\alpha. \end{cases}$$

Proof. Begin by noting that $\partial_x F(\alpha, \alpha; \beta; x) = (\alpha^2/\beta)F(\alpha+1, \alpha+1; \beta+1; x)$, which can be represented as an absolutely convergent power series in x on $[0, 1]$. Since this power series representation also has nonnegative coefficients it follows that $F(\alpha, \alpha; \beta; x)$ must be an increasing function of x on this interval. Hence, $F(\alpha, \alpha; \beta; x) \leq F(\alpha, \alpha; \beta; 1)$ which upon inspection of Relation 12 yields the desired result for the case $\beta > 2\alpha$. The $\beta = 2\alpha$ case is given in [2, Lem. 2.3]. For $\beta < 2\alpha$ we apply the transformation [7, Eq. 15.8.1(iii)] yielding $F(\alpha, \alpha; \beta; x) = (1-x)^{\beta-2\alpha} F(\beta-\alpha, \beta-\alpha; \beta; x) \leq (1-x)^{\beta-2\alpha} F(\beta-\alpha, \beta-\alpha; \beta; 1)$. The proof is now complete. \square

After much effort we may finally derive the second moment of the generalized estimator \mathcal{T}_ν .

Theorem 9 (The second moment of \mathcal{T}_ν). *Let $\zeta \in \mathbb{R}_0^+$, $(\alpha_1, \alpha_2) \in \mathbb{R}^+ \times \mathbb{R}^+$: $\alpha_1 + \alpha_2 > 2$, and $\nu \in \mathbb{R} : -\alpha_2 < 2\nu < \alpha_1$. Then, $\mathbb{E}\mathcal{T}_\nu^2 < \infty$ where*

$$\mathbb{E}\mathcal{T}_\nu^2 = \frac{1}{\kappa_1^2} \sum_{k=0}^{\infty} \sum_{\ell=0}^k \frac{g_{k,\ell}^2(\zeta, \nu)}{(\alpha_1)_\ell (\alpha_2)_{k-\ell} \ell! (k-\ell)!},$$

and $g_{n,\omega}$ is given by Theorem 7 (ii). Additionally,

$$\begin{aligned} \mathbb{E}\mathcal{T}_\nu^2 &= \frac{\nu^2 \zeta^{2\nu}}{\kappa_1^2} \int_0^1 \int_0^1 F\left(\begin{matrix} 1+\nu, 1+\nu \\ \alpha_1 \end{matrix}; \frac{(1-x)(1-y)}{(1-(1-\zeta)x)(1-(1-\zeta)y)}\right) \\ &\quad F\left(\begin{matrix} 1-\nu, 1-\nu \\ \alpha_2 \end{matrix}; (1-x)(1-y)\right) ((1-(1-\zeta)x)(1-(1-\zeta)y))^{-\nu-1} dx dy. \end{aligned}$$

Proof. We begin with the expression for $\mathbb{E}\mathcal{T}_n^2$ derived in Lemma 20 which is finite for $n \in \mathbb{N}_0 : 0 \leq 2n < \alpha_1$. According to [7, §16.2(iii)], $F(k+1, \ell+1; \alpha_1; 1)$ can be expressed as an absolutely convergent series so long as $k + \ell + 2 < \alpha_1$ which is covered by the already imposed restriction on α_1 . Furthermore, $F(-k, -\ell; \alpha_2; 1)$ is degenerate and truncates after $m = \min\{k, \ell\} + 1$ terms due to the presence of nonpositive integers $-k$ and $-\ell$ in the top two arguments. Consequently, the product⁶

$$\begin{aligned} F\left(\begin{matrix} k+1, \ell+1 \\ \alpha_1 \end{matrix}; 1\right) F\left(\begin{matrix} -k, -\ell \\ \alpha_2 \end{matrix}; 1\right) \\ = \sum_{r=0}^{\infty} \sum_{s=0}^r \frac{(k+1)_s (\ell+1)_s (-k)_{r-s} (-\ell)_{r-s}}{(\alpha_1)_s (\alpha_2)_{r-s} s! (r-s)!} \end{aligned}$$

is absolutely convergent and thus permits rearrangement of its terms [23, Ch. 13]. Substituting the derived product series into the expression for $\mathbb{E}\mathcal{T}_n^2$ and rearranging the order of summation produces

$$\mathbb{E}\mathcal{T}_n^2 = \frac{1}{\kappa_1^2} \sum_{r=0}^{\infty} \sum_{s=0}^r \frac{f^2(n)}{(\alpha_1)_s (\alpha_2)_{r-s} s! (r-s)!}, \quad (2.16)$$

with $f(n) = \sum_{k=0}^{n-1} (k+1)_s (-k)_{r-s} \zeta^k$. Focusing on the Pochhammer terms in the summand of $f(n)$ we use Relations 8–9 to write

$$(k+1)_s (-k)_{r-s} = (-1)^{r-s} (k+1)_s (k+1-(r-s))_{r-s} = (-1)^s (-k-s)_r,$$

which upon expanding with Definition 23 and substituting into $f(n)$ gives

$$f(n) = (-1)^{r+s} \sum_{\ell=0}^r \mathcal{S}_r^{(\ell)} \sum_{k=0}^{n-1} (k+s)^\ell \zeta^k.$$

Identifying the interior sum over k as the incomplete Lerch Transcendent we have by Theorem 7 the unique generalization of $f(n)$ being given by $f_G(\nu) = (-1)^{r+s} g_{r,s}(\zeta, \nu)$. Substituting $f(n) \mapsto f_G(\nu)$ in (2.16) then gives the desired expression for the series expansion of $\mathbb{E}\mathcal{T}_\nu^2$.

⁶For the purpose of taking the product we can formally express the degenerate hypergeometric term as the infinite series $\sum_{s=0}^{\infty} \frac{(-k)_s (-\ell)_s}{(\alpha_2)_s s!} = \sum_{s=0}^{\min\{k, \ell\}} \frac{(-k)_s (-\ell)_s}{(\alpha_2)_s s!} + 0 + 0 + \dots$

Now, to obtain the integral representation we begin by writing $\mathbb{E}\mathcal{T}_\nu^2$ in the form

$$\mathbb{E}\mathcal{T}_\nu^2 = (\mathbb{E}\mathcal{T}_\nu)^2 \sum_{k=0}^{\infty} \sum_{\ell=0}^k \frac{\tilde{g}_{k,\ell}^2(\zeta, \nu)}{(\alpha_1)_\ell (\alpha_2)_{k-\ell} \ell! (k-\ell)!}.$$

Upon inspection of Proposition 3 we see that $\tilde{g}_{k,\ell}$ can be recast in terms of an expected value to produce

$$\mathbb{E}\mathcal{T}_\nu^2 = \left(\frac{\nu \zeta^\nu}{\kappa_1} \right)^2 \lim_{n \rightarrow \infty} \int_0^1 \int_0^1 f_n(x, y) \, dx dy,$$

where

$$f_n(x, y) = \sum_{k=0}^n \sum_{\ell=0}^k \frac{(\nu^{-1}(\ell + \nu)^{(k+1)})^2}{(\alpha_1)_\ell (\alpha_2)_{k-\ell} \ell! (k-\ell)!} \frac{((1-x)(1-y))^k}{((1-(1-\zeta)x)(1-(1-\zeta)y))^{\ell+1+\nu}}.$$

To interchange limits we must find an integrable function Υ that dominates the sequence $|f_n|$ on $(x, y) \in [0, 1]^2$. With this goal in mind let's first find an expression for $f = \lim_{n \rightarrow \infty} f_n$. Using properties of the Pochhammer symbol we may write $\nu^{-1}(\ell + \nu)^{(k+1)} = (-1)^k (1-\nu)_k (1+\nu)_\ell / (\nu-k)_\ell$ and $[(\alpha_2)_{k-\ell} (k-\ell)!]^{-1} = (-k)_\ell (1-\alpha_2-k)_\ell / (k! (\alpha_2)_k)$, which upon substituting into f_n , taking the limit $n \rightarrow \infty$, and utilizing Lemma 24 gives

$$f(x, y) = t^{-1-\nu} F\left(\begin{matrix} 1+\nu, 1+\nu \\ \alpha_1 \end{matrix}; \frac{s}{t}\right) F\left(\begin{matrix} 1-\nu, 1-\nu \\ \alpha_2 \end{matrix}; s\right),$$

where $s = (1-x)(1-y)$ and $t = (1-(1-\zeta)x)(1-(1-\zeta)y)$. Now upon closer inspection of f_n we see that it is the sum of nonnegative terms; hence, $0 \leq f_n < f$ showing that f dominates f_n . Given this observation we could choose $\Upsilon = f$, however, the complexity of f hinders demonstrating its integrability. As such, we seek a simpler function for Υ that bounds f from above.

Looking back at our expression for f we can see that it is the product of three nonnegative components and so we will build Υ by successively bounding each component from above. To bound $t^{-1-\nu}$ we decompose the set $(\zeta, \nu) \in \mathbb{R}^+ \times \mathbb{R}$ into the four regions: $(0, 1] \times (-\infty, -1]$, $(0, 1] \times [-1, \infty)$, $[1, \infty) \times (-\infty, -1]$, and $[1, \infty) \times [-1, \infty)$. Combining upper and lower bounds of each case gives

$$\min\{1, \zeta^{-2-2\nu}\} \leq t^{-1-\nu} \leq \max\{1, \zeta^{-2-2\nu}\}.$$

Furthermore, observe that $0 \leq s \leq 1$ and $0 \leq s/t \leq 1$ everywhere on $(x, y) \in [0, 1]^2$ so that we may call on Lemma 23 to bound each hypergeometric term in f . This leads us to propose

$$\Upsilon(x, y) = \max\{1, \zeta^{-2-2\nu}\} v(1+\nu, \alpha_1, s/t) v(1-\nu, \alpha_2, s),$$

with $v(\alpha, \beta, x)$ given by Lemma 23. The function $v(\alpha, \beta, x)$ is piecewise with three possible cases depending on the value of $\text{sign}(\beta - 2\alpha)$. Therefore, we must determine the integrability of Υ for nine different cases which we categorize

into four regions of the set $(\alpha_1, \alpha_2, \nu) \in \mathbb{R}^+ \times \mathbb{R}^+ \times \mathbb{R}$. Table 2.2 presents the four regions which are roughly ordered according to the severity of singularities present in Υ (IV most severe). Included in the table is the domain of each region, number of cases contained in each region, and any additional constraints determined from Lemma 22 (use $a = \alpha_1 + 2\nu$ and $b = \alpha_2 - 2\nu$ in lemma) such that Υ remains integrable. Working with the domains and additional constraints we determine that each of the four regions implicitly requires $\alpha_1 + \alpha_2 > 2$. As such, we may combine the domains and constraints of each region to deduce

$$\alpha_1 + \alpha_2 > 2 \wedge -\alpha_2 < 2\nu < \alpha_1 \implies \int_0^1 \int_0^1 \Upsilon(x, y) dx dy < \infty.$$

Hence if the parameters satisfy these constraints, Υ is integrable and $\mathbb{E}\mathcal{T}_\nu^2 = \iint f(x, y) dx dy < \infty$. The proof is now complete. \square

Region	Domain	# Cases	Constraint(s)
(I)	$\alpha_1 - 2\nu \geq 2 \wedge \alpha_2 + 2\nu \geq 2$	4	—
(II)	$\alpha_1 - 2\nu < 2 \wedge \alpha_2 + 2\nu \geq 2$	2	$0 < \alpha_1 - 2\nu$
(III)	$\alpha_1 - 2\nu \geq 2 \wedge \alpha_2 + 2\nu < 2$	2	$0 < \alpha_2 + 2\nu$
(IV)	$\alpha_1 - 2\nu < 2 \wedge \alpha_2 + 2\nu < 2$	1	$0 < \alpha_1 - 2\nu$ $0 < \alpha_2 + 2\nu$ $2 < \alpha_1 + \alpha_2$

Table 2.2: Regions of the parameter space $(\alpha_1, \alpha_2, \nu) \in \mathbb{R}^+ \times \mathbb{R}^+ \times \mathbb{R}$ ordered by severity of singularities in Υ along with number of cases contained in each region and additional constraint determined by Lemma 22.

Corollary 11. *For the parameter constraints given by Theorem 9*

$$\text{Var}\mathcal{T}_\nu = \mathbb{E}\mathcal{T}_\nu^2 - (\mathbb{E}\mathcal{T}_\nu)^2 < \infty.$$

In particular,

$$\text{Var}\mathcal{T}_\nu = \frac{1}{\kappa_1^2} \sum_{k=1}^{\infty} \sum_{\ell=0}^k \frac{g_{k,\ell}^2(\zeta, \nu)}{(\alpha_1)_\ell (\alpha_2)_{k-\ell} \ell! (k-\ell)!},$$

where $g_{n,\omega}$ is given in Theorem 7.

Proof. Using the shorthand $\mathbb{E}\mathcal{T}_\nu^2 = \sum_{r=0}^{\infty} a_r$ observe that

$$a_0 = \kappa_1^{-2} g_{0,0}^2(\zeta, \nu) = (\kappa_1^{-1} {}_1F_0(1; -; z)_\nu)^2 = (\mathbb{E}\mathcal{T}_\nu)^2;$$

thus, subtracting the a_0 term from $\mathbb{E}\mathcal{T}_\nu^2$ yields $\text{Var}\mathcal{T}_\nu$ as desired. \square

Proposition 4. *Evaluating the $k = 1$ term of $\text{Var } \mathcal{T}_\nu$ yields the following asymptotic approximation for large α_1 and α_2 .*

$$\begin{aligned} \text{Var } \mathcal{T}_\nu = \frac{1}{\alpha_1} \left(\frac{1 - \zeta^\nu(1 + \nu(1 - \zeta))}{\kappa_1(1 - \zeta)^2} \right)^2 \\ + \frac{1}{\alpha_2} \left(\frac{\zeta - \zeta^\nu(1 + (\nu - 1)(1 - \zeta))}{\kappa_1(1 - \zeta)^2} \right)^2 + \dots \end{aligned}$$

The following is a generalization of Theorem 9, which shows that the mixed partial derivatives of $\mathbb{E} \mathcal{T}_\nu^2$ w.r.t. α_1 and α_2 converge for the same set of parameters as $\mathbb{E} \mathcal{T}_\nu^2$ itself. Such a result is a key ingredient to Corollary 13 and Section 3.5.2 on optimal sample sizes.

Theorem 10. *For all $n, m \in \mathbb{N}_0$, $\partial_{\alpha_1}^n \partial_{\alpha_2}^m \mathbb{E} \mathcal{T}_\nu^2 < \infty$ whenever $\mathbb{E} \mathcal{T}_\nu^2 < \infty$.*

Proof sketch. The proof amounts to studying the convergence of the double integral representation for $\partial_{\alpha_1}^n \partial_{\alpha_2}^m \mathbb{E} \mathcal{T}_\nu^2$. Using the results of Theorem 22 in Appendix E we may construct a function that bounds the magnitude of the differentiated integrand in the form

$$\Upsilon_{n,m}(x, y) = \max\{1, \zeta^{-2-2\nu}\} v_n(1 + \nu, \alpha_1, s/t) v_m(1 - \nu, \alpha_2, s),$$

where $s = (1 - x)(1 - y)$, $t = (1 - (1 - \zeta)x)(1 - (1 - \zeta)y)$, and

$$v_n(\alpha, \beta, x) = \begin{cases} \frac{n!}{B(|\alpha|, |\alpha|)} \frac{1}{(\beta - 2\alpha \mathbb{1}_{\alpha > 0})^{n+1}} + \mathbb{1}_{n=0}, & \beta > 2\alpha \\ \frac{n!}{B(\alpha, \alpha)} \left(\frac{1}{2\alpha} - \log(1 - x) \right)^{n+1} + \mathbb{1}_{n=0}, & \beta = 2\alpha \\ \frac{n!}{B(\alpha, \alpha)} (1 - x)^{\beta - 2\alpha} \left(\frac{1}{\beta} - \log(1 - x) \right)^{n+1} + \mathbb{1}_{n=0}, & \beta < 2\alpha. \end{cases}$$

Notice that $\Upsilon_{n,m}$ is very similar to the bounding function Υ in Theorem 9 with the exception of possibly additional constant and higher-order multiplicative logarithmic terms. Using Lemma 22, we can easily verify that these additional constant and logarithmic terms do not affect convergence of the integral $\iint \Upsilon_{n,m} dx dy$ and so the claim follows. \square

2.4.3 Coefficient of variation

With minimal effort we can now derive an expression for the coefficient of variation which gives us a signed measure of relative uncertainty in \mathcal{T}_ν . Making use of the results for $\tilde{g}_{n,\omega}$ back in Section 2.4.1, we will show that this quantity is a monotone function of the unknown parameter ζ which will lead directly to obtaining exact confidence intervals of its absolute value in Section 2.5. Also important is the absolute coefficient of variation which will be discussed extensively in latter sections and—in particular—used to define optimal sample sizes for \mathcal{T}_ν in Section 3.5.

Corollary 12 (Corollary of Theorem 9). *For the parameter constraints given by Theorem 9*

$$\begin{aligned}\text{CV } \mathcal{T}_\nu &= \text{sign}(\mathbb{E} \mathcal{T}_\nu) \sqrt{\text{Var } \mathcal{T}_\nu / (\mathbb{E} \mathcal{T}_\nu)^2} \\ \text{ACV } \mathcal{T}_\nu &= |\text{CV } \mathcal{T}_\nu|,\end{aligned}$$

with $\text{Var } \mathcal{T}_\nu$ given in Corollary 11 are finite. In particular,

$$\text{CV } \mathcal{T}_\nu = \text{sign}(\nu) \left(\sum_{k=1}^{\infty} \sum_{\ell=0}^k \frac{\tilde{g}_{k,\ell}^2(\zeta, \nu)}{(\alpha_1)_\ell (\alpha_2)_{k-\ell} \ell! (k-\ell)!} \right)^{1/2},$$

with $\tilde{g}_{n,\omega}$ given by Corollary 10.

Proof. The proof follows from the following facts:

- (1) $\text{sign}(\mathbb{E} \mathcal{T}_\nu) = \text{sign}(\nu)$,
- (2) $g_{k,\ell}^2(\zeta, \nu) / (\mathbb{E} \mathcal{T}_\nu)^2 = \kappa_1^2 \tilde{g}_{k,\ell}^2(\zeta, \nu)$.

A few simple algebraic manipulations then yield the desired form for $\text{CV } \mathcal{T}_\nu$. \square

The results of the previous section can now be used to show that mixed partial derivatives of $\text{ACV}^2 \mathcal{T}_\nu$ w.r.t. α_1 and α_2 converge. This will be used in Section 3.5.2 when studying optimal sample sizes.

Corollary 13 (Corollary of Theorem 10). *Let $\text{ACV}^2 \mathcal{T}_\nu(\alpha_1, \alpha_2)$ denote the squared absolute coefficient of variation of \mathcal{T}_ν as a function of α_1 and α_2 . Then for all $n \in \mathbb{N}_0$, $\partial_{\alpha_2}^n \text{ACV}^2 \mathcal{T}_\nu(A - \alpha_2, \alpha_2)|_{A=\alpha_1+\alpha_2} < \infty$ whenever $\mathbb{E} \mathcal{T}_\nu^2 < \infty$.*

Proof. By definition $\text{ACV}^2 \mathcal{T}_\nu = \mathbb{E} \mathcal{T}_\nu^2 / (\mathbb{E} \mathcal{T}_\nu)^2 - 1$ and since $\mathbb{E} \mathcal{T}_\nu$ is independent of α_1 and α_2 we conclude that the convergence of $\partial_{\alpha_2}^n \text{ACV}^2 \mathcal{T}_\nu(A - \alpha_2, \alpha_2)|_{A=\alpha_1+\alpha_2}$ will agree with that of $\partial_{\alpha_2}^n \mathbb{E} \mathcal{T}_\nu^2(A - \alpha_2, \alpha_2)|_{A=\alpha_1+\alpha_2}$. With a straightforward calculation we find

$$\partial_{\alpha_2}^n \mathbb{E} \mathcal{T}_\nu^2(A - \alpha_2, \alpha_2)|_{A=\alpha_1+\alpha_2} = \sum_{k=0}^n \binom{n}{k} (-1)^k \partial_{\alpha_1}^k \partial_{\alpha_2}^{n-k} \mathbb{E} \mathcal{T}_\nu^2(\alpha_1, \alpha_2),$$

where according to Theorem 10 the magnitude of each term is finite whenever $\mathbb{E} \mathcal{T}_\nu^2$ is finite. \square

With an expression for $\text{CV } \mathcal{T}_\nu$ at hand we seek to establish its monotony in the parameter ζ . We will accomplish this by working with the series expansion of $\text{CV } \mathcal{T}_\nu$ to show that: (1) the series converges at the boundary values $\zeta \rightarrow 0$ and $\zeta \rightarrow \infty$ and (2) the series terms are montone functions in ζ . With these results we will call upon Fubini's theorem on differentiation to conclude that $\partial_\zeta \text{CV } \mathcal{T}_\nu$ is positive. Before proceeding we present an explicit expression for product of hypergeometric series that will be used many times in the rest of the work.

Lemma 24 (Hypergeometric product, [27, Eq. 07.23.16.0006.01]).

$$F\left(\begin{matrix} a, b \\ c \end{matrix}; gz\right) F\left(\begin{matrix} \alpha, \beta \\ \gamma \end{matrix}; hz\right) = \sum_{k=0}^{\infty} c_k z^k,$$

where

$$c_k = \frac{g^k (a)_k (b)_k}{k! (c)_k} {}_4F_3\left(\begin{matrix} -k, 1-c-k, \alpha, \beta \\ 1-a-k, 1-b-k, \gamma \end{matrix}; \frac{h}{g}\right).$$

Lemma 25 (Boundary values of $\text{CV } \mathcal{T}_\nu$). *If the parameters α_1 , α_2 , and ν adhere to the constraints given by Theorem 9*

$$\begin{aligned} \text{(i)} \quad \lim_{\zeta \rightarrow 0} \text{CV } \mathcal{T}_\nu &= \begin{cases} -\left(\frac{(\alpha_1 - \nu - 1)_{-\nu-1} (\alpha_2 + \nu)_\nu}{(\alpha_1)_{-\nu-1} (\alpha_2)_\nu} - 1\right)^{1/2}, & \nu < 0 \\ \frac{1}{\sqrt{\alpha_1 - 2}}, & \nu > 0 \end{cases} \\ \text{(ii)} \quad \lim_{\zeta \rightarrow \infty} \text{CV } \mathcal{T}_\nu &= \begin{cases} -\frac{1}{\sqrt{\alpha_2 - 2}}, & \nu < 0 \\ \left(\frac{(\alpha_1 - \nu)_{-\nu} (\alpha_2 + \nu - 1)_{\nu-1}}{(\alpha_1)_{-\nu} (\alpha_2)_{\nu-1}} - 1\right)^{1/2}, & \nu > 0. \end{cases} \end{aligned}$$

Proof. We will only prove (i) since the proof for (ii) being nearly identical. Working with the series expansion for $\text{CV}^2 \mathcal{T}_\nu$ we call on Lemma 15 and Relation 3 to deduce for $\nu < 0$: $\tilde{g}_{k,\ell}(0, \nu) = (-1)^k (-\ell - \nu)_k$; hence,

$$\lim_{\zeta \rightarrow 0} \text{CV}^2 \mathcal{T}_\nu = \sum_{k=1}^{\infty} \sum_{\ell=0}^k \frac{(-\ell - \nu)_k^2}{(\alpha_1)_\ell (\alpha_2)_{k-\ell} \ell! (k-\ell)!}. \quad (2.17)$$

Working with the properties of the Pochhammer symbol, several algebraic manipulations reveal

$$\frac{(-\ell - \nu)_k^2}{(\alpha_2)_{k-\ell} (k-\ell)!} = \frac{(-\nu)_k^2}{(\alpha_2)_k k!} \frac{(-k)_\ell (1-k-\alpha_2)_\ell (\nu+1)_\ell (\nu+1)_\ell}{(\nu+1-k)_\ell (\nu+1-k)_\ell},$$

which upon substitution into (2.17) and identifying the resulting sum over ℓ as a degenerate hypergeometric function yields

$$\lim_{\zeta \rightarrow 0} \text{CV}^2 \mathcal{T}_\nu = \sum_{k=1}^{\infty} \frac{(-\nu)_k^2}{(\alpha_2)_k k!} {}_4F_3\left(\begin{matrix} -k, 1-k-\alpha_2, \nu+1, \nu+1 \\ \nu+1-k, \nu+1-k, \alpha_1 \end{matrix}; 1\right).$$

Now calling on Lemma 24 the remaining series in k is readily identified as a product of hypergeometric series such that

$$\lim_{\zeta \rightarrow 0} \text{CV}^2 \mathcal{T}_\nu = F\left(\begin{matrix} \nu+1, \nu+1 \\ \alpha_1 \end{matrix}; 1\right) F\left(\begin{matrix} -\nu, -\nu \\ \alpha_2 \end{matrix}; 1\right) - 1. \quad (2.18)$$

By Relation 12 this result can be recast in terms of the ratio of gamma functions. Simplifying in terms of Pochhammer symbols, taking the square root, and reintroducing the appropriate sign then yields the desired expression for the $\nu < 0$

case. Now looking back at Lemma 15 we see for $\nu > 0$: $\tilde{g}_{k,\ell}(0, \nu) = (-1)^k(-\ell)_k$, which is equivalent to the $\nu < 0$ case evaluated at $\nu = 0$. Therefore, to find $\lim_{\zeta \rightarrow 0} \text{CV} \mathcal{T}_\nu$ for $\nu > 0$ we simply substitute $\nu = 0$ into (2.18) and evaluate the square root yielding

$$\lim_{\zeta \rightarrow 0} \text{CV} \mathcal{T}_\nu = \left(F \left(\begin{matrix} 1, 1 \\ \alpha_1 \end{matrix}; 1 \right) - 1 \right)^{1/2} = \frac{1}{\sqrt{\alpha_1 - 2}}.$$

The proof is now complete. \square

Theorem 11 (Monotony of $\text{CV} \mathcal{T}_\nu$ in ζ). *Under the conditions of Theorem 9 if $|\nu| > 1$ the coefficient of variation for \mathcal{T}_ν is a strictly increasing function in ζ , that is, $\partial_\zeta \text{CV} \mathcal{T}_\nu > 0$ for all $\zeta \in \mathbb{R}^+$.*

Proof. For brevity we write

$$\text{CV}^2 \mathcal{T}_\nu = \sum_{k=1}^{\infty} f_k(\zeta, \nu),$$

where $f_k(\zeta, \nu) = \sum_{\ell=0}^k \tilde{g}_{k,\ell}^2(\zeta, \nu) / c_{k,\ell}$ and $c_{k,\ell} = (\alpha_1)_\ell (\alpha_2)_{k-\ell} \ell! (k-\ell)!$. Since $c_{k,\ell} > 0$, if $\nu > 1$ it follows from Theorem 8 that: (i) $f_k(\zeta, \nu)$ is nonnegative and increasing in ζ for all $k \in \mathbb{N}$ and (ii) $\exists k \in \mathbb{N}$ where $f_k(\zeta, \nu)$ is strictly increasing in ζ . Consequently,

$$\text{CV}^2 \mathcal{T}_\nu < \sum_{k=1}^{\infty} \lim_{\zeta \rightarrow \infty} f_k(\zeta, \nu),$$

which was shown to converge in Lemma 25; thus, the series expansion for $\text{CV}^2 \mathcal{T}_\nu$ must converge uniformly for all $\zeta \in \mathbb{R}_0^+$ [23, Thm. 7.10]. Since each f_k is increasing and the series expansion for $\text{CV}^2 \mathcal{T}_\nu$ converges uniformly, Fubini's theorem on differentiation asserts

$$\partial_\zeta \text{CV}^2 \mathcal{T}_\nu = \sum_{k=1}^{\infty} \partial_\zeta f_k(\zeta, \nu) > 0,$$

almost everywhere on $\zeta \in \mathbb{R}^+$. But now observe that $\nu > 1 \implies \text{CV} \mathcal{T}_\nu > 0$, so it follows

$$\partial_\zeta \text{CV}^2 \mathcal{T}_\nu > 0 \implies \partial_\zeta \text{CV} \mathcal{T}_\nu > 0,$$

which establishes $\text{CV} \mathcal{T}_\nu$ being strictly increasing in ζ when $\nu > 1$. For the case $\nu < -1$, we can follow the same process to show $\text{CV}^2 \mathcal{T}_\nu$ is positive and strictly decreasing in ζ . However, $\nu < -1 \implies \text{CV} \mathcal{T}_\nu < 0$ so again we find $\text{CV} \mathcal{T}_\nu$ to be strictly increasing in ζ which completes the proof. \square

2.5 Confidence intervals

An important aspect of any estimation procedure is quantifying the error and precision of the estimate itself. In the context of estimating $\tau = (\kappa_1 - \kappa_2)^{-1}$

with the estimator \mathcal{T}_ν , two relevant quantities for providing relative error and precision come to mind, namely, the absolute relative bias $\text{ARB}\mathcal{T}_\nu$ and absolute coefficient of variation $\text{ACV}\mathcal{T}_\nu$. Due to their dependence on the value of ζ , neither of these quantities can ever be known with exact certainty; however, one can resort to confidence sets as a useful alternative. For clarity the following two lemmas state the conditions for which $\text{ARB}\mathcal{T}_\nu$ and $\text{ACV}\mathcal{T}_\nu$ are monotone functions of ζ which is needed for deriving the corresponding confidence sets in Theorems 12 and 13.

Lemma 26. *If $-\alpha_2 < \nu < \alpha_1$ then $\text{ARB}\mathcal{T}_\nu$ is strictly decreasing in ζ for $\nu < 0$ and strictly increasing in ζ for $\nu > 0$.*

Proof. We have $\text{ARB}\mathcal{T}_\nu = |\mathbb{E}\mathcal{T}_\nu/\tau - 1| = \zeta^\nu$, where $\mathbb{E}\mathcal{T}_\nu$ is finite if $-\alpha_2 < \nu < \alpha_1$. Since $\zeta > 0$, the monotonicity of $\text{ARB}\mathcal{T}_\nu$ immediately follows. \square

Lemma 27. *If $\alpha_1 + \alpha_2 > 2$ and $-\alpha_2 < 2\nu < \alpha_1$ then $\text{ACV}\mathcal{T}_\nu$ is strictly decreasing in ζ for $\nu < -1$ and strictly increasing in ζ for $\nu > 1$.*

Proof. According to Corollary 12, $\text{ACV}\mathcal{T}_\nu$ is finite if $\alpha_1 + \alpha_2 > 2$ and $-\alpha_2 < 2\nu < \alpha_1$. Furthermore, Theorem 11 states that $\text{CV}\mathcal{T}_\nu$ is: (1) positive and strictly increasing in ζ for $\nu > 1$ and (2) negative and strictly increasing in ζ for $\nu < -1$. Given $\text{ACV}\mathcal{T}_\nu = |\text{CV}\mathcal{T}_\nu|$ the result immediately follows. \square

Theorem 12. *Let F_{α,d_1,d_2} denote the $(1-\alpha)$ th quantile for the F_{d_1,d_2} distribution, $V = Y_2/Y_1$, and $Z_\alpha = VF_{\alpha,2\alpha_1,2\alpha_2}$. If $-\alpha_2 < \nu < \alpha_1$ then*

$$\text{CI}_\alpha(\text{ARB}\mathcal{T}_\nu) = \begin{cases} (0, Z_{1-\alpha}^\nu], & \nu < 0 \\ (0, Z_\alpha^\nu], & \nu > 0 \end{cases}$$

is a upper bound confidence set for $\text{ARB}\mathcal{T}_\nu$ with coverage probability $(1-\alpha)$.

Proof. Recall the distributional forms for Y_1 and Y_2 are $Y_i \sim \mathcal{G}(\alpha_i, \alpha_i/\kappa_i)$ where α_i is known. Since $Y_1 \perp Y_2$ one can define the pivotal quantity

$$\frac{\zeta}{V} \sim F_{2\alpha_1, 2\alpha_2}.$$

It follows that $\text{CI}_\alpha(\zeta) = [Z_{1-\alpha}, \infty)$ is a lower bound confidence set for ζ with coverage probability $(1-\alpha)$, that is, $\mathbb{P}(\text{CI}_\alpha(\zeta) \ni \zeta) = 1-\alpha$. Furthermore, if $\nu < 0$ then $\text{ARB}\mathcal{T}_\nu$ is monotone decreasing in ζ with $\lim_{\zeta \rightarrow \infty} \text{ARB}\mathcal{T}_\nu = 0$; thus,

$$\text{CI}_\alpha(\text{ARB}\mathcal{T}_\nu) = \text{ARB}\mathcal{T}_\nu(\text{CI}_\alpha(\zeta)) = (0, Z_{1-\alpha}^\nu]$$

is a upper bound confidence set for $\text{ARB}\mathcal{T}_\nu$ with coverage probability $(1-\alpha)$. If instead $\nu > 0$, $\text{ARB}\mathcal{T}_\nu$ is monotone increasing in ζ so we use $\text{CI}_\alpha(\zeta) = (0, Z_\alpha]$ as an upper bound confidence set for ζ to obtain the corresponding set estimator of $\text{ARB}\mathcal{T}_\nu$ for the $\nu > 0$ case. \square

Theorem 13. Let Z_α be as defined in Theorem 12 and $\text{ACV}\mathcal{T}_\nu(\zeta)$ represent the absolute coefficient as a function of ζ . If $\alpha_1 + \alpha_2 > 2$ and $-\alpha_2 < 2\nu < \alpha_1$ then

$$\text{CI}_\alpha(\text{ACV}\mathcal{T}_\nu) = \begin{cases} ((\alpha_2 - 2)^{-1/2}, \text{ACV}\mathcal{T}_\nu(Z_{1-\alpha})] & \nu < -1 \\ ((\alpha_1 - 2)^{-1/2}, \text{ACV}\mathcal{T}_\nu(Z_\alpha)] & \nu > 1 \end{cases}$$

is a upper bound confidence set for $\text{ACV}\mathcal{T}_\nu$ with coverage probability $(1 - \alpha)$.

Proof. The proof follows much along the same line of reasoning given in Theorem 12 and therefore is omitted. Lemma 25 provides the the expressions for the lower boundary of each set estimator. \square

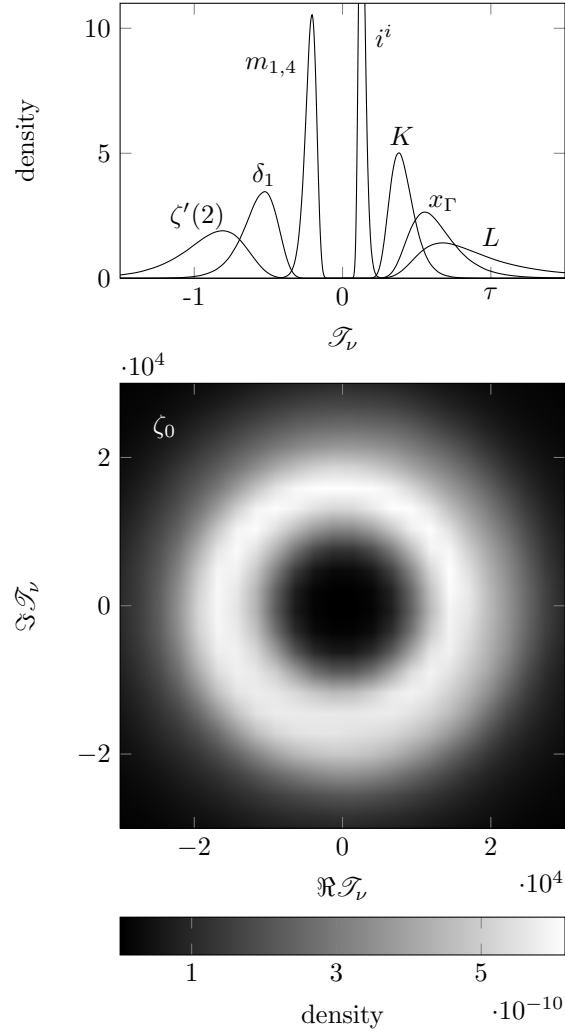


Figure 2.2: Kernel density estimates of the \mathcal{T}_ν probability density for select values of ν given in Table 2.1. Each density estimate is labeled with the value of ν used to generate it.

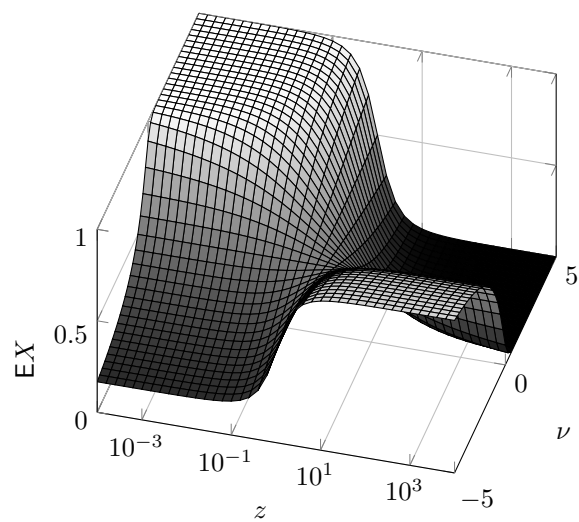


Figure 2.3: Surface plot of EX from Lemma [16](#).

Chapter 3

Photon Transfer Conversion Gain Estimation

At this point we have completed the first part of the goal set forth which was to derive an estimator for the reciprocal difference of independent normal variances. Several fundamental results were found for this estimator including: (1) an asymptotic expansion for large shape parameters α_1 and α_2 , (2) the first two moments $E\mathcal{T}_\nu$ and $E\mathcal{T}_\nu^2$ along with the associated quantities $\text{Var}\mathcal{T}_\nu$ and $\text{CV}\mathcal{T}_\nu$, and (3) exact confidence intervals for the absolute relative bias $\text{ARB}\mathcal{T}_\nu$ and absolute coefficient of variation $\text{ACV}\mathcal{T}_\nu$. With these results at hand, we are finally ready to turn to the tackling the second part of our goal: the problem of conversion gain estimation.

To accomplish this we will first briefly recap and expound upon the discussion and notation surrounding photon transfer theory found in the introduction of Chapter 1. Then we will introduce our newly developed estimator \mathcal{G}_ν for the conversion gain g and use the results for \mathcal{T}_ν in Chapter 2 to derive analogous results for \mathcal{G}_ν . Next, we will rigorously establish a long observed phenomenon about estimators for g , that is, their dispersion is dominated at *high illumination* by the dispersion contributed by estimates of variances. Indeed, Section 3.5.1 we will take this claim a step further by using the theoretical foundation laid in the previous chapter to show that this dominance can be achieved even at illumination levels near zero if we adopt a notation of *optimal sample sizes*. This observation opens the door to not only justifying the estimation of g and its confidence intervals under low illumination but also provides a pathway for design and control of experiment of g -estimation at low illumination; thus, addressing the *low-illumination problem* of conversion gain estimation introduced in [12]. Finally, this chapter will end by demonstrating the effectiveness of the theoretical results derived herein with an experiment measuring g under low illumination conditions.

3.1 A brief review of photon transfer theory

3.1.1 Bose-Einstein statistics and the uncertain nature of light

The theory of photon transfer is fundamentally premised on the uncertainty of electro-magnetic radiation emitted by a source. Such uncertainty means that even if the mean photon production of a source per unit time—which we shall simply call the *illumination level*—remains fixed, the observed number of photons emitted over any specific, fixed, time interval will vary; giving rise to the presence of *noise* in the photon stream. From Bose-Einstein statistics the noise in the photon stream of a blackbody source, described by the variance in the number of photons emitted per unit time σ_γ^2 can be related to the mean photon production per unit time μ_γ , photon energy $E_\gamma = h\nu$ and thermal energy of the source $E_T = kT$ by [18]

$$\sigma_\gamma^2 = \mu_\gamma \left[\frac{e^{h\nu/kT}}{e^{h\nu/kT} - 1} \right],$$

where the quantity in square brackets is the so-called *boson factor*. In the regime where the photon energy is significantly larger than the thermal energy $h\nu \gg kT$, which corresponds to photon wavelengths of $0.3 - 30 \mu\text{m}$ and temperatures $T < 500\text{K}$, the boson factor is near unity such that $\sigma_\gamma^2 \approx \mu_\gamma$ and the number of photons k emitted from the source per unit time is accurately modeled by the Poisson mass function

$$P(k) = \frac{\mu_\gamma^k e^{-\mu_\gamma}}{k!}, \quad k \in \mathbb{N}_0.$$

Light sources with these characteristics are referred to as *Poissonian* and are assumed in the photon transfer method.

3.1.2 Photon transfer $\gamma \rightarrow \text{DN}$ and conversion gain

Detection of photons is done via electro-optical image sensors where the pixels comprising the sensor convert, that is, *transfer* photons (γ) to electrons (e^-). After exposing the sensor to a light source for some *integration time*, the packets of electrons collected by each pixel are passed through the sensor's circuitry whereby each charge packet is first converted to a voltage (V) and then digitized to produce a *digital number* (DN) representing the intensity of the source at each pixel. As one can see, several conversions, e.g. $\gamma \rightarrow e^-$, $e^- \rightarrow V$, and $V \rightarrow \text{DN}$, take place in the process of image formation. Treating each conversion process as a mapping from one unit to another gives rise to the concept of the system *transfer function* $\mathcal{T} : \gamma \rightarrow \text{DN}$ which represents the aggregate mapping of photons to digital numbers. It is important to note that in general each pixel will have its own unique transfer function and must be characterized individually. For sensors where each pixel's transfer function can be assumed identical we

say the sensor is *uniform*. Unless otherwise specified, whenever we discuss the transfer function and measurement thereof, we will assume it is for an individual pixel.

In most cases it is desirable to characterize a pixel in terms of electrons; thus removing the dependence of photon wavelength. Luckily, for Silicon based electro-optical sensors and photons in the visible band $0.4 - 0.7 \mu\text{m}$ the conversion of photons to electrons, described by the quantum yield η is unity; therefore rendering the photon-to-digital number transfer function $\mathcal{T} : \gamma \rightarrow \text{DN}$ equivalent to the electron-to-digital number transfer function $\mathcal{T} : e^- \rightarrow \text{DN}$. The rather lofty goal of the photon transfer method is to measure the transfer function solely by observing the pixel's digital output and then use the estimated transfer function to convert the digital numbers back to a physical quantity of electrons produced in the pixel over the integration time. The ability to reverse engineer the transfer function in this way ultimately allows one to characterize the pixel in terms of key imaging performance metrics like read noise and dynamic range all while treating the sensor system as a black box.

Perhaps the simplest transfer function one could have is that represented by the linear equation $\mathcal{T}(e^-) = e^-/g$ where g is a constant with units (e^-/DN). Pixels that admit such a transfer function are naturally called *linear* and the constant g is referred to as the *conversion gain*. In the special case of linearity, an expression for g is simple to derive. Assuming Poisson photon statistics and unity quantum yield $\eta = 1$ (γ/e^-), the number of electrons collected by a pixel over the integration time is modeled by $N \sim \text{Poisson}(\mu_{e^-})$, where $\mu_{e^-} = \mu_\gamma \text{QE}_\lambda$ is the mean number of electrons collected per integration time, μ_γ is the corresponding mean number of incident photons per integration time, i.e. the illumination level, and QE_λ is the wavelength dependent quantum efficiency describing the probability that an incident photon with wavelength λ produces a free electron. In this context, the transfer function can be viewed as a transformation of the random variable N so that if we let $P = \mathcal{T}(N)$ denote the random variable representing the *photon induced* digital output then $\mu_p(\text{DN}) = \mathbf{E}P = \mu_{e^-}/g$ and $\sigma_p^2(\text{DN}^2) = \text{Var}P = \mu_{e^-}/g^2$; giving rise to the fundamental photon transfer relationship

$$g = \frac{\mu_p}{\sigma_p^2}. \quad (3.1)$$

The remarkable aspect of the model that led up to the relationship (3.1) is that it provides a natural and simple way to estimate g based solely on observing the random output of a pixel exposed to incident illumination. If we denote $\mathbf{P} = \{P_i\}_{i=1}^n$ as a sample of n digital observations generated by a pixel under illumination and $T(\mathbf{P}) = (\bar{P}, \hat{P})$, where $\bar{P} = \frac{1}{n} \sum_{i=1}^n P_i$ is the sample mean and $\hat{P} = \frac{1}{n-1} \sum_{i=1}^n (P_i - \bar{P})^2$ as the sample variance, then T is an unbiased estimator of the parameter $\theta = (\mu_p, \sigma_p^2)$ so that g can be estimated by

$$G = \frac{\bar{P}}{\hat{P}}. \quad (3.2)$$

While simple, the estimator (3.2) has an inherent weakness due to the fact

that the relationship (3.1) does not account for the background signal and noise produced by real pixels in the absence of photon interaction. In some cases, given a sensor of sufficiently high quality, it can be possible to expose the pixels to high levels of illumination so that this background noise is dominated by photon noise and $g \approx \mu_p/\sigma_p^2$ approximately holds. Such sensors are said to achieve a *shot noise limited* response and the measurement of g is said to be performed in the shot noise limited region of the pixel's dynamic range.

It is of no surprise that many sensors cannot achieve a shot noise-limited response such that the background signal and noise produced by the pixels cannot be ignored. To extend our model to include such cases we first let $D \sim F_D$ represent the digital output of the pixels in the absence of illumination (dark), which is distributed according to some distribution F_D with mean μ_d (DN) = $\mathbb{E}D$ and variance σ_d^2 (DN²) = $\text{Var}D$. Assuming D is independent of P , the population mean and variance of the pixels digital output under illumination becomes

$$\begin{aligned}\mathbb{E}(P + D) &:= \mu_{p+d} = \mu_p + \mu_d = \mu_{e-}/g + \mu_d \\ \text{Var}(P + D) &:= \sigma_{p+d}^2 = \sigma_p^2 + \sigma_d^2 = \mu_{e-}/g^2 + \sigma_d^2,\end{aligned}$$

respectively, which leads us to the modify the gain relationship (3.1) as

$$g = \frac{\mu_{p+d} - \mu_d}{\sigma_{p+d}^2 - \sigma_d^2}. \quad (3.3)$$

Unlike the one-sample, shot noise-limited estimator for g given by (3.2), one can see from (3.3) that the measurement of g in a sub shot noise-limited regime will require two separate samples captured under dark and illuminated conditions. Denoting the sample under illumination by $\mathbf{X} = \{X_i\}_{i=1}^{n_1}$ and the sample in the dark by $\mathbf{Y} = \{Y_i\}_{i=1}^{n_2}$, the unknown parameter vector $\theta = (\mu_{p+d}, \sigma_{p+d}^2, \mu_d, \sigma_d^2)$ can be estimated with the unbiased two-sample statistic $T(\mathbf{X}, \mathbf{Y}) = (\bar{X}, \hat{X}, \bar{Y}, \hat{Y})$ with \bar{X} and \hat{X} representing the sample mean and sample variance of \mathbf{X} and likewise for the sample \mathbf{Y} . Substituting the components of T directly into (3.3) gives an estimator for g of the form

$$G = \frac{\bar{X} - \bar{Y}}{\hat{X} - \hat{Y}} = \frac{\bar{P}}{\hat{P}}, \quad (3.4)$$

where \bar{P} and \hat{P} are the new estimators of the photon induced mean μ_p and variance σ_p^2 , respectively.

By accounting for the effects of dark signal and noise with (\bar{Y}, \hat{Y}) , the estimator (3.4) does relieve the need for a pixel to achieve a shot noise limited response. However, as was discussed in the introduction of Chapter 1, the introduction of these dark corrections, in particular that of \hat{Y} , lead to (3.4) exhibiting ill-behaved characteristics in low illumination conditions. To combat this one may measure g with (3.4) under high illumination conditions where the estimator will be most well-behaved. That said, such a procedure becomes invalid if the pixel admits a nonlinear transfer function.

Characterizing pixels with nonlinear transfer functions using only sample statistics of the output signal is a much more challenging task. The inherent complexity of characterizing nonlinear pixels comes from the fact that we can no longer impose the very restrictive assumption that g is a constant and instead must treat it as some unknown function $g(\cdot)$ that varies with illumination level. In years past, two methods for nonlinear characterization have been proposed, namely, the nonlinear compensation (NLC) and nonlinear estimation (NLE) techniques [16, 21, 4]. In the NLC technique, the approach taken is to not directly measure g but rather measure analogous gains for the first two moments of the photon induced signal P . What makes the NLC method work is the observation that pixels with nonlinear transfer functions typically exhibit a linear response at low illumination [15, 16]. As such, if one assumes Poisson photon statistics and exposes the pixel to a sufficiently low level of illumination μ_γ^* , the mean number of electrons collected in the pixel can be described by

$$\mu_{e-}^* = (\mu_{p+d}^* - \mu_d) \times g^*,$$

where μ_{p+d}^* and g^* represent the the corresponding quantities at the illumination level μ_γ^* . If we then define the relative illumination level $r = \mu_\gamma / \mu_\gamma^*$ one can subsequently define the illuminated population parameters and mean electron signal as functions of r whereby $\mu_{e-}^* = \mu_{e-}(1)$, $\mu_{p+d}^* = \mu_{p+d}(1)$, $\sigma_{p+d}^{2*} = \sigma_{p+d}^2(1)$. Using this notation the expected mean number of electrons at relative illumination level r becomes

$$\mu_{e-}(r) = \mu_{e-}^* \times r.$$

Having an explicit expression for this quantity then allows us to define a *signal gain* and *noise gain* in terms of relative illumination level as

$$\begin{aligned} s(r) &= \frac{\mu_{e-}(r)}{\mu_{p+d}(r) - \mu_d} \\ n(r) &= \sqrt{\frac{\mu_{e-}(r)}{\sigma_{p+d}^2(r) - \sigma_d^2}}, \end{aligned} \tag{3.5}$$

where both functions have units of (e-/DN).

In practice, NLC photon transfer characterization is performed by first identifying the linear region of the pixel and measuring g^* . Then, $s(r)$ and $n(r)$ are measured at several illumination levels. At each illumination level, r is recorded and the transfer functions are estimated by according to the formulas in (3.5) above. The estimated transfer functions are then fit by some curve to produce signal and noise gains, which allow one to convert sample means and standard deviations in units of digital numbers back into meaningful quantities of electrons.

3.2 Noise model

Dark noise $D \sim F_D$ represents the sum of many different noise sources present in the pixel and downstream circuitry and therefore is justifiably modeled as normal. We further assume that individual observations D_i of dark noise are mutually independent such that the sample $\mathbf{D} = (D_1, \dots, D_n)^\top$ is modeled by $\mathbf{D} \sim \mathcal{N}(\mu_d \mathbf{1}_n, \sigma_d^2 \mathbf{I}_n)$ where $\mathbf{1}_n \in \mathbb{R}^{n \times 1}$ denotes a column vector of ones and $\mathbf{I}_n \in \mathbb{R}^{n \times n}$ is the $n \times n$ identity matrix. Furthermore, photon induced noise P , although Poissonian by assumption, quickly approaches a normal approximation for even small values of μ_γ ¹. Since the arrival of photons is independent of the dark noise D and individual observations P_i are mutually independent, the observed vector $\mathbf{P} + \mathbf{D} = ((P + D)_1, \dots, (P + D)_n)^\top$ is modeled as $(\mathbf{P} + \mathbf{D}) \sim \mathcal{N}(\mu_{p+d} \mathbf{1}_n, \sigma_{p+d}^2 \mathbf{I}_n)$. With these underlying assumptions we will let $\mathbf{X} = (X_1, \dots, X_{n_1})^\top$ be a sequences of n_1 digital observations of a pixel under some level of illumination and $\mathbf{Y} = (Y_1, \dots, Y_{n_2})^\top$ be a separate sample of n_2 observations of the same pixel in the dark so that the joint vector is modeled by

$$\begin{pmatrix} \mathbf{X} \\ \mathbf{Y} \end{pmatrix} \sim \mathcal{N} \left(\begin{pmatrix} \mu_{p+d} \mathbf{1}_{n_1} \\ \mu_d \mathbf{1}_{n_2} \end{pmatrix}, \begin{pmatrix} \sigma_{p+d}^2 \mathbf{I}_{n_1} & \mathbf{0} \\ \mathbf{0} & \sigma_d^2 \mathbf{I}_{n_2} \end{pmatrix} \right). \quad (3.6)$$

Under the proposed model, the two-sample statistic $T(\mathbf{X}, \mathbf{Y}) = (\bar{X}, \hat{X}, \bar{Y}, \hat{Y})^\top$, where

$$\begin{aligned} \bar{X} &= \frac{1}{n_1} \sum_{k=1}^{n_1} X_k, & \hat{X} &= \frac{1}{n_1 - 1} \sum_{k=1}^{n_1} (X_k - \bar{X})^2, \\ \bar{Y} &= \frac{1}{n_2} \sum_{k=1}^{n_2} Y_k, & \hat{Y} &= \frac{1}{n_2 - 1} \sum_{k=1}^{n_2} (Y_k - \bar{Y})^2, \end{aligned}$$

forms a vector of mutually independent components and constitutes a complete-sufficient statistic for the unknown parameter vector $\theta = (\mu_{p+d}, \sigma_{p+d}^2, \mu_d, \sigma_d^2)$. Normal sampling theory gives the distributional results

$$\begin{aligned} \bar{X} &\sim \mathcal{N}(\mu_{p+d}, \sigma_{p+d}^2/n_1), & \hat{X} &\sim \mathcal{G}(\alpha_1, \alpha_1/\sigma_{p+d}^2), \\ \bar{Y} &\sim \mathcal{N}(\mu_d, \sigma_d^2/n_2), & \hat{Y} &\sim \mathcal{G}(\alpha_2, \alpha_2/\sigma_d^2), \end{aligned}$$

where $\alpha_i = (n_i - 1)/2$. Since the shapes parameters α_i are directly related to the sample sizes n_i in this manner, we will use the term *sample size* to refer to both quantities when it is expedient to do so. Further denoting the estimator for the photon induced mean as $\bar{P} = \bar{X} - \bar{Y}$ also gives the sometimes useful result

$$\bar{P} \sim \mathcal{N}(\mu_p, \sigma_{p+d}^2/n_1 + \sigma_d^2/n_2).$$

We will further assume that the observed data $(\mathbf{X}^\top \mathbf{Y}^\top)^\top$ is produced by a pixel with a linear transfer function or equivalently is produced in the linear region of a pixel with nonlinear transfer function. This assumption implies

¹A typical rule of thumb is the normal approximation is useful for $\mu_\gamma > 30$.

$\mu_{p+d} = \mu_d + \mu_{e-}/g$ and $\sigma_{p+d}^2 = \sigma_d^2 + \mu_{e-}/g^2$ where g is the conversion gain given by (3.3). Since $\mu_{e-} \geq 0$ it follows that $\mu_{p+d} \geq \mu_d > 0$ and $\sigma_{p+d}^2 \geq \sigma_d^2 > 0$ with equality reached at zero illumination. Throughout the remaining sections, we will also use the notation of Chapter 2 to denote the ratio of dark and illuminated variances by $\zeta = \sigma_d^2/\sigma_{p+d}^2$ where $\zeta \in [0, 1]$, $\zeta = 1$ is achieved at zero illumination, and $\zeta = 0$ is achieved at infinite illumination which is the shot noise limit².

3.3 The estimator \mathcal{G}_ν

We are finally ready to present our new estimator for the photon transfer conversion gain. Our first result shows that under the proposed noise model, if an unbiased estimator for g exists, it must have infinite variance on at least a portion of the ζ -domain.

Theorem 14 (Corollary of Theorem 1). *Under the normal model of pixel noise in (3.6), if an unbiased estimator of g exists it must have infinite variance for at least $\zeta \in (1/2, 1]$.*

Proof. Assuming the model (3.6), $T(\mathbf{X}, \mathbf{Y}) = (\bar{P}, \hat{X}, \hat{Y})^\top$ is a complete-sufficient statistic for the parameter $\theta = (\mu_p, \sigma_{p+d}^2, \sigma_d^2)^\top$. Since the components of T are mutually independent and $E\bar{P} = \mu_p$, it follows that if unbiased estimator of g exists it will be of the form $\mathcal{G}(T) = \bar{P} \times \mathcal{T}(\hat{X}, \hat{Y})$ with $\mathcal{T}(\hat{X}, \hat{Y})$ denoting an unbiased estimator of $(\sigma_{p+d}^2 - \sigma_d^2)^{-1}$. Again making use of the independence of \bar{P} and \mathcal{T} we then write

$$\text{Var}\mathcal{G} = (E\bar{P}^2)\text{Var}\mathcal{T} + (E\mathcal{T})^2\text{Var}\bar{P}.$$

But according to Theorem 1, if the estimator \mathcal{T} exists it must have infinite variance on at least $\zeta \in (1/2, 1]$. Since \mathcal{G} is an UMVUE for g and $\text{Var}\mathcal{T} < \text{Var}\mathcal{G}$ the desired result immediately follows. \square

Given that there is no unbiased estimator for g that can achieve finite variance on the entire ζ -domain we again turn to biased estimation. The following theorem presents a biased estimator based on the estimator \mathcal{T}_ν derived in Chapter 2.

Proposition 5. *Under the assumed model we have $\sigma_{p+d}^2 = \sigma_d^2/\zeta$, $\sigma_p^2 = \sigma_d^2\zeta^{-1}(1-\zeta)$, and $\mu_p = \sigma_d^2\zeta^{-1}(1-\zeta)g$.*

Proof. The first two relationships are derived from $\sigma_{p+d}^2 = \sigma_p^2 + \sigma_d^2$ and $\zeta = \sigma_d^2/\sigma_{p+d}^2$. To derive the relationship for μ_p we use $\mu_p = \mu_{e-}/g$ and $\sigma_p^2 = \mu_{e-}/g^2$ to write $\mu_p = \sigma_p^2 g$. \square

² $\zeta = 0$ can be treated as the mathematical definition of the shot noise limit. In practice, the term *shot noise limited* is a subjective term meant to describe a pixel that can achieve a ζ -value near zero before saturating.

Theorem 15. Let $T = (\bar{P}, \hat{X}, \hat{Y})^\top$ and

$$\mathcal{G}_\nu(T) = \bar{P} \times \mathcal{T}_\nu(\hat{X}, \hat{Y}), \quad \nu > 0.$$

Then, \mathcal{G}_ν is the unique uniformly minimum variance unbiased estimator of

$$\mathbb{E}\mathcal{G}_\nu = (1 - \zeta^\nu)g,$$

with

$$\text{Var}\mathcal{G}_\nu = \frac{\sigma_d^2}{\zeta} \left(\frac{1}{n_1} + \frac{\zeta}{n_2} + \frac{(\sigma_d g)^2}{\zeta} (1 - \zeta)^2 \right) \mathbb{E}\mathcal{T}_\nu^2 - (1 - \zeta^\nu)^2 g^2$$

and $\mathbb{E}\mathcal{T}_\nu^2$ is given by Theorem 9 for $\kappa_1 = \sigma_d^2/\zeta$ and $\alpha_i = (n_i - 1)/2$.

Proof. First, note that $\sigma_{p+d}^2 > \sigma_d^2$ for any nonzero illumination level; thus, by Remark 2 we must require $\nu > 0$ to guarantee $\text{ARB}\mathcal{T}_\nu < 1$. Next, for the proposed normal model $T(\mathbf{X}, \mathbf{Y}) = (\bar{X}, \bar{Y}, \hat{X}, \hat{Y})$ is a complete-sufficient statistic for the parameter $\theta = (\mu_{p+d}, \mu_d, \sigma_{p+d}^2, \sigma_d^2)$; thus by the Lehmann-Scheffé theorem \mathcal{G}_ν is the unique UMVUE of its expected value. To evaluate the expected value, we use the independence of \bar{P} and $\mathcal{T}_\nu(\hat{X}, \hat{Y})$ to write $\mathbb{E}\mathcal{G}_\nu = (\mathbb{E}\bar{P})(\mathbb{E}\mathcal{T}_\nu)$. We know $\mathbb{E}\bar{P} = \mu_p$ and $\mathbb{E}\mathcal{T}_\nu$ is given in Theorem 4. Using the formula for g in (3.3) then gives the desired result for $\mathbb{E}\mathcal{G}_\nu$. To obtain the variance we again use independence of \bar{P} and \mathcal{T}_ν to write

$$\text{Var}\mathcal{G}_\nu = (\text{Var}\bar{P} + (\mathbb{E}\bar{P})^2)(\mathbb{E}\mathcal{T}_\nu^2) - (1 - \zeta^\nu)^2 g^2.$$

Recalling $\bar{P} \sim \mathcal{N}(\mu_p, \sigma_{p+d}^2/n_1 + \sigma_d^2/n_2)$ and the relations of Proposition 5 then leads to the desired result. \square

In the following analysis we will derive many results involving the coefficient of variation of \mathcal{G}_ν . Given the restrictions $\nu > 0$ and $\zeta \in (0, 1)$ we know that $\mathbb{E}\mathcal{G}_\nu > 0$ so that $\text{CV}\mathcal{G}_\nu = \text{ACV}\mathcal{G}_\nu$. As such, to maintain some level of congruence between the following results and those of Chapter 2 we will use these quantities interchangeably when its convenient to do so. We now show that $\text{ARB}\mathcal{G}_\nu$ and $\text{ACV}\mathcal{G}_\nu$ are strictly increasing functions of ζ .

Proposition 6. $\text{ARB}\mathcal{G}_\nu$ is a strictly increasing function of ζ . Furthermore, if $\nu > 1$ then $\text{ACV}\mathcal{G}_\nu$ is also a strictly increasing function of ζ .

Proof. Given the definition of the absolute relative bias we have

$$\text{ARB}\mathcal{G}_\nu = \left| \frac{(1 - \zeta^\nu)g - g}{g} \right| = \zeta^\nu.$$

Since $\nu > 0$ it immediately follows that $\partial_\zeta \text{ARB}\mathcal{G}_\nu > 0$ on $\zeta \in (0, 1)$. Next, we use the independence of \bar{P} and \mathcal{T}_ν to write

$$\text{ACV}^2\mathcal{G}_\nu = \text{CV}^2\mathcal{T}_\nu + (\text{CV}^2\mathcal{T}_\nu)(\text{CV}^2\bar{P}) + \text{CV}^2\bar{P} \quad (3.7)$$

so that

$$\partial_\zeta \text{ACV}^2\mathcal{G}_\nu = (\text{CV}^2\bar{P} + 1)(\partial_\zeta \text{CV}^2\mathcal{T}_\nu) + (\text{CV}^2\mathcal{T}_\nu + 1)(\partial_\zeta \text{CV}^2\bar{P}). \quad (3.8)$$

Using the relations in Proposition 5 we have

$$\text{CV}^2 \bar{P} = \frac{1}{(\sigma_d g)^2} \frac{\zeta}{(1 - \zeta)^2} \left(\frac{1}{n_1} + \frac{\zeta}{n_2} \right), \quad (3.9)$$

which is easily shown to be decreasing in ζ on $\zeta \in (0, 1)$ ³. Likewise, for $\nu > 1$ we know from Lemma 27 that $\partial_\zeta \text{ACV}^2 \mathcal{T}_\nu > 0$ which implies all terms in (3.8) are positive. Noting that $\text{ACV} \mathcal{G}_\nu$ is positive completes the proof. \square

In the following Lemma we establish a property of \mathcal{G}_ν that agrees with a long standing observation about estimators of g in the literature, that is, the dispersion of \mathcal{G}_ν is dominated by the dispersion of the estimator for $(\sigma_{p+d}^2 - \sigma_d^2)^{-1}$ as the illumination increases. To accomplish this we will consider the quantity

$$\mathcal{E} = \frac{\text{CV}^2 \mathcal{T}_\nu}{\text{CV}^2 \mathcal{G}_\nu}.$$

This ratio is useful for studying the dominance of $\text{Var} \mathcal{G}_\nu$ by the dispersion of \mathcal{T}_ν for a couple reasons. First, using the definition of the coefficient of variation and independence of \bar{P} and $\mathcal{T}_\nu(\hat{X}, \hat{Y})$ we are able to write

$$\text{CV}^2 \mathcal{G}_\nu = \text{CV}^2 \mathcal{T}_\nu (1 + (1 + \text{CV}^{-2} \mathcal{T}_\nu) \text{CV}^2 \bar{P}),$$

and thus

$$\mathcal{E} = [1 + (1 + \text{CV}^{-2} \mathcal{T}_\nu) \text{CV}^2 \bar{P}]^{-1}. \quad (3.10)$$

Since the quantity inside the brackets is bounded below by one it follows that $0 < \mathcal{E} < 1$ and so \mathcal{E} gives an intuitive measure of dominance. Second, if we define the random variable $\mathcal{G}_\nu^* = \mu_p \mathcal{T}_\nu(\hat{X}, \hat{Y})$ which estimates g when μ_p is known, i.e. has zero variance, then \mathcal{E} is equivalent to

$$\mathcal{E} = \frac{\text{Var} \mathcal{G}_\nu^*}{\text{Var} \mathcal{G}_\nu}.$$

So in this context we see that $\mathcal{E} \approx 1$ corresponds to \bar{P} behaving like a fixed constant in comparison to \mathcal{T}_ν ; hence, $\text{Var} \mathcal{G}_\nu$ is completely dominated by the dispersion of \mathcal{T}_ν .

Lemma 28. *As the illumination level increases $\mathcal{E} \searrow 1$.*

Proof. We have already shown that $\mathcal{E} < 1$; thus, if it approaches one then it must do so from below. All that is left is to show that $\mathcal{E} = 1$ in the limit of infinite illumination. Our starting point is the expression for \mathcal{E} in (3.10), namely,

$$\mathcal{E} = (1 + (1 + \text{CV}^{-2} \mathcal{T}_\nu) \text{CV}^2 \bar{P})^{-1}.$$

³In (3.9) we see the quantity $\sigma_d g$ which is the sensor dark noise in units of electrons. This quantity represents the sum of read noise and dark current noise present in the pixel and is a function of integration time.

As the illumination level increases without bound, $\zeta \rightarrow 0$ and from Lemma 25

$$\text{CV}^2 \mathcal{T}_\nu \rightarrow \begin{cases} \frac{2}{n_1-5}, & n_1 > 5 \\ \infty, & n_1 \leq 5. \end{cases}$$

Hence, $1 + \text{CV}^{-2} \mathcal{T}_\nu$ approaches a positive and finite constant in the limit. Next we turn our attention to the $\text{CV}^2 \bar{P}$ term. Using (3.9) it is immediately obvious that $\text{CV}^2 \bar{P} \rightarrow 0$ as $\zeta \rightarrow 0$. Thus, as the illumination increases without bound $(1 + \text{CV}^{-2} \mathcal{T}_\nu) \text{CV}^2 \bar{P} \rightarrow 0$ which completes the proof. \square

Theorem 16. *For the estimator \mathcal{G}_ν in Theorem 15*

$$\text{ARB} \mathcal{G}_\nu = \text{ARB} \mathcal{T}_\nu$$

and as illumination increases

$$\text{ACV} \mathcal{G}_\nu \sim \text{ACV} \mathcal{T}_\nu.$$

In particular, if $\alpha_1 + \alpha_2 > 2$, $\alpha_1 > 2\nu$, and $\nu > 1$ then as illumination increases, $\zeta \nearrow 0$ and

$$\text{ACV} \mathcal{G}_\nu \sim \text{ACV} \mathcal{T}_\nu \left(1 + \frac{n_1 - 3}{4n_1} \frac{\zeta}{(\sigma_{\text{dg}})^2} + \mathcal{O}(\zeta^2) \right).$$

Proof. The first two claims follow directly from Proposition 6 and Lemma 28, respectively. For the last claim we assume $\nu > 1$ and use (2.7) to deduce

$$\tilde{g}_{k,\ell}^2(\zeta, \nu) \sim \begin{cases} (k!)^2 + \mathcal{O}(\zeta), & k = \ell \\ \mathcal{O}(\zeta^2), & k > \ell. \end{cases}$$

If in addition $\alpha_1 + \alpha_2 > 2$ and $\alpha_1 > 2\nu$ then $\text{CV} \mathcal{T}_\nu$ is finite and it follows that as $\zeta \nearrow 0$

$$\text{CV}^2 \mathcal{T}_\nu \sim \sum_{k=1}^{\infty} \frac{k!}{(\alpha_1)_k} + \mathcal{O}(\zeta) = \frac{1}{\alpha_1 - 2} + \mathcal{O}(\zeta)$$

and

$$1 + \text{CV}^{-2} \mathcal{T}_\nu \sim \alpha_1 - 1 + \mathcal{O}(\zeta) = \frac{n_1 - 3}{2} + \mathcal{O}(\zeta).$$

Multiplying this result by

$$\text{CV}^2 \bar{P} \sim \frac{1}{(\sigma_{\text{dg}})^2} \frac{\zeta}{n_1} + \mathcal{O}(\zeta^2)$$

and using $\sqrt{1 + f(x)} \sim 1 + \frac{1}{2}f(x) + \mathcal{O}(f^2(x))$ as $f(x) \rightarrow 0$ then gives

$$\mathcal{E}^{-1/2} = \frac{\text{ACV} \mathcal{G}_\nu}{\text{ACV} \mathcal{T}_\nu} \sim 1 + \frac{n_1 - 3}{4n_1} \frac{\zeta}{(\sigma_{\text{dg}})^2} + \mathcal{O}(\zeta^2),$$

which is the desired result. \square

The main conclusion of Theorem 16 is that confidence intervals for $\text{ARB}\mathcal{T}_\nu$ are equal to those of $\text{ARB}\mathcal{G}_\nu$ and that for sufficiently high illumination confidence intervals for $\text{ACV}\mathcal{T}_\nu$ may be used to approximate those of $\text{ACV}\mathcal{G}_\nu$. That said, these results do not give any indication as to how high the illumination level must be to achieve a good approximation or how $\text{ACV}\mathcal{G}_\nu$ compares to $\text{ACV}\mathcal{T}_\nu$ under low illumination when taking into account other parameters like the dark noise σ_d , conversion gain g , and sample sizes. We will return to this problem later and for now will be content with knowing that given a sufficiently high illumination level $\text{ACV}\mathcal{T}_\nu \approx \text{ACV}\mathcal{G}_\nu$.

3.4 A demonstration of g -estimation with confidence intervals

With Theorem 16 at hand, we now bring together several of the results derived thus far and demonstrate the process of estimating g in the context of the photon transfer method. Using the parameter values in Table 3.1, $N = 10^6$ pseudo-random observations of $T = (\bar{P}, \hat{X}, \hat{Y})$ were generated. The parameter values chosen represent what one might typically see in the photon transfer method. Since the sample sizes used are large we use (2.6) to derive the *first order* approximation

$$\mathcal{G}_{\nu,1}(T) = \bar{P} \times \mathcal{T}_{\nu,1}(\hat{X}, \hat{Y}),$$

where

$$\begin{aligned} \mathcal{T}_{\nu,1}(\hat{X}, \hat{Y}) = & \frac{1}{\hat{Y}} \left(\left(1 - \frac{1}{\alpha_1}\right) \nu F\left(\begin{matrix} 1, 1+\nu \\ 2 \end{matrix}; 1 - \frac{\hat{X}}{\hat{Y}}\right) \right. \\ & \left. - \frac{1}{\alpha_1} (\nu)^{(2)} F\left(\begin{matrix} 2, 1+\nu \\ 3 \end{matrix}; 1 - \frac{\hat{X}}{\hat{Y}}\right) - \frac{\alpha_1 + \alpha_2}{6\alpha_1\alpha_2} (\nu)^{(3)} F\left(\begin{matrix} 3, 1+\nu \\ 4 \end{matrix}; 1 - \frac{\hat{X}}{\hat{Y}}\right) \right) \end{aligned}$$

and $\alpha_i = (n_i - 1)/2$. Note that the presence of integers in the top and bottom parameters of the hypergeometric terms mean they reduce to elementary functions of the argument $1 - \hat{X}/\hat{Y}$.

Computation of the confidence intervals was done by first computing $Z_\alpha = \hat{Y}/\hat{X} F_{\alpha, 2\alpha_1, 2\alpha_2}$ for each pair of (\hat{X}, \hat{Y}) and confidence level $\alpha = 0.05$. The 95% confidence intervals for $\text{ARB}\mathcal{G}_\nu$ were then computed by substituting the values for Z_α into Theorem 12. As for the confidence intervals of $\text{ACV}\mathcal{G}_\nu$, a quick computation of \mathcal{E} using the parameters in Table 3.1 shows that despite the relatively low level of illumination used in the simulation $\mathcal{E} = 0.998685\dots$ so that we may approximate these intervals with those for \mathcal{T}_ν in Theorem 13. The relatively large values used for α_1 and α_2 means computation of these interval estimates will have to be done with the series expansion for $\text{ACV}\mathcal{T}_\nu$ which introduces the practical problem of truncation error. If we define

$$\text{ACV}_n \mathcal{T}_\nu = \left(\sum_{k=1}^n \sum_{\ell=0}^k \frac{\tilde{g}_{k,\ell}^2(z, \nu)}{(\alpha_1)_\ell (\alpha_2)_{k-\ell} \ell! (k-\ell)!} \right)^{1/2},$$

then the absolute relative error incurred in using this truncated expansion is given by

$$R_{n,1} = \left| \frac{\text{ACV}_n \mathcal{T}_\nu}{\text{ACV} \mathcal{T}_\nu} - 1 \right|.$$

Corollary 17 (see Appendix D) provides an upper bound, $R_{n,m,1}^*$, for $R_{n,1}$ so that one may compute the number of terms $n = K^*$ that guarantees $R_n < \epsilon$ according to

$$K^* = \min\{K | R_{K,m,1}^* \leq \epsilon \wedge K \in \mathbb{N}\}.$$

Note that the quantity $R_{n,m,1}^*$ in Corollary 17 provides a single upper bound for the entire set of Z_α values so that K^* is the appropriate number of terms needed in computing all 10^6 interval estimates within the specified error tolerance. The approximate interval estimates for $\text{ACV} \mathcal{G}_\nu$ may then be computed by substituting $\text{ACV}_{K^*} \mathcal{T}_\nu$ and Z_α into Theorem 13.

Table 3.2 presents the results of the simulation. Using the simulated values for Z_α and choosing $m = 0$ and an absolute relative truncation error tolerance $\epsilon = 5 \times 10^{-4}$ led to only needing the first $K^* = 3$ terms in the series expansion for $\text{ACV} \mathcal{T}_\nu$. Substituting K^* into $R_{n,0,1}^*$ subsequently showed that using this number of terms guaranteed the relative truncation error was less than 2.7×10^{-4} for all 10^6 values of Z_α . Additionally, note the relative difference between the exact and estimated values for $\text{E} \mathcal{G}_\nu$ and $\text{Var} \mathcal{G}_\nu$ are

$$R_{\text{E} \mathcal{G}_\nu} = \left| \frac{\widehat{\text{E}} \mathcal{G}_{\nu,1}}{\text{E} \mathcal{G}_\nu} - 1 \right| \times 100\% = 0.001\%$$

and

$$R_{\text{Var} \mathcal{G}_\nu} = \left| \frac{\widehat{\text{Var}} \mathcal{G}_{\nu,1}}{\text{Var} \mathcal{G}_\nu} - 1 \right| \times 100\% = 0.24\%,$$

which indicates no significant error was incurred from using the asymptotic approximation $\mathcal{G}_{\nu,1}$ in place of \mathcal{G}_ν . Lastly, we see that the estimated coverage probability for the 95% confidence intervals for $\text{ARB} \mathcal{G}_\nu$ and $\text{ACV} \mathcal{G}_\nu$ agree with the target values, the latter of which is due to the fact that $\mathcal{E} \approx 1$ for the chosen parameters.

This exercise raises additional questions as no instruction is given on the appropriate values for ν , n_1 and n_2 to achieve desired values of $\text{ARB} \mathcal{G}_\nu$ and $\text{ACV} \mathcal{G}_\nu$. In particular, for real experiments, gathering large numbers of observations takes time and so knowledge of *optimal* sample sizes would be useful in reducing the time required to gather data. We will take a closer look at this problem in the following section.

3.5 Optimal sample sizes

When discussing the notion of optimal sample sizes we must first begin with a definition of what is optimal. Typically, experimenters wish to achieve the smallest possible uncertainty with the fewest number of total observations. This goal is manifested in the following definition.

Parameter	Equation	Value	Unit
α	—	0.05	—
n_1	—	3001	—
n_2	—	1501	—
g	—	5	e^-/DN
ν	—	$\frac{1}{2}e^\pi$	—
μ_{e^-}	—	150	e^-
μ_d	—	10	DN
σ_d^2	—	16	DN^2
μ_{p+d}	$\mu_d + \mu_{e^-}/g$	40	DN
σ_{p+d}^2	$\sigma_d^2 + \mu_{e^-}/g^2$	22	DN^2
ζ	$\sigma_d^2/\sigma_{p+d}^2$	$\frac{8}{11}$	—
$\mu_{\bar{P}}$	$\mu_{p+d} - \mu_d$	30	DN
$\sigma_{\bar{P}}^2$	$\sigma_{p+d}^2/n_1 + \sigma_d^2/n_2$	$\frac{81038}{4504501}$	DN^2
α_1	$(n_1 - 1)/2$	1500	—
α_2	$(n_2 - 1)/2$	750	—
β_1	α_1/σ_{p+d}^2	$\frac{750}{11}$	DN^{-2}
β_2	α_2/σ_d^2	$\frac{375}{8}$	DN^{-2}

Table 3.1: Simulation parameters.

Quantity	Exact Value	Estimated Value	Unit
K^\star	3	—	—
$R_{K^\star,0,1}^\star$	0.02671	—	%
$E\mathcal{G}_\nu$	4.87447	4.87440	e^-/DN
$\text{Var}\mathcal{G}_\nu$	0.36671	0.36759	$(e^-/\text{DN})^2$
$P(\text{CI}_\alpha(\text{ARB}\mathcal{T}_\nu) \ni \text{ARB}\mathcal{G}_\nu)$	0.95	0.95008	—
$P(\text{CI}_\alpha(\text{ACV}\mathcal{T}_\nu) \ni \text{ACV}\mathcal{G}_\nu)$	~ 0.95	0.94945	—

Table 3.2: Simulation results based on $N = 10^6$ pseudo-random observations.

Definition 11 (Optimal sample sizes). Let $\mathbf{X}_j = (X_{i,j}, \dots, X_{n_j,j})$ with $X_{i,j} \stackrel{\text{iid}}{\sim} F_j(\theta_j)$ denote a random sample of size n_j drawn from the distribution F_j with parameters θ_j . Furthermore, let $T(\mathbf{X})$ denote an estimator based on M random samples $\mathbf{X} = (\mathbf{X}_1, \dots, \mathbf{X}_M)$ and $\text{ACVT}(n|\theta_T)$ denote its absolute coefficient of variation as a function of the sample sizes $n = (n_1, \dots, n_M)$ with parameters $\theta_T = \cup_j \theta_j$. Then the optimal sample sizes are defined as the vector-valued function $n^{\text{opt}}(\mathbf{N}, \theta_T) = (n_1^{\text{opt}}, \dots, n_M^{\text{opt}})(\mathbf{N}, \theta_T)$ that minimizes $\text{ACVT}(n|\theta_T)$ subject to $\mathbf{N} = n_1 + \dots + n_M$ for some fixed $\mathbf{N} > 0$.

In the case where there are two samples, so that $n = (n_1, n_2)$, this definition of optimality requires solving the single-variable optimization problem

$$n_2^{\text{opt}}(\mathbf{N}, \theta_T) = \arg \inf_{n_2 \in [0, \mathbf{N}]} \text{ACV}^2 T(\mathbf{N} - n_2, n_2 | \theta_T) \quad (3.11a)$$

$$n_1^{\text{opt}}(\mathbf{N}, \theta_T) = \mathbf{N} - n_2^{\text{opt}}(\mathbf{N}, \theta_T), \quad (3.11b)$$

for some total number of samples \mathbf{N} and parameters θ_T . Note that while this formulation does give the optimal sample sizes according to definition 11, it does not allow one to specify a predetermined value (desired outcome) for ACVT . Since it may be desirable to specify the outcome of ACVT instead of \mathbf{N} we can introduce the constraint $\text{ACVT}(n_1^{\text{opt}}, n_2^{\text{opt}} | \theta_T) = \text{acv}_0$ and reformulate (3.11) into the equivalent two-variable problem

$$\inf_{n_2 \in [0, \mathbf{N}]} \text{ACV}^2 T(\mathbf{N} - n_2, n_2 | \theta_T) \Big|_{(\mathbf{N}, n_2) = (n_1^{\text{opt}} + n_2^{\text{opt}}, n_2^{\text{opt}})} \quad (3.12a)$$

$$\text{ACV}^2 T(n_1^{\text{opt}}, n_2^{\text{opt}} | \theta_T) - \text{acv}_0^2 = 0, \quad (3.12b)$$

which can then be solved for $(n_1^{\text{opt}}, n_2^{\text{opt}})$ in terms of acv_0 and θ_T .

Before proceeding, let's consider what this system of equations says and how we solve it. Three cases must be considered which we shall denote as: *nondegenerate* ($n_1^{\text{opt}}, n_2^{\text{opt}} \neq 0$), *weakly degenerate* ($n_1^{\text{opt}} = 0$ or $n_2^{\text{opt}} = 0$ but not both), and *degenerate* ($n_1^{\text{opt}}, n_2^{\text{opt}} = 0$). For the nondegenerate case we begin with equation (3.12a) by fixing the total number of samples to \mathbf{N} and then minimizing $\text{ACV}^2 T$ in n_2 subject to this constraint. This process gives the optimal sample size n_2^{opt} in terms of \mathbf{N} and θ_T ⁴, which upon substituting $\mathbf{N} = n_1^{\text{opt}} + n_2^{\text{opt}}$ yields an equation representing the optimal relationship, a.k.a. the *optimality relation*, between the two sample sizes. Solving the optimality relation for either n_1^{opt} or n_2^{opt} and then substituting into (3.12b) we then obtain one of the optimal sample sizes parameterized in terms of acv_0 and θ_T . This solution may then be used in conjunction with the optimality relation to obtain the solution for the remaining optimal sample size. In the case of weak degeneracy, the infimum of $\text{ACV}^2 T(\mathbf{N} - n_2, n_2 | \theta_T)$ occurs at the boundary $n_2 = 0, \mathbf{N}$ and so our two-sample problem reduces to that of finding a single optimal sample size via (3.12b). Lastly, the case of degeneracy results when $\text{ACVT} \rightarrow 0$ and so zero samples are needed to achieve the desired outcome $\text{ACVT} = \text{acv}_0$. As will be seen in the latter analysis, this situation can occur at boundary points of the parameter space and thus be treated as a limit of the nondegenerate case.

⁴In fact, if we were to stop here equation (3.12a) would be identical to (3.11a)

3.5.1 Asymptotic properties at low illumination

One of the unanswered curiosities of Section 3.4 was how the quantity \mathcal{E} behaves at low illumination w.r.t. the parameters (σ_d, g, n_1, n_2) . If we fix these parameters and consider what only happens as the illumination decreases, i.e. as $\zeta \searrow 1$, we see that $\text{CV}\bar{P} \rightarrow \infty$ while $\text{CV}\mathcal{T}_\nu$ approaches a constant and thus $\mathcal{E} \rightarrow 0$. From this observation one might conclude that the only way to achieve \mathcal{E} -values near unity is to perform measurements at high illumination; thus, extinguishing the possibility of approximating confidence intervals and optimal sample sizes for \mathcal{G}_ν with those of \mathcal{T}_ν under low illumination conditions. However, if we instead consider \mathcal{E} as a function of the optimal samples sizes for \mathcal{T}_ν or \mathcal{G}_ν , which vary with the illumination level, the limiting behavior at low illumination changes drastically. The following analysis takes a look at the behavior of the optimal sample sizes for \bar{P} , \mathcal{T}_ν , and \mathcal{G}_ν under low illumination conditions. The main results are found in Lemma 29, Theorem 17, and Corollary 14, which show for each estimator that the optimal samples sizes are asymptotically equal and proportional to $(1 - \zeta)^{-2}$ as $\zeta \searrow 1$. We will then conclude this section by using these asymptotic results in Corollary 15 to study how \mathcal{E} behaves at low illumination when subject to optimal sample sizes.

Lemma 29. *Let $(n_1^{\text{opt}}, n_2^{\text{opt}})$ denote the optimal sample sizes for \bar{P} that also satisfy $\text{ACV}\bar{P}(n_1^{\text{opt}}, n_2^{\text{opt}}|\zeta, \sigma_d, g) = \text{acv}_0$ for some fixed $\text{acv}_0 \in \mathbb{R}^+$. Then as illumination decreases, $\zeta \searrow 1$, $n_2^{\text{opt}}/n_1^{\text{opt}} \rightarrow 1$, and $n_i^{\text{opt}} \sim C_{\bar{P}}(1 - \zeta)^{-2}$ where $C_{\bar{P}} = 2((\sigma_d g)^2 \text{acv}_0^2)^{-1}$.*

Proof. For the sake of brevity, we begin by letting $a = \frac{1}{(\sigma_d g)^2} \frac{\zeta}{(1-\zeta)^2}$ and writing

$$\text{ACV}^2 \bar{P}(n_1, n_2|\zeta, \sigma_d, g) = a \left(\frac{1}{n_1} + \frac{\zeta}{n_2} \right).$$

If $\zeta \in (0, 1)$, then $a \neq 0$ and $\text{ACV}^2 \bar{P}(N - n_2, n_2|\theta_{\bar{P}})$ is smooth and strictly convex in n_2 on $(0, N)$. Additionally, the limiting value of $\text{ACV}^2 \bar{P}(N - n_2, n_2|\theta_{\bar{P}})$ at the endpoints $n_2 = 0, N$ is infinite and so we know our optimization problem is nondegenerate. These observations lead us to conclude that (3.12) can be uniquely solved by

$$\begin{aligned} \partial_{n_2} \text{ACV}^2 \bar{P}(N - n_2, n_2|\theta_{\bar{P}}) \Big|_{(N, n_2) = (n_1^{\text{opt}} + n_2^{\text{opt}}, n_2^{\text{opt}})} &= 0 \\ \text{ACV}^2 \bar{P}(n_1^{\text{opt}}, n_2^{\text{opt}}|\theta_{\bar{P}}) - \text{acv}_0^2 &= 0, \end{aligned}$$

which upon substituting appropriate values produces the system of equations

$$\begin{aligned} (1) \quad & a \left(\frac{1}{(n_1^{\text{opt}})^2} - \frac{\zeta}{(n_2^{\text{opt}})^2} \right) = 0 \\ (2) \quad & a \left(\frac{1}{n_1^{\text{opt}}} + \frac{\zeta}{n_2^{\text{opt}}} \right) - \text{acv}_0^2 = 0. \end{aligned}$$

Upon inspection, (1) gives us the optimality relation $n_2^{\text{opt}}/n_1^{\text{opt}} = \sqrt{\zeta}$ and so as $\zeta \searrow 1$ we have $n_2^{\text{opt}}/n_1^{\text{opt}} \rightarrow 1$ which is the first claim. Substituting the optimality relation into (2) and solving for n_2^{opt} further yields $n_2^{\text{opt}} = a/\text{acv}_0^2(\sqrt{\zeta} + \zeta)$. Making use of this result and again calling on the optimality relation we have after reintroducing a :

$$\begin{aligned} n_1^{\text{opt}} &= \frac{1}{(\sigma_{\text{dg}})^2 \text{acv}_0^2} \frac{\zeta(1 + \sqrt{\zeta})}{(1 - \zeta)^2} \\ n_2^{\text{opt}} &= \frac{1}{(\sigma_{\text{dg}})^2 \text{acv}_0^2} \frac{\zeta(\sqrt{\zeta} + \zeta)}{(1 - \zeta)^2}. \end{aligned}$$

Now as $\zeta \searrow 1$, $\zeta(1 + \sqrt{\zeta}) \sim \zeta(\sqrt{\zeta} + \zeta) \sim 2 + \mathcal{O}(1 - \zeta)$; hence,

$$n_i^{\text{opt}} \sim \frac{2}{(\sigma_{\text{dg}})^2 \text{acv}_0^2} (1 - \zeta)^{-2} + \mathcal{O}((1 - \zeta)^{-1}), \quad i = 1, 2$$

which proves the second claim. Recall that we assumed $\zeta \in (0, 1)$ so as to render our optimization problem nondegenerate. However, one can obtain the optimal sample sizes at the endpoints $\zeta = 1$ and $\zeta = 0$ by considering the appropriate limits, the latter of which gives us the degenerate case $(n_1^{\text{opt}}, n_2^{\text{opt}}) = (0, 0)$. The proof is now complete. \square

In Lemma 29 we studied the optimal sample sizes for \bar{P} that satisfied Definition 11 and the constraint $\text{ACV}\bar{P} = \text{acv}_0$. Unlike \bar{P} , the estimator \mathcal{T}_ν is biased so we will investigate its optimal sample sizes w.r.t. a desired outcome for both $\text{ACV}\mathcal{T}_\nu$ and $\text{ARB}\mathcal{T}_\nu$. We could also choose $\text{ARB}\mathcal{T}_\nu = \text{arb}_0$ to be constant but this may not always be desirable as will be seen in later sections. In particular, notice that for any $\nu > 0$, $\text{ARB}\mathcal{T}_\nu = \zeta^\nu \rightarrow 0$ in the shot noise limit $\zeta \nearrow 0$. As such, forcing a bias on \mathcal{T}_ν in the shot noise limit by requiring $\text{ARB}\mathcal{T}_\nu = \text{arb}_0$ could be viewed as counterproductive in certain contexts. These observations steer us in the direction of specifying a constraint on $\text{ARB}\mathcal{T}_\nu$ that varies with illumination level and vanishes in the shot noise limit. To help aid in our discussion we introduce the notion of the *bias profile*.

Definition 12 (Bias profile). *Let $T \sim F_T(\theta_T)$ be an estimator of $g(\theta_T) \neq 0$ for which $\text{ARB}T = \rho(\theta_T)$. Then we say $\rho(\theta_T)$ is the bias profile for T .*

Given the simplicity of the expression for $\text{ARB}\mathcal{T}_\nu$ we can choose just about any bias profile we desire by setting $\nu = \log_\zeta \rho$. With so many available options we will aim for simplicity and proceed with the following.

Definition 13. *For $\zeta \in [0, 1]$, $\text{arb}_0 \in (0, 1)$, and $b \in \mathbb{R}_0^+$, $\nu^\dagger := \log_\zeta \text{arb}_0 + b$.*

Proposition 7. *Let ν^\dagger be as defined in Definition 13. Then, the bias profile of $\mathcal{T}_{\nu^\dagger}$ is $\rho = \text{arb}_0 \zeta^b$.*

This choice of bias profile is useful since it is simple and guarantees $\text{ARB}\mathcal{T}_{\nu^\dagger} \leq \text{arb}_0$ everywhere on $\zeta \in [0, 1]$. Furthermore, the parameter b provides the flexibility to choose a constant bias profile ($b = 0$) or a profile that vanishes to zero

in the shot noise limit ($b > 0$). With this matter out of the way we present Lemmas 30-32, which provide us with the necessary results for studying the behavior of the optimal sample sizes of $\mathcal{T}_{\nu^\dagger}$ under low-illumination conditions in Theorem 17.

Definition 14 (Lower-incomplete gamma function). *For $\Re s > 0$*

$$\gamma(s, z) := \int_0^z t^{s-1} e^{-t} dt.$$

Lemma 30. *Let ν^\dagger be as define in Definition 13. Then as $\zeta \searrow 1$*

$$\tilde{g}_{n,\omega}(\zeta, \nu^\dagger) \sim \frac{\gamma(n+1, -\log \text{arb}_0)}{1 - \text{arb}_0} (1 - \zeta)^{-n} + \mathcal{O}((1 - \zeta)^{1-n}),$$

where $\gamma(s, z)$ is the lower-incomplete gamma function of Definition 14.

Proof. From Corollary 10 form (iii) we have

$$(1 - \zeta)^n \tilde{g}_{n,\omega}(\zeta, \nu^\dagger) = n! \frac{\zeta^{n-\omega} - \text{arb}_0 \zeta^b \sum_{k=0}^n \frac{(\log_\zeta \text{arb}_0 + b - n + \omega)_k}{k!} (1 - \zeta)^k}{1 - \text{arb}_0 \zeta^b}.$$

As $\zeta \searrow 1$, one may use the generalized binomial theorem to deduce $\zeta^x \sim 1 + \mathcal{O}(1 - \zeta)$. Furthermore, we also determine as $\zeta \searrow 1$: $\log_\zeta \text{arb}_0 \rightarrow \infty$ so that $(\log_\zeta \text{arb}_0 + b - n + \omega)_k \sim \log_\zeta^k \text{arb}_0$ and $[(1 - \zeta) \log_\zeta \text{arb}_0]^k \sim (-\log \text{arb}_0)^k (1 + \mathcal{O}(1 - \zeta))$. After making the appropriate substitutions and collecting terms we find

$$(1 - \zeta)^n \tilde{g}_{n,\omega}(\zeta, \nu^\dagger) \sim \Gamma(n+1) \frac{1 - \text{arb}_0 \sum_{k=0}^n \frac{(-\log \text{arb}_0)^k}{k!}}{1 - \text{arb}_0} + \mathcal{O}(1 - \zeta),$$

which according to [27, Eq. 06.06.03.0009.01] can be written in terms of the lower incomplete gamma function. Solving for $\tilde{g}_{n,\omega}$ completes the proof. \square

Definition 15 (Polygamma function). *For $n \in \mathbb{N}_0$,*

$$\psi^{(n)}(z) := \partial_z^{n+1} \log \Gamma(z).$$

Lemma 31. *Let $(\alpha_1, \alpha_2) \in \mathbb{R}^+ \times \mathbb{R}^+$ and*

$$f_k(\alpha_1, \alpha_2) = \sum_{\ell=0}^k \frac{1}{(\alpha_1)_\ell (\alpha_2)_{k-\ell} \ell! (k-\ell)!}, \quad k \in \mathbb{N}.$$

Then for all k and some constant $A > 0$, the optimal pair $(\alpha_1^{\text{opt}}, \alpha_2^{\text{opt}})$ that minimize f_k subject to $A = \alpha_1 + \alpha_2$ is

$$(\alpha_1^{\text{opt}}, \alpha_2^{\text{opt}}) = (\tfrac{1}{2}A, \tfrac{1}{2}A).$$

Proof. Working with the properties of the Pochhammer symbol and Relation 12 we may write f_k in the equivalent form

$$f_k(\alpha_1, \alpha_2) = \frac{1}{k!} \frac{(\alpha_1 + \alpha_2 - 1 + k)_k}{(\alpha_1)_k (\alpha_2)_k}.$$

Substituting $A = \alpha_1 + \alpha_2$ and differentiating w.r.t. α_2 yields

$$\partial_{\alpha_2} f_k(A - \alpha_2, \alpha_2) = f_k(A - \alpha_2, \alpha_2) \Psi_k^{(0)}(A - \alpha_2, \alpha_2),$$

where

$$\Psi_k^{(0)}(\alpha_1, \alpha_2) = \psi^{(0)}(\alpha_1 + k) - \psi^{(0)}(\alpha_1) - \psi^{(0)}(\alpha_2 + k) + \psi^{(0)}(\alpha_2)$$

and $\psi^{(n)}(z)$ is the polygamma function of Definition 15. By repeated application of the recurrence relation $\psi^{(n)}(z + 1) = \psi^{(n)}(z) + (-1)^n n! z^{-n-1}$ we deduce

$$\Psi_k^{(0)}(\alpha_2) = \sum_{m=0}^{k-1} \left(\frac{1}{A - \alpha_2 + m} - \frac{1}{\alpha_2 + m} \right) \begin{cases} < 0, & 0 < \alpha_2 < \frac{1}{2}A \\ = 0, & \alpha_2 = \frac{1}{2}A \\ > 0, & \frac{1}{2}A < \alpha_2 < A. \end{cases}$$

Further noting that $f_k(A - \alpha_2, \alpha_2)$ is positive proves it has a unique global minimum at $\alpha_2 = \frac{1}{2}A$, which completes the proof. \square

Definition 16 (Exponential integral function).

$$\text{Ei}(z) := \int_0^z \frac{e^t - 1}{t} dt + \frac{1}{2} \left(\log z - \log \left(\frac{1}{z} \right) \right) + \gamma,$$

where $\gamma = 0.577216 \dots$ is the Euler-Mascheroni constant.

Lemma 32. For $c, x \in \mathbb{R}$

$$\int_{[0, x]^2} e^{-u+cu v-v} du dv = \frac{1}{c} e^{-1/c} \left(\text{Ei} \left(\frac{1}{c} \right) - 2 \text{Ei} \left(\frac{1}{c}(1 - cx) \right) + \text{Ei} \left(\frac{1}{c}(1 - cx)^2 \right) \right),$$

where $\text{Ei}(z)$ is the exponential integral function of Definition 16.

Proof. Let I denote the integral in question. Integrating w.r.t. u and then substituting $t = (cv - 1)x$ yields

$$I = \frac{1}{c} e^{-1/c} \int_{-x}^{x(cx-1)} e^{-t/(cx)} \frac{e^t - 1}{t} dt.$$

With a bit of algebra we may further write

$$I = \frac{1}{c} e^{-1/c} \left(\int_{-x}^{x(cx-1)} \frac{e^{(1-1/(cx))t} - 1}{t} dt - \int_{-x}^{x(cx-1)} \frac{e^{-1/(cx)t} - 1}{t} dt \right).$$

Now substituting $s = (1 - 1/(cx))t$ and $s = -1/(cx)t$ into the first and second integral, respectively, we have after some simplification

$$I = \frac{1}{c} e^{-1/c} \left(\int_0^{1/c} -2 \int_0^{(1-cx)/c} + \int_0^{(1-cx)^2/c} \right) \frac{e^s - 1}{s} ds.$$

From Definition 16, if $z \in \mathbb{R}$ then $\int_0^z \frac{1}{t} (e^t - 1) dt = \text{Ei}(z) - \log|z| - \gamma$. Substituting this result into I , all of the logarithmic and constant terms cancel leaving us with the desired result. \square

Theorem 17. Let $(n_1^{\text{opt}}, n_2^{\text{opt}})$ denote the optimal sample sizes for $\mathcal{T}_{\nu^\dagger}$ that also satisfy $\text{ACV}_{\mathcal{T}_{\nu^\dagger}}(n_1^{\text{opt}}, n_2^{\text{opt}} | \zeta, \nu^\dagger) = \text{acv}_0$ and $\text{ARB}_{\mathcal{T}_{\nu^\dagger}} = \text{arb}_0 \zeta^b$ for $\text{acv}_0 \in \mathbb{R}^+$, $\text{arb}_0 \in (0, 1)$, and $b \in \mathbb{R}_0^+$ fixed. Then as illumination decreases, $\zeta \searrow 1$, $n_2^{\text{opt}}/n_1^{\text{opt}} \rightarrow 1$, and $n_i^{\text{opt}} \sim C_{\mathcal{T}_{\nu^\dagger}}(1 - \zeta)^{-2}$ where $C_{\mathcal{T}_{\nu^\dagger}}$ is the solution to

$$\overline{\text{ACV}^2 \mathcal{T}_{\nu^\dagger}}(C_{\mathcal{T}_{\nu^\dagger}}, \text{arb}_0) - \text{acv}_0^2 = 0$$

with

$$\begin{aligned} \overline{\text{ACV}^2 \mathcal{T}_{\nu^\dagger}} = \frac{(C_{\mathcal{T}_{\nu^\dagger}}/4)e^{-C_{\mathcal{T}_{\nu^\dagger}}/4}}{(1 - \text{arb}_0)^2} & \left(\text{Ei}\left(\frac{C_{\mathcal{T}_{\nu^\dagger}}}{4}\right) - 2 \text{Ei}\left(\log \text{arb}_0 + \frac{C_{\mathcal{T}_{\nu^\dagger}}}{4}\right) \right. \\ & \left. + \text{Ei}\left(\frac{(C_{\mathcal{T}_{\nu^\dagger}}/4 + \log \text{arb}_0)^2}{C_{\mathcal{T}_{\nu^\dagger}}/4}\right) \right) - 1 \end{aligned}$$

and $\text{Ei}(z)$ is the exponential integral function of Definition 16.

Proof. First note that $\mathcal{T}_{\nu^\dagger}$ satisfies the constraint $\text{ARB}_{\mathcal{T}_{\nu^\dagger}} = \text{arb}_0 \zeta^b$ independent of n_1 and n_2 . Using the result of Lemma 30 and the relationship $\alpha_i = (n_i - 1)/2$ we deduce as $\zeta \searrow 1$

$$\text{ACV}^2 \mathcal{T}_{\nu^\dagger}(n_1, n_2 | \zeta, \text{arb}_0, b) \sim \sum_{k=1}^{\infty} \frac{f_k\left(\frac{n_1-1}{2}, \frac{n_2-1}{2}\right)}{(1 - \zeta)^{2k}} (a_k^2(\text{arb}_0) + \mathcal{O}(1 - \zeta)),$$

where $f_k(\alpha_1, \alpha_2)$ is as defined in Lemma 31 and $a_k(\text{arb}_0) = \gamma(k+1, -\log \text{arb}_0)/(1 - \text{arb}_0)$. By Lemma 31 we know that the optimal sample sizes $(n_1^{\text{opt}}, n_2^{\text{opt}})$ that minimizes f_k with $N = n_1 + n_2$ fixed occurs when $n_1 = n_2$; thus, $n_2^{\text{opt}}/n_1^{\text{opt}} \rightarrow 1$ as $\zeta \searrow 1$ which is our first claim. Letting $n_1^{\text{opt}} = n_2^{\text{opt}} = n^{\text{opt}}$ we have

$$\text{ACV}^2 \mathcal{T}_{\nu^\dagger}(n_1^{\text{opt}}, n_2^{\text{opt}} | \theta_{\mathcal{T}_{\nu^\dagger}}) \sim \sum_{k=1}^{\infty} \frac{f_k\left(\frac{n^{\text{opt}}-1}{2}, \frac{n^{\text{opt}}-1}{2}\right)}{(1 - \zeta)^{2k}} (a_k^2(\text{arb}_0) + \mathcal{O}(1 - \zeta)),$$

Since $(1 - \zeta)^{-2k}$ becomes arbitrarily large in the neighborhood of $\zeta = 1$ the function f_k must simultaneously become arbitrarily small as to maintain a finite value of $\text{ACV}^2 \mathcal{T}_{\nu^\dagger}$ in the limit. But $f_k((n^{\text{opt}} - 1)/2, (n^{\text{opt}} - 1)/2)$ is a decreasing function of n^{opt} so it must be that $n^{\text{opt}} \rightarrow \infty$ as $\zeta \searrow 1$. Making use of the

asymptotic relation $(s)_k \sim s^k(1 + \mathcal{O}(s^{-1}))$ as $s \rightarrow \infty$ and binomial theorem we deduce for $n^{\text{opt}} \rightarrow \infty$:

$$f_k\left(\frac{n^{\text{opt}}-1}{2}, \frac{n^{\text{opt}}-1}{2}\right) \sim \frac{1}{k!} \left(\frac{4}{n^{\text{opt}}}\right)^k + \mathcal{O}((n^{\text{opt}})^{-k-1}),$$

which upon substitution into our expression for $\text{ACV}^2 \mathcal{T}_{\nu^\dagger}$ gives

$$\begin{aligned} \text{ACV}^2 \mathcal{T}_{\nu^\dagger}(n_1^{\text{opt}}, n_2^{\text{opt}} | \theta_{\mathcal{T}_{\nu^\dagger}}) &\sim \sum_{k=1}^{\infty} \left(\frac{1}{k!} \left(\frac{4}{(1-\zeta)^2 n^{\text{opt}}} \right)^k + \frac{\mathcal{O}((n^{\text{opt}})^{-k-1})}{(1-\zeta)^{2k}} \right) \\ &\quad \cdots \times (a_k^2(\text{arb}_0) + \mathcal{O}(1-\zeta)). \end{aligned}$$

Given that we require $\text{ACV} \mathcal{T}_{\nu^\dagger} = \text{acv}_0 < \infty$ in the limit it follows that we must have $n^{\text{opt}} \sim C_{\mathcal{T}_{\nu^\dagger}}(1-\zeta)^{-2} + \mathcal{O}((1-\zeta)^{-1})$ for some positive constant $C_{\mathcal{T}_{\nu^\dagger}}$ which proves our second claim. Substituting this asymptotic form for n^{opt} into our expression for $\text{ACV}^2 \mathcal{T}_{\nu^\dagger}$ we see that all error terms are $\mathcal{O}(1-\zeta)$ so that upon passing to the limit we obtain

$$\lim_{\substack{\zeta \searrow 1 \\ \text{ACV} \mathcal{T}_{\nu^\dagger} = \text{acv}_0 \\ \text{ARB} \mathcal{T}_{\nu^\dagger} = \text{arb}_0 \zeta^b}} \text{ACV}^2 \mathcal{T}_{\nu^\dagger}(n_1^{\text{opt}}, n_2^{\text{opt}} | \theta_{\mathcal{T}_{\nu^\dagger}}) = \sum_{k=1}^{\infty} \frac{\gamma^2(k+1, -\log \text{arb}_0)}{(1-\text{arb}_0)^2} \frac{(4/C_{\mathcal{T}_{\nu^\dagger}})^k}{k!},$$

where $C_{\mathcal{T}_{\nu^\dagger}}$ is the positive constant that solves

$$\sum_{k=1}^{\infty} \frac{\gamma^2(k+1, -\log \text{arb}_0)}{(1-\text{arb}_0)^2} \frac{(4/C_{\mathcal{T}_{\nu^\dagger}})^k}{k!} = \text{acv}_0^2. \quad (3.13)$$

Letting $\overline{\text{ACV}^2 \mathcal{T}_{\nu^\dagger}}$ denote the series on the l.h.s. of (3.13) we use the integral representation of the lower incomplete gamma function in Definition 14 to write

$$\overline{\text{ACV}^2 \mathcal{T}_{\nu^\dagger}} = \lim_{n \rightarrow \infty} \int_{[0, -\log \text{arb}_0]^2} \frac{e^{-(u+v)}}{(1-\text{arb}_0)^2} \sum_{k=1}^n \frac{(4uv/C_{\mathcal{T}_{\nu^\dagger}})^k}{k!} du dv.$$

The integrand is the sum of nonnegative terms and is bounded above by its limiting form as $n \rightarrow \infty$ which in turn is integrable on the domain of integration; thus, by argument of dominated convergence we have

$$\overline{\text{ACV}^2 \mathcal{T}_{\nu^\dagger}} = \int_{[0, -\log \text{arb}_0]^2} \frac{e^{-u+4uv/C_{\mathcal{T}_{\nu^\dagger}}-v}}{(1-\text{arb}_0)^2} du dv - 1,$$

which is evaluated in terms of the exponential integral function with Lemma 32. The proof is now complete. \square

Figure 3.1 plots $C_{\mathcal{T}_{\nu^\dagger}}$ on the unit square. These values for $C_{\mathcal{T}_{\nu^\dagger}}$ were computed in MATHEMATICA using a Newton-Raphson iteration with starting point

$$C_{\mathcal{T}_{\nu^\dagger}}^* = \frac{2\gamma^2(2, -\log \text{arb}_0)}{\text{acv}_0^2(1-\text{arb}_0)^2} \left(1 + \left(1 + 2\text{acv}_0^2(1-\text{arb}_0)^2 \frac{\gamma^2(3, -\log \text{arb}_0)}{\gamma^4(2, -\log \text{arb}_0)} \right)^{1/2} \right),$$

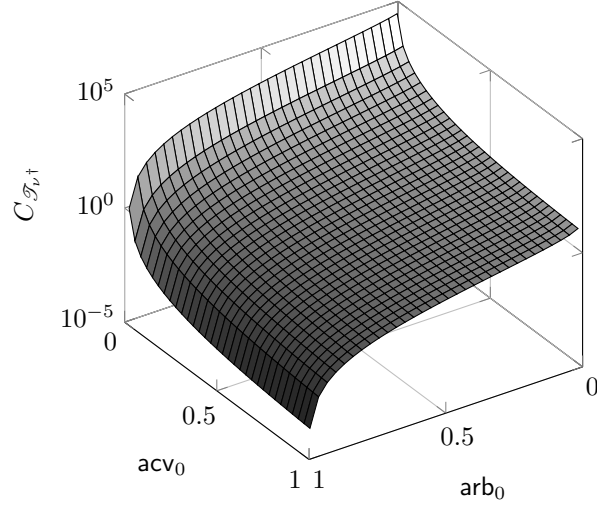


Figure 3.1: Plot of $C_{\mathcal{T}_{\nu^\dagger}}(arb_0, acv_0)$ on the unit square.

which is the solution to (3.13) using only the $k = 1, 2$ terms.

Since $ARB_{\mathcal{G}_\nu} = ARB_{\mathcal{T}_\nu}$ we may combine the results of Lemma 29 and Theorem 17 to make the following claims about the optimal sample sizes for $\mathcal{G}_{\nu^\dagger}$ at low illumination.

Corollary 14. *Let $(n_1^{\text{opt}}, n_2^{\text{opt}})$ denote the optimal sample sizes for $\mathcal{G}_{\nu^\dagger}$ that also satisfy $ACV_{\mathcal{G}_{\nu^\dagger}}(n_1^{\text{opt}}, n_2^{\text{opt}} | \zeta, \nu^\dagger, \sigma_d, g) = acv_0$ and $ARB_{\mathcal{G}_{\nu^\dagger}} = arb_0 \zeta^b$ for $acv_0 \in \mathbb{R}^+$, $arb_0 \in (0, 1)$, and $b \in \mathbb{R}_0^+$ fixed. Then as illumination decreases, $\zeta \searrow 1$, $n_2^{\text{opt}}/n_1^{\text{opt}} \rightarrow 1$, and $n_i^{\text{opt}} \sim C_{\mathcal{G}_{\nu^\dagger}}(1 - \zeta)^{-2}$ where $C_{\mathcal{G}_{\nu^\dagger}}$ is the solution to*

$$\overline{ACV^2_{\mathcal{G}_{\nu^\dagger}}}(C_{\mathcal{G}_{\nu^\dagger}}, arb_0, \sigma_d, g) - acv_0^2 = 0$$

with

$$\overline{ACV^2_{\mathcal{G}_{\nu^\dagger}}} = \overline{ACV^2_{\mathcal{T}_{\nu^\dagger}}}(C_{\mathcal{G}_{\nu^\dagger}}, arb_0) + 2 \frac{\overline{ACV^2_{\mathcal{T}_{\nu^\dagger}}}(C_{\mathcal{G}_{\nu^\dagger}}, arb_0)}{(\sigma_d g)^2 C_{\mathcal{G}_{\nu^\dagger}}} + \frac{2}{(\sigma_d g)^2 C_{\mathcal{G}_{\nu^\dagger}}}$$

and $\overline{ACV^2_{\mathcal{T}_{\nu^\dagger}}}$ given in Theorem 17.

Proof. Begin by writing

$$ACV^2_{\mathcal{G}_{\nu^\dagger}} = ACV^2_{\mathcal{T}_{\nu^\dagger}} + (ACV^2_{\mathcal{T}_{\nu^\dagger}})(ACV^2 \bar{P}) + ACV^2 \bar{P}.$$

As was the case in Theorem 17, $\mathcal{G}_{\nu^\dagger}$ satisfies the constraint on $ARB_{\mathcal{G}_\nu}$ independent of n_1 and n_2 . Furthermore, from Lemma 29 and Theorem 17 we know in the limit $\zeta \searrow 1$ that the optimal sample sizes for \bar{P} and $\mathcal{T}_{\nu^\dagger}$ are asymptotically equal and proportional to $(1 - \zeta)^{-2}$. Substituting $n_1^{\text{opt}} = n_2^{\text{opt}} \sim C_{\mathcal{G}_{\nu^\dagger}}(1 - \zeta)^{-2}$ and passing to the limit gives the desired expression for $\overline{ACV^2_{\mathcal{G}_{\nu^\dagger}}}$. \square

We are finally able to return to the questions surrounding the behavior of \mathcal{E} as a function of the optimal sample sizes at low illumination.

Corollary 15. *Let T stand in place for $\mathcal{T}_{\nu^\dagger}$ or $\mathcal{G}_{\nu^\dagger}$ and $(n_1^{\text{opt}}, n_2^{\text{opt}})$ denote the optimal sample sizes for T such that $\text{ACVT} = \text{acv}_0$ and $\text{ARBT} = \text{arb}_0 \zeta^b$ with $\text{acv}_0 \in \mathbb{R}^+$, $\text{arb}_0 \in (0, 1)$, and $b \in \mathbb{R}_0^+$ fixed. Furthermore, define \mathcal{E}_T to be the quantity \mathcal{E} as a function of $(n_1^{\text{opt}}, n_2^{\text{opt}})$ and $\overline{\mathcal{E}_T} = \lim_{\zeta \searrow 1} \mathcal{E}_T$. Then,*

$$\overline{\mathcal{E}_T} = \left(1 + (1 + \overline{\text{ACV}^{-2} \mathcal{T}_{\nu^\dagger}}(C_T, \text{arb}_0)) \frac{2}{(\sigma_{\text{dg}})^2 C_T} \right)^{-1},$$

where $\overline{\text{ACV}^2 \mathcal{T}_{\nu^\dagger}}$ is given in Theorem 17. In particular, if $T = \mathcal{T}_{\nu^\dagger}$:

$$\mathcal{E}_{\mathcal{T}_{\nu^\dagger}} = \left(1 + \frac{1 + \text{acv}_0^{-2}}{(\sigma_{\text{dg}})^2} \frac{\zeta}{(1 - \zeta)^2} \left(\frac{1}{n_1^{\text{opt}}} + \frac{\zeta}{n_2^{\text{opt}}} \right) \right)^{-1}$$

and

$$\overline{\mathcal{E}_{\mathcal{T}_{\nu^\dagger}}} = \left(1 + \frac{2(1 + \text{acv}_0^{-2})}{(\sigma_{\text{dg}})^2 C_{\mathcal{T}_{\nu^\dagger}}} \right)^{-1}.$$

Corollary 15 shows us that when one substitutes the optimal sample sizes for $\mathcal{T}_{\nu^\dagger}$ or $\mathcal{G}_{\nu^\dagger}$ into \mathcal{E} , the limit $\lim_{\zeta \searrow 1} \mathcal{E}_{\mathcal{T}_{\nu^\dagger}}$ is nonzero. Additionally, for the special case where the optimal sample sizes for $\mathcal{T}_{\nu^\dagger}$ are chosen, both $\mathcal{E}_{\mathcal{T}_{\nu^\dagger}}$ and $\overline{\mathcal{E}_{\mathcal{T}_{\nu^\dagger}}}$ reduce to very simple and easy to compute expressions. To get a sense for how $\overline{\mathcal{E}_{\mathcal{T}_{\nu^\dagger}}}$ behaves w.r.t. its parameters, Table 3.3 presents numerical values of this quantity for select values of σ_{dg} , arb_0 , and acv_0 . One can see for the chosen parameter values that the dark noise, denoted σ_{dg} , plays a significant role in the proximity of $\overline{\mathcal{E}_{\mathcal{T}_{\nu^\dagger}}}$ to one. Indeed, for σ_{dg} greater than about 5 e - we observe $\overline{\mathcal{E}_{\mathcal{T}_{\nu^\dagger}}} \approx 1$, which implies that the optimal sample sizes for $\mathcal{T}_{\nu^\dagger}$ and $\mathcal{G}_{\nu^\dagger}$ are nearly identical even at near zero illumination.

Using the optimal sample sizes of $\mathcal{T}_{\nu^\dagger}$ in place of those for $\mathcal{G}_{\nu^\dagger}$ is not just convenient for producing a compact expression for \mathcal{E} . When measuring g in an actual experiment, one cannot know the optimal sample sizes with certainty because they are based on unknown parameters. For $\mathcal{T}_{\nu^\dagger}$, the optimal sample sizes are a function of $\zeta = \sigma_{\text{d}}^2 / \sigma_{\text{p+d}}^2$, which is itself a function of two unknown parameters that must be estimated. This problem is compounded when considering optimal sample sizes for $\mathcal{G}_{\nu^\dagger}$ which are a function of $(\sigma_{\text{d}}^2, g, \zeta)$ and thus require estimating four parameters, i.e. $(\mu_{\text{d}}, \mu_{\text{p+d}}, \sigma_{\text{d}}, \sigma_{\text{p+d}})$. The two additional degrees of freedom render estimating the optimal sample sizes for $\mathcal{G}_{\nu^\dagger}$ in a real experiment impractical due to the amount of uncertainty introduced in the process of estimation. Instead, it is far better to measure g in a region where $\mathcal{E} \approx 1$ so that the optimal sample sizes for $\mathcal{T}_{\nu^\dagger}$ can be substituted. As has been demonstrated here, this situation is possible even when the illumination level is near zero small provided a sufficiently large dark noise.

3.5.2 Computation of optimal sample sizes for $\mathcal{T}_{\nu^\dagger}$

Given that the optimal samples sizes for $\mathcal{T}_{\nu^\dagger}$ are most desirable for experimentation, this section is dedicated to further studying their characteristics as well

$\text{arb}_0/\text{acv}_0$	$\sigma_d g = 1 e-$			$\sigma_d g = 2 e-$		
	0.01	0.02	0.05	0.01	0.02	0.05
0.01	0.645	0.645	0.646	0.879	0.879	0.879
0.02	0.629	0.629	0.629	0.871	0.871	0.872
0.05	0.587	0.587	0.587	0.850	0.850	0.850

$\text{arb}_0/\text{acv}_0$	$\sigma_d g = 5 e-$			$\sigma_d g = 10 e-$		
	0.01	0.02	0.05	0.01	0.02	0.05
0.01	0.978	0.978	0.979	0.995	0.995	0.995
0.02	0.977	0.977	0.977	0.994	0.994	0.994
0.05	0.973	0.973	0.973	0.993	0.993	0.993

Table 3.3: $\overline{\mathcal{E}_{\mathcal{T}_{\nu^\dagger}}}$ for select values of $\sigma_d g$, arb_0 , and acv_0 .

as computing them. Our approach will be organized as follows. We will begin by using the analysis in Section 2.4.1 to derive a few results pertaining to zeros and special values of $\tilde{g}_{n,\omega}(z, \nu)$ evaluated at $(z, \nu) = (\zeta, \nu^\dagger)$. These results will then allow us to write the system of equations needed to solve for the optimal sample sizes $(n_1^{\text{opt}}, n_2^{\text{opt}})$ as well as provide exact solutions at two points of interest. From here we will derive explicit approximations for the optimal sample sizes and use our previous findings to determine the usefulness of these approximations. Finally, the derived approximations will be used as the starting point in numerical methods to compute $(n_1^{\text{opt}}, n_2^{\text{opt}})$, which will be demonstrated for some sample values.

The following proposition defines some notation needed to discuss the zeros of $\tilde{g}_{n,\omega}(\zeta, \nu^\dagger)$ in Lemma 33.

Proposition 8. *Let $\nu^\dagger(\zeta) = \log_\zeta \text{arb}_0 + b$ be a function of ζ as defined in Definition 13, $\mathbb{N}_b := \{n \in \mathbb{N}_0 : n \geq b\}$, $\zeta_{b,n} := \sqrt[n-b]{\text{arb}_0} \mathbb{1}_{b < n}$, and $Z_b := \{\zeta_{b,n} : n \in \mathbb{N}_b\}$. Then,*

- (1) $\nu^\dagger(\zeta)$ is strictly increasing from $[0, 1]$ onto $[b, \infty)$,
- (2) $\nu^\dagger[Z_b] = \mathbb{N}_b$.

Lemma 33 (Zeros of $\tilde{g}_{n,\omega}(\zeta, \nu^\dagger)$).

$$\tilde{g}_{n,\omega}(\zeta, \nu^\dagger) = 0 \iff (n, n - \omega) \in \mathbb{N}^2 \wedge (\zeta = 0 \vee (\zeta \in Z_b \setminus \{0\} \wedge n - \omega \geq \nu^\dagger)).$$

Proof. The proof follows from Lemma 17 which states

$$\tilde{g}_{n,\omega}(\zeta, \nu^\dagger) = 0 \iff A \vee B,$$

with $A = (n \in \mathbb{N} \wedge n > \omega \wedge \nu^\dagger \in \mathbb{R}_0^+ \wedge z = 0)$ and $B = (n - \omega - \nu^\dagger \in \mathbb{N}_0 \wedge \nu^\dagger \neq 0)$. Starting with A notice that $\nu^\dagger \in \mathbb{R}_0^+$ always holds so that we may equivalently

write $A = ((n, n - \omega) \in \mathbb{N}^2 \wedge \zeta = 0)$. Next, consider B and observe that a necessary condition for $\nu^\dagger = 0$ is $\zeta = 0$. Since the condition $\zeta = 0$ is already covered by A we may write $B = (n - \omega - \nu^\dagger \in \mathbb{N}_0 \wedge \zeta \neq 0)$. Furthermore, $n - \omega - \nu^\dagger \in \mathbb{N}_0$ requires ν^\dagger to be an integer and $n - \omega \geq \nu^\dagger$. But ν^\dagger can only be an integer if $\zeta \in Z_b$ so that $B = (n - \omega \geq \nu^\dagger \wedge \zeta \in Z_b \setminus \{0\})$. But the conditions specified by B implicitly require $n - \omega \geq 1 \implies (n, n - \omega) \in \mathbb{N}^2$ so that this requirement can be factored out of A and B leaving us with the desired result. \square

Corollary 16. *For all $(\zeta, \nu^\dagger) \in [0, 1] \times [b, \infty)$*

$$n = \omega \implies \tilde{g}_{n,\omega}(\zeta, \nu^\dagger) \neq 0.$$

Furthermore,

$$\tilde{g}_{n,\omega}(\zeta, \nu^\dagger) = 0, \forall (n, n - \omega) \in \mathbb{N}^2 \iff \zeta \in \{0, \zeta_{b,1}\}.$$

Proof. The first claim immediately follows from Lemma 33 since $n = \omega \implies n - \omega = 0 \notin \mathbb{N}$. Furthermore, the conditions of Lemma 33 are always satisfied if $(n, n - \omega) \in \mathbb{N}^2$ and $\zeta = 0 \vee \nu^\dagger = 1$, where the latter holds if and only if $\zeta \in \{0, \zeta_{b,1}\}$. \square

Corollary 16 will turn out to be very important in determining the behavior of optimal sample sizes of $\mathcal{T}_{\nu^\dagger}$. In particular, the results of this corollary indicate that $\zeta = 0$ and $\zeta = \zeta_{b,1}$ are the only values of ζ for which $\tilde{g}_{n,\omega}(\zeta, \nu^\dagger) = 0$ for all $n > \omega$. We shall see that these two points of interest corresponds to the only ζ -values that render the optimization problem for the optimal sample sizes of $\mathcal{T}_{\nu^\dagger}$ weakly degenerate. Before proceeding, we need one more result, which gives us the expression for $\tilde{g}_{n,n}(\zeta, \nu^\dagger)$ at $\zeta = 0, \zeta_{b,1}$.

Lemma 34. *Let $L \in \{0, \zeta_{b,1}\}$. Then $\lim_{\zeta \nearrow L} \tilde{g}_{n,n}(\zeta, \nu^\dagger) = n!$ for all $n \in \mathbb{N}_0$.*

Proof. From Corollary 10 form (iii) we have for all $n \in \mathbb{N}_0$:

$$\tilde{g}_{n,n}(\zeta, \nu^\dagger) = n! \frac{1 - \text{arb}_0 \zeta^b \sum_{k=0}^n \frac{(\nu^\dagger)_k}{k!} (1 - \zeta)^k}{(1 - \zeta)^n (1 - \text{arb}_0 \zeta^b)}.$$

Each case is now examined separately.

(1) $\zeta \nearrow 0$.

Proof. If $b > 0$ then $\zeta \nearrow 0 \implies \zeta^b \nearrow 0$ and so $\tilde{g}_{n,n}(\zeta, \nu^\dagger_{b>0}) \rightarrow n!$. Likewise, if $b = 0$ then $\zeta^b = 1$ while $(\nu^\dagger)_k \rightarrow \mathbf{1}_{k=0}$ and so again we find $\tilde{g}_{n,n}(\zeta, \nu^\dagger_{b=0}) \rightarrow n!$ as expected. \blacksquare

(2) $\zeta \nearrow \zeta_{b,1}$.

Proof. If $b \geq 1$ then $\zeta_{b,1} = 0$, which was already covered in part (1). Now suppose $0 \leq b \leq 1$. As $\zeta \nearrow \zeta_{b,1}$: $\nu^\dagger \rightarrow 1$ and $\text{arb}_0 \zeta^b \rightarrow \zeta_{b,1}$; hence

$$\lim_{\zeta \nearrow \zeta_{b,1}} \tilde{g}_{n,n}(\zeta, \nu^\dagger_{b \in [0,1]}) = n! \frac{1 - \zeta_{b,1} \sum_{k=0}^n (1 - \zeta_{b,1})^k}{(1 - \zeta_{b,1})^{n+1}} = n!,$$

which completes the proof. ■

□

Our next task is to derive the system of equations needed for computing the optimal sample sizes. Since $\text{ACV} \mathcal{T}_{\nu^\dagger}$ is naturally parameterized in terms of the shape parameters α_1 and α_2 and not the sample sizes n_1 and n_2 our discussion will focus on finding the optimal shape parameters according to Definition 11, knowing that we may convert these optimal shape parameters to their corresponding sample sizes through the relation $n_i^{\text{opt}} = 2\alpha_i^{\text{opt}} + 1$. As was done in Lemma 29 we will accomplish this task by letting $A = \alpha_1 + \alpha_2$ be constant and then showing that $\text{ACV}^2 \mathcal{T}_\nu(A - \alpha_2, \alpha_2)$ is: (1) twice continuously differentiable and strictly convex on $\alpha_2 \in (0, A)$ and (2) is infinite at the endpoints $\alpha_2 = 0, A$ with the exception of two points of interest. These findings will then be used to show that the minimization in (3.12) can be uniquely solved by equating a derivative with zero. The following result presents and intermediate step in demonstrating convexity of $\text{ACV}^2 \mathcal{T}_\nu(A - \alpha_2, \alpha_2)$.

Lemma 35. *Let $k \in \mathbb{N}$, $A > 0$, $\zeta \in [0, 1]$, and ν^\dagger be as defined in Definition 13. Then,*

$$f_k(\alpha_2 | A, \zeta, \nu^\dagger) := \sum_{\ell=0}^k \frac{\tilde{g}_{k,\ell}^2(\zeta, \nu^\dagger)}{(A - \alpha_2)_\ell (\alpha_2)_{k-\ell} \ell! (k - \ell)!}$$

is positive and strictly convex on $\alpha_2 \in (0, A)$. Furthermore,

$$\lim_{\alpha_2 \nearrow 0} f_k(\alpha_2 | \cdot) = \begin{cases} k! / (A)_k, & \zeta \in \{0, \zeta_{b,1}\} \\ \infty, & \text{otherwise} \end{cases}$$

and

$$\lim_{\alpha_2 \searrow A} f_k(\alpha_2 | \cdot) = \infty.$$

Proof. The claim of positivity comes from the fact that the summand of f_k is nonnegative and from Corollary 16 which implies $\tilde{g}_{n,\omega}(\zeta, \nu^\dagger) \neq 0$ for at least one $\ell \in \{0, \dots, k\}$. For the claim of convexity we first write

$$\partial_{\alpha_2}^2 \frac{1}{(A - \alpha_2)_\ell (\alpha_2)_{k-\ell}} = \frac{[\Psi_{k,\ell}^{(0)}(A - \alpha_2, \alpha_2)]^2 + \Psi_{k,\ell}^{(1)}(A - \alpha_2, \alpha_2)}{(A - \alpha_2)_\ell (\alpha_2)_{k-\ell}},$$

where

$$\begin{aligned} \Psi_{k,\ell}^{(0)}(\alpha_1, \alpha_2) &= \psi^{(0)}(\alpha_1) - \psi^{(0)}(\alpha_1 + \ell) - \psi^{(0)}(\alpha_2) + \psi^{(0)}(\alpha_2 + k - \ell) \\ \Psi_{k,\ell}^{(1)}(\alpha_1, \alpha_2) &= \psi^{(1)}(\alpha_1) - \psi^{(1)}(\alpha_1 + \ell) + \psi^{(1)}(\alpha_2) - \psi^{(1)}(\alpha_2 + k - \ell). \end{aligned}$$

Certainly, $[\Psi_{k,\ell}^{(0)}(A - \alpha_2, \alpha_2)]^2 \geq 0$ for all k, ℓ , and $\alpha_2 \in (0, A)$. Furthermore,

$$\Psi_{k,\ell}^{(1)}(A - \alpha_2, \alpha_2) = \sum_{j=0}^{\ell-1} \frac{1}{(A - \alpha_2 + j)^2} + \sum_{j=0}^{k-\ell-1} \frac{1}{(\alpha_2 + j)^2}.$$

Since $(k, \ell) \in (\mathbb{N}, \mathbb{N}_0)$ with $\ell \leq k$, it follows that at least one of these sums will be nonzero such that $\Psi_{k,\ell}^{(1)}(A - \alpha_2, \alpha_2) > 0$ and $[(A - \alpha_2)_\ell (\alpha_2)_{k-\ell}]^{-1}$ is a strictly convex function of α_2 on $(0, A)$. Combining this observation with the fact that there is always at least one $\ell \in \{0, \dots, k\}$ for which $\tilde{g}_{k,\ell}(\zeta, \nu^\dagger) \neq 0$ further implies that f_k is a finite sum of at least one positive strictly convex function with the rest of the terms being either being zero or also positive and strictly convex; hence, f_k is positive and strictly convex on $\alpha_2 \in (0, A)$.

Now turning to the limits notice that if $\zeta \in \{0, \zeta_{b,1}\}$ then by Corollary 16 and Lemma 34 we have $f_k(\alpha_2|\cdot) = \tilde{g}_{k,k}^2(\zeta, \nu^\dagger)/((A - \alpha_2)_k k!) \rightarrow k!/(A)_k$ as $\alpha_2 \nearrow 0$. For the complementary case $\zeta \in [0, 1] \setminus \{0, \zeta_{b,1}\}$ we may use the asymptotic expansion $\frac{1}{(x)_m} \sim \frac{1}{\Gamma(m)}(\frac{1}{x} - H_{m-1} + \mathcal{O}(x))$ for $x \rightarrow 0$ and Lemma 34 to further deduce

$$f_k(\alpha_2|\cdot) \sim \frac{k!}{(A)_k} + \mathcal{O}(\alpha_2^{-1}) \rightarrow \infty$$

as $\alpha_2 \nearrow 0$. For the other limit $\alpha_2 \searrow A$, Corollary 16 tells us that the $\ell = 0$ term in f_k is always positive; hence, as $\alpha_2 \searrow A$

$$f_k(\alpha_2|\cdot) \sim \mathcal{O}((A - \alpha_2)^{-1}) \rightarrow \infty,$$

which completes the proof. \square

Theorem 18 (Optimal sample sizes of $\mathcal{T}_{\nu^\dagger}$). *Let $(n_1^{\text{opt}}, n_2^{\text{opt}})(\theta_{\mathcal{T}_{\nu^\dagger}})$ with $\theta_{\mathcal{T}_{\nu^\dagger}} = (\zeta, \text{acv}_0, \text{arb}_0, b)$ denote the optimal sample sizes for $\mathcal{T}_{\nu^\dagger}$ as a function of $\theta_{\mathcal{T}_{\nu^\dagger}}$ that also satisfy $\text{ACV}_{\mathcal{T}_{\nu^\dagger}}(n_1^{\text{opt}}, n_2^{\text{opt}}|\theta_{\mathcal{T}_{\nu^\dagger}}) = \text{acv}_0$ and $\text{ARB}_{\mathcal{T}_{\nu^\dagger}} = \text{arb}_0 \zeta^b$ for $\text{acv}_0 \in \mathbb{R}^+$, $\text{arb}_0 \in (0, 1)$, and $b \in \mathbb{R}_0^+$ fixed. Then, for $\zeta \in \{0, \zeta_{b,1}\}$:*

$$(n_1^{\text{opt}}, n_2^{\text{opt}})(\theta_{\mathcal{T}_{\nu^\dagger}}) = (2\text{acv}_0^{-2} + 5, 1).$$

Likewise, for all remaining $\zeta \in [0, 1] \setminus \{0, \zeta_{b,1}\}$:

$$(n_1^{\text{opt}}, n_2^{\text{opt}})(\theta_{\mathcal{T}_{\nu^\dagger}}) = (2\alpha_1^{\text{opt}} + 1, 2\alpha_2^{\text{opt}} + 1)(\theta_{\mathcal{T}_{\nu^\dagger}}),$$

where α_1^{opt} and α_2^{opt} satisfy

$$\begin{aligned} \partial_{\alpha_2} \text{ACV}^2 \mathcal{T}_{\nu^\dagger}(A - \alpha_2, \alpha_2|\theta_{\mathcal{T}_{\nu^\dagger}}) \Big|_{(A, \alpha_2) = (\alpha_1^{\text{opt}} + \alpha_2^{\text{opt}}, \alpha_2^{\text{opt}})} &= 0 \\ \text{ACV}^2 \mathcal{T}_{\nu^\dagger}(\alpha_1^{\text{opt}}, \alpha_2^{\text{opt}}|\theta_{\mathcal{T}_{\nu^\dagger}}) - \text{acv}_0^2 &= 0. \end{aligned} \quad (3.14)$$

Proof. We begin with the special case $\zeta \in \{0, \zeta_{b,1}\}$ and call upon Corollary 16 and Lemma 34 to find

$$\text{ACV}^2 \mathcal{T}_{\nu^\dagger}(\alpha_1, \alpha_2|\theta_{\mathcal{T}_{\nu^\dagger}}) = \sum_{k=1}^{\infty} \frac{(1)_k (1)_k}{(\alpha_1)_k k!} = \frac{1}{\alpha_1 - 2}.$$

Since $\text{ACV}^2 \mathcal{T}_{\nu^\dagger}$ is independent of α_2 it follows that the optimization problem (3.14) is weakly degenerate so that $\alpha_2^{\text{opt}} = 0$ and α_1^{opt} satisfies

$$\frac{1}{\alpha_1^{\text{opt}} - 2} = \text{acv}_0^2.$$

Solving for α_1^{opt} and then using the relation $n_i^{\text{opt}} = 2n_i^{\text{opt}} + 1$ then gives the desired result for the special case $\zeta \in \{0, \zeta_{b,1}\}$.

Now consider the complementary case $\zeta \in [0, 1] \setminus \{0, \zeta_{b,1}\}$. Upon inspection of the double integral representation of $\text{E} \mathcal{T}_\nu^2$ in Theorem 9 and assuming appropriate values of (ζ, ν^\dagger) to guarantee convergence, we see that $\text{E} \mathcal{T}_\nu^2(A - \alpha_2, \alpha_2 | \theta_{\mathcal{T}_{\nu^\dagger}})$ is a smooth function of α_2 and hence so is $\text{ACV}^2 \mathcal{T}_{\nu^\dagger}(A - \alpha_2, \alpha_2 | \theta_{\mathcal{T}_{\nu^\dagger}})$. Additionally, upon writing

$$\text{ACV}^2 \mathcal{T}_\nu(A - \alpha_2, \alpha_2 | \theta_{\mathcal{T}_{\nu^\dagger}}) = \sum_{k=1}^{\infty} f_k(\alpha_2 | A, \theta_{\mathcal{T}_{\nu^\dagger}}),$$

we conclude from Lemma 35 that $\text{ACV}^2 \mathcal{T}_\nu(A - \alpha_2, \alpha_2 | \theta_{\mathcal{T}_{\nu^\dagger}})$ is: 1) positive and strictly convex on $\alpha_2 \in (0, A)$ and 2) infinite at the endpoints $\alpha_2 = 0, A$. As such, it follows that for every set of parameters $\theta_{\mathcal{T}_{\nu^\dagger}}$ with $\zeta \notin \{0, \zeta_{b,1}\}$ that $\alpha_2^{\text{opt}}(A, \theta_{\mathcal{T}_{\nu^\dagger}}) = \arg \inf_{\alpha_2 \in (0, A)} \text{ACV}^2 \mathcal{T}_\nu(A - \alpha_2, \alpha_2 | \theta_{\mathcal{T}_{\nu^\dagger}})$ is unique and corresponds to

$$\partial_{\alpha_2} \text{ACV}^2 \mathcal{T}_\nu(A - \alpha_2, \alpha_2 | \theta_{\mathcal{T}_{\nu^\dagger}})_{\alpha_2 = \alpha_2^{\text{opt}}} = 0.$$

This in turn implies the optimization problem for finding $(\alpha_1^{\text{opt}}, \alpha_2^{\text{opt}})$ is nondegenerate and is given by (3.14). The proof is now complete. \square

Taking a small detour, we now relate the optimal sample sizes for $\mathcal{T}_{\nu^\dagger}$ in Theorem 18 back to a classical result given by James Janesick in his book *Photon Transfer*.

Remark 3 (Optimal sample sizes in the shot noise limit). *Using the expression for $\mathcal{E}_{\mathcal{T}_{\nu^\dagger}}$ in Corollary 15 as well as the results from Theorem 18 it is straightforward to deduce*

$$\lim_{\zeta \nearrow 0} \mathcal{E}_{\mathcal{T}_{\nu^\dagger}} = 1,$$

which shows that the optimal sample sizes for $\mathcal{T}_{\nu^\dagger}$ equal those for $\mathcal{G}_{\nu^\dagger}$ in the shot noise limit. If one wants to obtain a 1% relative uncertainty for the measurement of g in the shot noise limit, i.e. $\lim_{\zeta \nearrow 0} \text{ACV} \mathcal{G}_{\nu^\dagger} = 0.01$, then according to Theorem 18 the optimal total number of samples needed is $N^{\text{opt}} = 20,006$. This exact result agrees with Janesick's estimate $N^{\text{opt}} \approx 20,000$ of [16, pgs. 79–81].

Up to this point we have made a significant amount of progress in studying the optimal sample sizes of $\mathcal{T}_{\nu^\dagger}$. In particular, we have established uniqueness of these optimal sample sizes, derived their exact expressions at the two points of interest $\zeta \in \{0, \zeta_{b,1}\}$, determined a system of equations for evaluating them at all remaining $\zeta \in [0, 1] \setminus \{0, \zeta_{b,1}\}$, studied their asymptotic behavior in the

low illumination limit $\zeta \searrow 1$, and derived the expression $\mathcal{E}_{\mathcal{T}_{\nu^\dagger}}$, which allow us to determine when they give a good approximation to the optimal sample sizes of $\mathcal{G}_{\nu^\dagger}$. With so much theoretical understanding of these optimal sample sizes we're in a good place to begin discussing how we actually compute them.

It is of no surprise that the system of equations for evaluating the optimal sample sizes given in (3.14) lacks a closed-form solution and so we must turn to numerical methods to solve it. This of course introduces the practical problem of implementing root finding algorithms. We already know the bounds of the parameters $\theta_{\mathcal{T}_{\nu^\dagger}}$ and so the only thing left to implement (3.14) is a good approximation for $(n_1^{\text{opt}}, n_2^{\text{opt}})$ to use as a starting point. Because $\text{ACV}_{\mathcal{T}_{\nu^\dagger}}$ is naturally parameterized in terms of (α_1, α_2) we will seek an approximate solution for the optimal pair $(\alpha_1^{\text{opt}}, \alpha_2^{\text{opt}})$ and then transform it into $(n_1^{\text{opt}}, n_2^{\text{opt}})$ via the relation $n_i^{\text{opt}} = 2\alpha_i^{\text{opt}} + 1$.

To begin deriving our approximation we call on the series expansion given in Corollary 12 to write $\text{ACV}^2_{\mathcal{T}_{\nu^\dagger}}(\alpha_1, \alpha_2|\theta_{\mathcal{T}_{\nu^\dagger}}) \approx \text{ACV}^2_{\mathcal{T}_{\nu^\dagger}}^*(\alpha_1, \alpha_2|\theta_{\mathcal{T}_{\nu^\dagger}})$, where

$$\text{ACV}^2_{\mathcal{T}_{\nu^\dagger}}^*(\alpha_1, \alpha_2|\theta_{\mathcal{T}_{\nu^\dagger}}) = \frac{1}{\alpha_1} \tilde{g}_{1,1}^2(\zeta, \nu^\dagger) + \frac{1}{\alpha_1 \alpha_2} \tilde{g}_{2,1}^2(\zeta, \nu^\dagger) + \frac{1}{\alpha_2} \tilde{g}_{1,0}^2(\zeta, \nu^\dagger) \quad (3.15)$$

and $\tilde{g}_{k,\ell}(z, \nu)$ given by Corollary 10 (i). Upon substituting $\alpha_1 = A - \alpha_2$ into this approximation we see that it possesses the same useful properties of the exact form of $\text{ACV}^2_{\mathcal{T}_{\nu^\dagger}}(A - \alpha_2, \alpha_2|\theta_{\mathcal{T}_{\nu^\dagger}})$, namely, positivity, smoothness, strictly convexity on $\alpha_2 \in (0, A)$, as well as the same limiting properties at the endpoints $\alpha_2 = 0, A$. For the sake of brevity we let $a = \tilde{g}_{1,1}(\zeta, \nu^\dagger)$, $b = \tilde{g}_{2,1}(\zeta, \nu^\dagger)$, $c = \tilde{g}_{1,0}(\zeta, \nu^\dagger)$, and $d = \text{acv}_0$ and then substitute $\text{ACV}^2_{\mathcal{T}_{\nu^\dagger}}^*$ into (3.14) yielding the system of equations

$$\begin{aligned} (1) \quad & \frac{a^2}{\alpha_1^2} + \frac{b^2}{\alpha_1^2 \alpha_2} - \frac{b^2}{\alpha_1 \alpha_2^2} - \frac{c^2}{\alpha_2^2} = 0 \\ (2) \quad & \frac{a^2}{\alpha_1} + \frac{b^2}{\alpha_1 \alpha_2} + \frac{c^2}{\alpha_2} - d^2 = 0. \end{aligned}$$

To put this system into a more useful form we perform the transformations $(1)' = (2)/\alpha_1 - (1)$ and $(2)' = (2)/\alpha_2 + (1)$ to get the equivalent set of equations

$$\begin{aligned} (1)' \quad & \alpha_1 = \frac{1}{c^2} (d^2 \alpha_2^2 - c^2 \alpha_2 - b^2) \\ (2)' \quad & \alpha_2 = \frac{1}{a^2} (d^2 \alpha_1^2 - a^2 \alpha_1 - b^2). \end{aligned}$$

Now substituting the r.h.s. of $(1)'$ into $(2)'$ and the r.h.s. of $(2)'$ into $(1)'$ separates the variables α_1 and α_2 into two quartic equations, each of which yields four roots for a total of sixteen possible solutions to our problem. Substituting all sixteen potential solutions back into our original system we find only two work, namely,

$$(\alpha_1, \alpha_2) = \left(\frac{a^2 \pm \sqrt{a^2 c^2 + b^2 d^2}}{d^2}, \frac{c^2 \pm \sqrt{a^2 c^2 + b^2 d^2}}{d^2} \right). \quad (3.16)$$

To obtain the final solution we must determine which sign in front of the root to take. Taking the positive sign clearly yields a nonnegative solution for α_1 and α_2 so to verify this is the correct choice we must show that choosing the negative sign yields a nonsensical solution. The following two lemmas show that if we choose the negative sign then the solution for α_2 is nonpositive and thus is not the desired choice. Since the choice of sign for both α_1 and α_2 must be the same it follows that the positive sign is indeed the correct choice.

Lemma 36. *Let ν^\dagger be as defined in Definition 13. Then for all $\zeta \in (0, 1)$: $\tilde{g}_{1,0}(\zeta, \nu^\dagger) \geq -\frac{1}{2}$.*

Proof. We begin with the explicit form

$$\tilde{g}_{1,0}(\zeta, \nu^\dagger) = \frac{\zeta}{1 - \zeta} - \frac{(\log_\zeta \text{arb}_0 + b)\text{arb}_0\zeta^b}{1 - \text{arb}_0\zeta^b}.$$

Our approach will be to put a lower bound on $\tilde{g}_{1,0}(\zeta, \nu^\dagger)$ by successively minimizing it w.r.t. each of its variables. Differentiating w.r.t. b we find

$$\partial_b \tilde{g}_{1,0}(\zeta, \nu^\dagger) = \frac{x(x - \log x - 1)}{(1 - x)^2} \Big|_{x=\text{arb}_0\zeta^b}.$$

For the specified parameter restriction we have $0 < \text{arb}_0\zeta^b < \text{arb}_0 < 1 \implies x \in (0, 1)$; thus, it is straightforward to show that the above expression in x is positive. It follows that

$$\tilde{g}_{1,0}(\zeta, \nu^\dagger) \geq \tilde{g}_{1,0}(\zeta, \nu^\dagger_{b=0}) = \frac{\zeta}{1 - \zeta} - \frac{(\log_\zeta \text{arb}_0)\text{arb}_0}{1 - \text{arb}_0}.$$

Now differentiating w.r.t. arb_0 we have

$$\partial_{\text{arb}_0} \tilde{g}_{1,0}(\zeta, \nu^\dagger_{b=0}) = \frac{1}{\log \zeta} \frac{\text{arb}_0 - \log \text{arb}_0 - 1}{(1 - \text{arb}_0)^2}.$$

The quantity involving arb_0 is positive on $\text{arb}_0 \in (0, 1)$ while $\log \zeta < 0$ on $\zeta \in (0, 1)$. Therefore, $\partial_{\text{arb}_0} \tilde{g}_{1,0}(\zeta, \nu^\dagger_{b=0}) < 0$ and

$$\tilde{g}_{1,0}(\zeta, \nu^\dagger_{b=0}) \geq \lim_{\text{arb}_0 \searrow 1} \tilde{g}_{1,0}(\zeta, \nu^\dagger_{b=0}) = \frac{\zeta}{1 - \zeta} + \frac{1}{\log \zeta}.$$

The resulting function of ζ is strictly decreasing in ζ . Taking the limit $\zeta \searrow 1$ subsequently gives

$$\tilde{g}_{1,0}(\zeta, \nu^\dagger_{b=0}) \geq \lim_{\zeta \searrow 1} \frac{\zeta}{1 - \zeta} + \frac{1}{\log \zeta} = -\frac{1}{2}.$$

The proof is now complete. \square

Lemma 37. *Choosing the negative sign in (3.16) leads to $\alpha_2 \leq 0$.*

Proof. For brevity we will use $\tilde{g}_{n,\omega}$ to denote $\tilde{g}_{n,\omega}(\zeta, \nu^\dagger)$. We need to show

$$\tilde{g}_{1,0}^2 - \sqrt{\tilde{g}_{1,0}^2 \tilde{g}_{1,1}^2 + \tilde{g}_{2,0}^2 \text{acv}_0^2} \leq 0.$$

Since all quantities under the radical are positive it follows that

$$\tilde{g}_{1,0}^2 - \sqrt{\tilde{g}_{1,0}^2 \tilde{g}_{1,1}^2 + \tilde{g}_{2,0}^2 \text{acv}_0^2} \leq \tilde{g}_{1,0}^2 - \sqrt{\tilde{g}_{1,0}^2 \tilde{g}_{1,1}^2}.$$

From Lemma 13 we have $\tilde{g}_{1,1} = \tilde{g}_{1,0} + 1$; hence,

$$\tilde{g}_{1,0}^2 - \sqrt{\tilde{g}_{1,0}^2 \tilde{g}_{1,1}^2 + \tilde{g}_{2,0}^2 \text{acv}_0^2} \leq \tilde{g}_{1,0}^2 - \sqrt{\tilde{g}_{1,0}^4 + \tilde{g}_{1,0}^2 (2\tilde{g}_{1,0} + 1)}.$$

But now recall from Lemma 36 that $\tilde{g}_{1,0} \geq -\frac{1}{2} \implies \tilde{g}_{1,0}^2 (2\tilde{g}_{1,0} + 1) \geq 0$. So it follows that

$$\tilde{g}_{1,0}^2 - \sqrt{\tilde{g}_{1,0}^2 \tilde{g}_{1,1}^2 + \tilde{g}_{2,0}^2 \text{acv}_0^2} \leq \tilde{g}_{1,0}^2 - \sqrt{\tilde{g}_{1,0}^4} = 0,$$

which completes the proof. \square

Now knowing that we must choose the positive sign in (3.16) we have after reintroducing a, b, c, d , and $n_i = 2\alpha_i + 1$:

$$\begin{aligned} n_1 &= \frac{2}{\text{acv}_0^2} \left(\tilde{g}_{1,1}^2 + \sqrt{\tilde{g}_{1,1}^2 \tilde{g}_{1,0}^2 + \tilde{g}_{2,1}^2 \text{acv}_0^2} \right) + 1 \\ n_2 &= \frac{2}{\text{acv}_0^2} \left(\tilde{g}_{1,0}^2 + \sqrt{\tilde{g}_{1,1}^2 \tilde{g}_{1,0}^2 + \tilde{g}_{2,1}^2 \text{acv}_0^2} \right) + 1, \end{aligned}$$

which is the desired solution for the approximate optimal sample sizes of $\mathcal{T}_{\nu^\dagger}$. So how good are these approximations? First note that with the results of Corollary 16 and Lemma 34 we have

$$\lim_{\zeta \nearrow L} (n_1, n_2)(\theta_{\mathcal{T}_{\nu^\dagger}}) = (2\text{acv}_0^{-2} + 1, 1), \quad L \in \{0, \zeta_{b,1}\}.$$

Comparing this with Theorem 18 we see that our approximate solutions can be made exact at $\zeta = \{0, \zeta_{b,1}\}$ by instead using the slightly modified solution

$$\begin{aligned} n_1^* &= \frac{2}{\text{acv}_0^2} \left(\tilde{g}_{1,1}^2 + \sqrt{\tilde{g}_{1,1}^2 \tilde{g}_{1,0}^2 + \tilde{g}_{2,1}^2 \text{acv}_0^2} \right) + 5 \\ n_2^* &= \frac{2}{\text{acv}_0^2} \left(\tilde{g}_{1,0}^2 + \sqrt{\tilde{g}_{1,1}^2 \tilde{g}_{1,0}^2 + \tilde{g}_{2,1}^2 \text{acv}_0^2} \right) + 1. \end{aligned} \tag{3.17}$$

At the opposite end of the ζ -domain, we may use Lemma 30 to deduce as $\zeta \searrow 1$: $n_2^*/n_1^* \rightarrow 1$ and $n_i^* \sim C_{\mathcal{T}_{\nu^\dagger}}^* (1 - \zeta)^{-2}$, where

$$C_{\mathcal{T}_{\nu^\dagger}}^* = \frac{2\gamma^2(2, -\log \text{arb}_0)}{\text{acv}_0^2(1 - \text{arb}_0)^2} \left(1 + \left(1 + \text{acv}_0^2(1 - \text{arb}_0)^2 \frac{\gamma^2(3, -\log \text{arb}_0)}{\gamma^4(2, -\log \text{arb}_0)} \right)^{1/2} \right).$$

$\text{arb}_0/\text{acv}_0$	0.01	0.02	0.05	0.10	0.20
0.01	0.9999	0.9999	0.9999	0.9999	0.9999
0.02	0.9997	0.9997	0.9997	0.9997	0.9998
0.05	0.9978	0.9980	0.9982	0.9984	0.9985
0.10	0.9913	0.9919	0.9927	0.9934	0.9942
0.20	0.9655	0.9679	0.9714	0.9743	0.9771

Table 3.4: $C_{\mathcal{T}_{\nu^\dagger}}^*/C_{\mathcal{T}_{\nu^\dagger}}$ for various values of arb_0 and acv_0 .

Table 3.4 tabulates the ratio $C_{\mathcal{T}_{\nu^\dagger}}^*/C_{\mathcal{T}_{\nu^\dagger}}$ for a variety of values for arb_0 and acv_0 . One can see that the ratio is near unity for these values which indicates our approximate solutions for $(n_1^{\text{opt}}, n_2^{\text{opt}})$ given by (3.17) are not only exact at $\zeta = \{0, \zeta_{b,1}\}$ but are also exceptionally accurate for small arb_0 and acv_0 in the neighborhood of $\zeta = 1$.

With a suitable approximation to the optimal sample sizes we may finally turn to implementing a numerical routine for computing them. Numerically solving the system (3.14) ultimately requires a method for computing $\text{ACV}^2_{\mathcal{T}_{\nu^\dagger}}$ and its partial derivative w.r.t. α_2 . The fact that the approximation for $\text{ACV}^2_{\mathcal{T}_{\nu^\dagger}}$ in (3.15) lead to excellent approximations for the optimal sample sizes across the entire ζ -domain tells us that we may compute the optimal sample sizes by substituting

$$\text{ACV}^2_{n, \mathcal{T}_{\nu^\dagger}} = \sum_{k=1}^n \sum_{\ell=0}^k \frac{\tilde{g}_{k,\ell}^2(\zeta, \nu^\dagger)}{(\alpha_1)_\ell (\alpha_2)_{k-\ell} \ell! (k-\ell)!}. \quad (3.18)$$

into (3.14) for some appropriate value of n . To determine an appropriate value for n we consider the absolute relative error

$$R_{n,2} = \left| \frac{\text{ACV}^2_{n, \mathcal{T}_{\nu^\dagger}}}{\text{ACV}^2_{\mathcal{T}_{\nu^\dagger}}} - 1 \right|,$$

which according to Corollary 17 is bounded above by $R_{n,2} \leq R_{n,m,2}^*$ with

$$R_{n,m,2}^* = \left| \left(1 + \frac{E_{n,m}^*}{\text{ACV}^2_{n, \mathcal{T}_{\nu^\dagger}}} \right)^{-1} - 1 \right|$$

and $E_{n,m}^*$ given in Theorem 20. Before proceeding, the following result gives us an exact value for $R_{n,2}$ at $\zeta \in \{0, \zeta_{b,1}\}$.

Lemma 38. *For $\zeta \in \{0, \zeta_{b,1}\}$*

$$R_{n,2}|_{(n_1, n_2) = (n_1^{\text{opt}}, n_2^{\text{opt}})} = \frac{(n+1)!}{(\text{acv}_0^{-2} + 2)_n}.$$

Proof. The proof follows from noting that at $\zeta = 0, \zeta_{b,1}$:

$$\text{ACV}^2_{\mathcal{T}_{\nu^\dagger}} = \frac{1}{\alpha_1 - 2},$$

$$\text{ACV}_n^2 \mathcal{T}_{\nu^\dagger} = \frac{1}{\alpha_1 - 2} \left(1 - \frac{(n+1)!}{(\alpha_1)_n} \right),$$

and $\alpha_1^{\text{opt}} = \text{acv}_0^{-2} + 2$. \square

The sharpness of the upper bound $R_{n,m,2}^*$ improves with increasing m but the rate at which this happens significantly decreases for $m > n + 1$; thus, it seems reasonable to use $R_{n,n+1}^*$ as the upper bound in our numerical routine. To get a sense of how $R_{n,n+1,2}^*$ behaves, we evaluated it at $(n_1, n_2) = (n_1^*, n_2^*)$ for $\text{arb}_0 = 0.5$, $\text{acv}_0 = 0.05$, and various values of b and n as plotted in Figure 3.2. We observe that as n increases, the upper bound decreases rapidly except for values of ζ in the neighborhood of $\zeta = 0, \zeta_{b,1}, 1$. However, notice that for the exact value of $R_{n,2}$ given by Lemma 38: $R_{1,2} = 4.98 \times 10^{-3}$, $R_{3,2} = 3.67 \times 10^{-7}$, $R_{5,2} = 6.69 \times 10^{-11}$, $R_{7,2} = 2.26 \times 10^{-14}$. Since the approximations n_1^* and n_2^* are exact as $\zeta \rightarrow L$, $L \in \{0, \zeta_{b,1}\}$, we can conclude that the high upper bound for $R_{n,2}$ near these values of ζ is the result of a deficiency of $R_{n,n+1,2}^*$ and not that the relative error isn't decrease rapidly with n . As such, estimates for the appropriate value of n in (3.18) determined using $R_{n,n+1,2}^*$ will be, in some cases, significantly overestimated near these points.

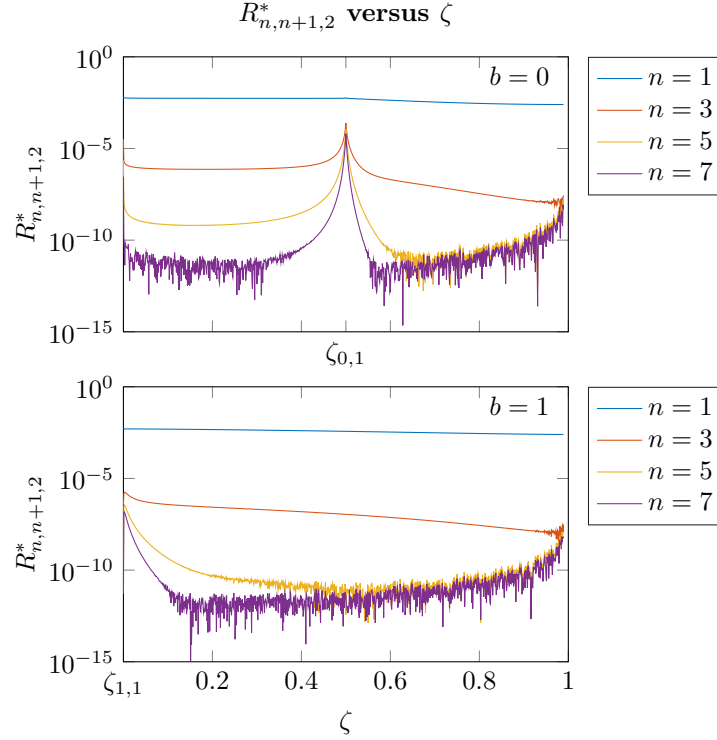


Figure 3.2: Absolute relative error bound $R_{n,n+1,2}^*$ versus ζ for $\text{arb}_0 = 0.5$, $\text{acv}_0 = 0.05$, $b = 0, 1$, and $n = 1, 3, 5, 7$.

Given these observations, Algorithm 1 presents a simple procedure for computing the optimal sample sizes for $\mathcal{T}_{\nu^\dagger}$.

Algorithm 1 Optimal sample size pseudo-code.

```

1: procedure OPTIMALSAMPLES( $\zeta$ ,  $\text{arb}_0$ ,  $b$ ,  $\text{acv}_0$ ,  $\epsilon$ ,  $n_{\max}$ )
2:   if  $\zeta \in \{0, \zeta_{b,1}\}$  then
3:      $(n_1^{\text{opt}}, n_2^{\text{opt}}) = (2\text{acv}_0^{-2} + 5, 1)$ ;
4:     return  $(n_1^{\text{opt}}, n_2^{\text{opt}})$ ;
5:   else
6:      $n = 1$ ;
7:     while  $R_{n,n+1,2}^*(\zeta, n_1^*, n_2^*) > \epsilon$  and  $n < n_{\max}$  do
8:        $n = n + 1$ ;
9:       Substitute  $\text{ACV}_n^2 \mathcal{T}_{\nu^\dagger}$  in (3.14);
10:      Solve for  $(n_1^{\text{opt}}, n_2^{\text{opt}})$  using starting point  $(n_1^*, n_2^*)$ ;
11:      if  $R_{n,n+1,2}^*(\zeta, n_1^{\text{opt}}, n_2^{\text{opt}}) \leq \epsilon$  or  $n = n_{\max}$  then
12:        return  $(n_1^{\text{opt}}, n_2^{\text{opt}})$ ;
13:      else
14:         $n = n + 1$ ;
15:      goto line 9;

```

To demonstrate its effectiveness, Algorithm 1 was implemented in MATHEMATICA using the `FindRoot[]` function for Line 10 to numerically solve the system (3.14). The procedure was executed for $\zeta \in [0, 1)$, $\text{arb}_0 = 0.5$, $\text{acv}_0 = 0.05$, and four different values of b ranging from zero to one. Figure 3.3 plots the computed sample sizes along with $\mathcal{E}_{\mathcal{T}_{\nu^\dagger}}$ evaluated at a dark noise of $\sigma_{\text{dg}} = 1e-$. The values chosen for arb_0 and σ_{dg} , while not typical, were chosen to exaggerate the features of the optimal sample size curves discussed in the preceding analysis.

Focusing first on the curve for n_2^{opt} we observe for values of $b < 1$ that the curve has a cusp at $\zeta = 0$ and $\zeta = \zeta_{b,1}$ where it takes on a value of one. As, $\zeta \searrow 1$ this curve approaches the n_1^{opt} curve; both of which approach $C_{\mathcal{T}_{\nu^\dagger}}(1 - \zeta)^{-2}$ in the limit. As for the $\mathcal{E}_{\mathcal{T}_{\nu^\dagger}}$ curve, we see that it equals one at $\zeta = 0$ and $\mathcal{E}_{\mathcal{T}_{\nu^\dagger}} = 0.15847\dots$ at $\zeta = 1$. Furthermore, the cusp present in the n_2^{opt} curve is also present in the curve for $\mathcal{E}_{\mathcal{T}_{\nu^\dagger}}$, which highlights the reason why choosing values of b less than one may yield undesirable results, in particular, unacceptably low values of $\mathcal{E}_{\mathcal{T}_{\nu^\dagger}}$.

As for the computational details of the routine, it was decided to use $\epsilon = 5 \times 10^{-7}$ so that $\text{ACV}_n^2 \mathcal{T}_{\nu^\dagger}$ was approximated to at least seven significant digits and $n_{\max} = 20$ to avoid issues of numerical stability. Figure 3.4 plots the number of terms, n , and upper bound on the absolute relative error, $R_{n,n+1,2}^*$, as a function of ζ obtained from the routine for the case $b = 0$. From the figure we observe that $R_{n,n+1,2}^*$ exhibits a sharp increase near the points $\zeta \in \{0, \zeta_{b,1}\}$; resulting in larger values for n . Only a few ζ -values near $\zeta_{b,1}$ hit the bound $n = 20$, which is the same behavior observed for all other values of b in Figure 3.3. To check the quality of the solution at these problematic points we note that in the neighborhood of $\zeta = \zeta_{b,1}$ that ν^\dagger and n_2^{opt} are quite small while

n_1^{opt} is large. Recalling the double integral representation of $\mathbb{E}\mathcal{T}_{\nu^\dagger}^2$ we may then approximate $\text{ACV}^2 \mathcal{T}_{\nu^\dagger}$ with

$$\begin{aligned} \text{ACV}_n^2 \mathcal{T}_{\nu^\dagger} &= \int_0^1 \int_0^1 \sum_{k=0}^n \frac{(1+\nu^\dagger)_k^2}{(\alpha_1)_k k!} \frac{((1-x)(1-y))^k}{((1-(1-\zeta)x)(1-(1-\zeta)y))^k} \\ &\quad \times F\left(\begin{matrix} 1-\nu^\dagger, 1-\nu^\dagger \\ \alpha_2 \end{matrix}; (1-x)(1-y)\right) f_{XY}(x, y) \, dx dy - 1, \end{aligned} \quad (3.19)$$

where

$$f_{XY}(x, y) = \frac{((1-(1-\zeta)x)(1-(1-\zeta)y))^{-\nu^\dagger-1}}{F(1, 1+\nu^\dagger; 2; 1-\zeta)^2}$$

and the error E_n such that $\text{ACV}^2 \mathcal{T}_{\nu^\dagger} = \text{ACV}_n^2 \mathcal{T}_{\nu^\dagger} + E_n$ is positive and bounded above by

$$\begin{aligned} E_n^* &= F\left(\begin{matrix} 1+\nu^\dagger, 1+\nu^\dagger \\ \alpha_1 \end{matrix}; 1\right)_{n+1}^c \int_0^1 \int_0^1 \frac{((1-x)(1-y))^{n+1}}{((1-(1-\zeta)x)(1-(1-\zeta)y))^{n+1}} \\ &\quad \times F\left(\begin{matrix} 1-\nu^\dagger, 1-\nu^\dagger \\ \alpha_2 \end{matrix}; (1-x)(1-y)\right) f_{XY}(x, y) \, dx dy \end{aligned}$$

with $F(\alpha, \beta; \gamma; z)_n^c$ given in Proposition 9. Looking back at the numerical data we observe that one of the problematic points in Figure 3.4 occurs at $\zeta = 0.499443$. Using this value for ζ and the optimal sample sizes computed from our routine we find

$$\left| \frac{\text{ACV}_{20}^2 \mathcal{T}_{\nu^\dagger}}{\text{ACV}^2 \mathcal{T}_{\nu^\dagger}} - 1 \right| \leq 6.21 \times 10^{-15},$$

which shows that the approximation $\text{ACV}_{20}^2 \mathcal{T}_{\nu^\dagger}$ given by (3.19) approximates the exact value $\text{ACV}^2 \mathcal{T}_{\nu^\dagger}$ to approximately fourteen significant digits at this point of interest. Substituting $\text{ACV}_{20}^2 \mathcal{T}_{\nu^\dagger}$ into (3.14) we then find

$$\begin{aligned} \partial_{\alpha_2} \text{ACV}_{20}^2 \mathcal{T}_{\nu^\dagger}(\mathbf{A} - \alpha_2, \alpha_2 | \theta_{\mathcal{T}_{\nu^\dagger}}) \Big|_{(\mathbf{A}, \alpha_2) = (\alpha_1^{\text{opt}} + \alpha_2^{\text{opt}}, \alpha_2^{\text{opt}})} &= -6.84 \times 10^{-9} \\ \text{ACV}_{20}^2 \mathcal{T}_{\nu^\dagger}(\alpha_1^{\text{opt}}, \alpha_2^{\text{opt}} | \theta_{\mathcal{T}_{\nu^\dagger}}) - \text{acv}_0^2 &= 9.48 \times 10^{-10}, \end{aligned}$$

which shows no significant deviation from the desired solution $(0, 0)$. This confirms that the solution to the optimal sample sizes obtained in our routine near $\zeta = \zeta_{b,1}$ are not in significant error as the upper bound $R_{n,n+1,2}^*$ might suggest.

3.6 Pixel-level conversion gain estimation: An introduction

Estimating conversion gain with the PT method is typically performed under the assumption that each pixel in the sensor array exhibits identical characteristics.

When this assumption holds we say the sensor is *uniform* and treat each pixel as a source of i.i.d. random noise. Such an assumption is very convenient for performing PT characterization as we can leverage the large number of pixels in a sensor array to obtain low-variance estimates of critical population values. Take for example the estimate of population dark variance σ_d^2 . When the assumption of uniformity holds, one can estimate this quantity from just two images captured under dark conditions. Denoting (D_1, D_2) as these two dark images each with R rows of pixels and C columns of pixels we first compute the pixelwise difference $\Delta D = D_1 - D_2$. Since this differencing operation effectively doubles the population variance we then estimate σ_d^2 by computing half of the sample variance of the difference-frame

$$\hat{\sigma}_d^2 = \frac{1}{2} \frac{1}{RC - 1} \sum_{i=1}^R \sum_{j=1}^C (\Delta D_{ij} - \overline{\Delta D})^2,$$

where ΔD_{ij} denotes the value of the difference-frame ΔD at row i and column j and $\overline{\Delta D} = \frac{1}{RC} \sum_{i=1}^R \sum_{j=1}^C \Delta D_{ij}$ denotes the sample mean of the difference-frame. For a sensor with a very modest one megapixel resolution $RC = 10^6$ and so from just two images we can obtain an estimate of σ_d^2 based on an effective sample size of one-million i.i.d. observations.

In actual sensors, the assumption of uniformity is rarely a good model and is only useful for a small number of pixel architectures. Indeed, in Janesick's book *Photon Transfer* he points out that nonuniformity is a key characteristic of the *Complementary Metal-Oxide Semiconductor* (CMOS) sensor architecture, which is by far the most prevalent architecture in modern imaging systems [16, pg. 82]. When the uniformity assumption is violated we no can longer provide global estimates of the necessary population parameters and must turn to estimates for each individual pixel. Going back to the example of estimating σ_d^2 , pixel-level estimation is performed by capturing a sequence of images, i.e. an *image stack*, and then computing the pixelwise temporal variance of the stack. Supposing we capture a stack of N dark images (D_1, \dots, D_N) to form a $R \times C \times N$ dark image stack, the estimate of σ_d^2 for the pixel in row i and column j becomes

$$(\hat{\sigma}_d^2)_{ij} = \frac{1}{N - 1} \sum_{k=1}^N (D_{ijk} - \overline{D}_{ij})^2, \quad (3.20)$$

where D_{ijk} is the value of pixel (i, j) in the k th image and $\overline{D}_{ij} = \frac{1}{N} \sum_{k=1}^N D_{ijk}$ is the temporal sample mean of that same pixel. From this, we can immediately see the challenge introduced in pixelwise estimation, for in order to estimate σ_d^2 for each pixel with the same level of uncertainty as in the uniform case a total of $N = 10^6$ images must be captured! Setting aside the sheer ammount of data this entails we also run into the practical problem of simply capturing the images in a short enough period of time so that drift does not corrupt the population parameters we are attempting to measure. So while the extension to pixelwise estimation is conceptually straightforward, implementation can be quite challenging.

Given that uniformity is generally the exception and not the rule, a generalized pixel-level approach to PT characterization is in order. Our goal here is to take the theoretical results presented in this work and apply them to develop a first attempt at the process of pixel-level conversion gain estimation. Before this is done we must discuss the topic of *pixel grouping*.

3.6.1 Pixel grouping

When the assumption of uniformity is removed and pixel-level measurement is performed, the characterization of each individual pixel effectively becomes its own experiment with its own unique optimal sample sizes. However, since we can only simultaneously sample all pixels by capturing full-frame images, the conclusion of any pixel-level characterization procedure will be a single set of sample sizes that must work for (nearly) all pixels in the sensor array⁵. Knowing that estimates for each pixel will ultimately be computed with the same number of samples, individually estimating optimal sample sizes is nonsensical and thus we should group pixels with similar characteristics to reduce the variance in estimates of the optimal sample sizes. This point is made evident by first recalling the asymptotic behavior of the optimal sample sizes in the low-illumination limit $\zeta \searrow 1$

$$(n_1^{\text{opt}}, n_2^{\text{opt}})(\zeta) \sim (C_{\mathcal{T}_{\nu^\dagger}}(1 - \zeta)^{-2}, C_{\mathcal{T}_{\nu^\dagger}}(1 - \zeta)^{-2}).$$

Letting $\hat{Y} = \hat{\sigma}_d^2$ be an estimate of σ_d^2 according to (3.20) and $\hat{X} = \hat{\sigma}_{p+d}^2$ be the analogous estimate of σ_{p+d}^2 for a single pixel based on dark and illuminated image stacks of n_2 and n_1 images, respectively, we can estimate ζ with

$$Z = \frac{n_1 - 3}{n_1 - 1} \frac{\hat{Y}}{\hat{X}}.$$

Under the assumed normal model, Z is the UMVUE for ζ with $\mathbb{E}Z = \zeta$ and

$$\text{Var}Z = \left(\frac{(n_1 - 3)(n_2 + 1)}{(n_1 - 5)(n_2 - 1)} - 1 \right) \zeta^2.$$

While Z possesses good characteristics as an estimator for ζ its density is nonzero in the neighborhood of $\zeta = 1$ and so the moments of the optimal sample size estimates $(\hat{n}_1^{\text{opt}}, \hat{n}_2^{\text{opt}}) = (n_1^{\text{opt}}, n_2^{\text{opt}})(Z)$ are strictly speaking undefined. However, if instead of measuring Z for each pixel individually we identify a group of m pixels with similar population values for σ_d^2 and σ_{p+d}^2 we may estimate ζ for the entire group with

$$Z = \frac{mn_1 - 3}{mn_1 - 1} \frac{\sum_{\text{group}} \hat{Y}_\ell}{\sum_{\text{group}} \hat{X}_\ell},$$

⁵We say nearly because typical sensors always contain some minority of defect pixels which are either non-functioning or exhibit statistical behavior too extreme to be properly characterized.

where \hat{Y}_ℓ and \hat{X}_ℓ denotes the estimates for the ℓ th pixel in the group. Grouping in this manner does not alter the unbiasedness of Z and effectively increases the dark and illuminated sample sizes by a factor of m . Hence, given sufficiently large n_1 , n_2 , and group size m , one may drive down the asymptotic variance of the optimal sample size estimates

$$\text{Var } \hat{n}_i^{\text{opt}} \sim (\partial_\zeta n_i^{\text{opt}}(\zeta))^2 \text{Var } Z, \quad i = 1, 2$$

to the point where they becomes useful.

Another important reason why grouping pixels in this manner is not only important but practically necessary is in estimating the quantity $\nu^\dagger(\zeta) = \log_\zeta(\text{arb}_0) + b$. In a similar manner to the optimal sample sizes we see as $\zeta \searrow 1$

$$\nu^\dagger(\zeta) \sim -\log \text{arb}_0 (1 - \zeta)^{-1}.$$

The pole of order one at $\zeta = 1$ again implies that the estimate $\hat{\nu}^\dagger = \nu^\dagger(Z)$ has undefined moments although we may assign it an asymptotic variance

$$\text{Var } \hat{\nu}^\dagger \sim \frac{\log_\zeta^2 \text{arb}_0}{\zeta^2 \log^2 \zeta} \text{Var } Z.$$

Since we ultimately want an estimate of ν^\dagger with nearly zero variance⁶, we need to turn to pixel grouping to leverage the asymptotics of large sample sizes to produce low-variance estimates of ν^\dagger for groups of similar pixels.

Identifying appropriate pixel groups for pixel-level characterization is largely determined by the architecture of the sensor under test. In what follows, we will demonstrate how to identify pixels groups through example as we step through the process of pixel-level conversion gain estimation for a real image sensor.

3.6.2 Experimental setup

For this experiment, the ON Semiconductor KAI-0407M monochrome interline transfer *Charge-Coupled Device* (CCD) sensor was chosen as an initial test case. This particular sensor was chosen for two main reasons. First, preliminary tests show that the noise it produces closely adheres to the normal model assumed in the development of the estimator \mathcal{G}_ν . Secondly, interline transfer CCDs typically exhibit only minor nonuniformities. Since we expect significant nonuniformities to complicate the experimental procedure, this particular sensor provides a gentle introduction into pixel-level characterization.

The experimental setup began with a 650 nm superluminescent light emitting diode (SLED), which was collimated and attached to a *Variable Optical Attenuator* (VOA) to facilitate control over total output power of the light source. The intensity of the light exiting the VOA could be adjusted from 0 – 100% power by rotating a half-wave plate inside the device. To illuminate the sensor with a uniform field, the SLED beam exiting the VOA was directed into a 12 in. diameter

⁶Recall that the derivation of the mean and variance of the estimator \mathcal{G}_ν assumed ν is a known constant.

integrating sphere and the sensor was placed at the output port of the sphere where uniformity is highest. The sensor was operated at its full bit-depth of 14-bits to minimize quantization error and image data was read off the sensor using a single readout register at its slowest setting (40 mhz) as not to introduce additional nonuniformities or smear. For the sake of reducing the total amount of data captured in the experiment, the source was turned on and a live-stream of the sensor output was examined to select the most uniformly illuminated 512×512 px subregion of the sensor array. All subsequent images captured in the experiment were cropped to this subregion prior to saving. Since image data needed to be captured under both dark and illuminated conditions, a motorized mirror was placed next to the path of the SLED beam. Moving the mirror into the beam path effectively redirected the light away from the integrating sphere and thus provided a dark environment for the sensor.

3.6.3 Design of experiment

Design of Experiment (DOE) for pixel-level conversion gain measurement at its core involves five major steps: (1) choosing values for arb_0 , b (bias profile), and acv_0 , (2) estimating a global lower bound on the dark noise $\sigma_d g$, (3) computing n_1^{opt} , n_2^{opt} , and $\mathcal{E}_{\mathcal{T}_{\dagger}}$ on $\zeta \in [0, 1]$, (4) choosing an illumination level, and (5) identifying pixel groups.

Beginning with the first step it was decided to use $\text{arb}_0 = 0.01$, $b = 0$ (constant bias profile), and $\text{acv}_0 = 0.05$ as these choices reflect typical values one might use. Then, to obtain a global lower bound estimate of the dark noise, two 512×512 px dark images (D_1, D_2) were captured. The pixelwise difference $\Delta D = D_1 - D_2$ of these two images was computed and σ_d^2 was estimated by half of the sample variance

$$\hat{\sigma}_d^2 = \frac{1}{2(512^2 - 1)} \sum_{i=1}^{512} \sum_{j=1}^{512} (\Delta D_{ij} - \overline{\Delta D})^2 = 39.94 \text{ DN}^2.$$

Since the value of the conversion gain is unknown, we make the safe assumption $g \geq 1$ and then obtain a single lower bound estimate of the dark noise for each pixel by

$$\widehat{\sigma_d g} = \hat{\sigma}_d (\text{DN}) \times 1(e-/ \text{DN}) = \sqrt{39.94} e-.$$

For the next step we compute the optimal sample size curves according to Algorithm 1. Figure 3.5 plots the computed curves for $N^{\text{opt}} = n_1^{\text{opt}} + n_2^{\text{opt}}$ and $\hat{\mathcal{E}}_{\mathcal{T}_{\dagger}}$ given by

$$\hat{\mathcal{E}}_{\mathcal{T}_{\dagger}} = \left(1 + \frac{1 + \text{acv}_0^{-2}}{(\widehat{\sigma_d g})^2} \frac{\zeta}{(1 - \zeta)^2} \left(\frac{1}{n_1^{\text{opt}}} + \frac{\zeta}{n_2^{\text{opt}}} \right) \right)^{-1}$$

along with the curves for n_1^{opt} and n_2^{opt} as functions of ζ . Due to the sufficiently large value of $\widehat{\sigma_d g}$ we see that $\hat{\mathcal{E}}_{\mathcal{T}_{\dagger}}$ is near unity for virtually any illumination level so that the requirement $\mathcal{E}_{\mathcal{T}_{\dagger}} \approx 1$ will not restrict what illumination levels we can choose for the experiment. To select an appropriate illumination level we

first note that this sensor can record images at ≈ 5 fps for the chosen readout rate of 40 mhz. Looking back at Figure 3.5 we observe that the illumination level corresponding to $\zeta \approx 0.4$ is paired with an optimal total sample size of $N^{\text{opt}} \approx 4000$. At a recording rate of 5 fps this number of images will take ≈ 13 min. to capture, which is short enough to avoid any significant drift in the sensor or source.

Now equipped with a desired value for ζ , the variable optical attenuator was adjusted until the illumination level at the sensor plane resulted in a mean pixel output of about 1% of the sensors dynamic range. Using the same process to estimate the dark noise, two illuminated frames (I_1, I_2) were captured and their difference $\Delta I = I_1 - I_2$ was used to obtain the estimate

$$\hat{\sigma}_{\text{p+d}}^2 = \frac{1}{2(512^2 - 1)} \sum_{i=1}^{512} \sum_{j=1}^{512} (\Delta I_{ij} - \overline{\Delta I})^2 = 112.89 \text{ DN}^2,$$

which then gave an estimate $\hat{\zeta} = Z$ equal to

$$Z = \frac{512^2 - 3}{512^2 - 1} \frac{\hat{\sigma}_{\text{d}}^2}{\hat{\sigma}_{\text{p+d}}^2} = 0.354.$$

This illumination was sufficiently close to the target $\zeta = 0.4$ and corresponded to $\hat{\mathcal{E}}_{\mathcal{I}_{\text{v}^\dagger}} = 0.9928$ and $N^{\text{opt}} = 3237$ images, which needs only ≈ 11 min. to capture.

The last step in the DOE process is to determine appropriate pixel groupings for the data collection algorithm. As discussed in Section 3.6.1, identifying these pixel groups is largely aided by knowledge of the sensor architecture under test. In this example, we know we are working with an interline transfer CCD architecture [20]. These devices work by transferring the packets of charge collected by each pixel into columnwise vertical shift registers that subsequently facilitate the transfer of the charge packets off the sensor to downstream readout circuitry. Since variations in the columnwise circuitry supporting these vertical shift registers is expected, nonuniformities in interline transfer CCDs is typically observed between its columns. To see this in action, a stack of dark images were captured with the KAI-0407M CCD and the pixelwise temporal average of the stack was computed as seen in Figure 3.6. From the figure we see clear columnwise variations in the estimated population dark mean μ_{d} , which supports our conclusions about the sensor nonuniformities. As such, we will group pixels according to their column number for the data collection procedure.

3.6.4 Data collection

The procedure for the data collection portion of this experiment centers around successively capturing images under dark and illuminated conditions, using these images to update sample statistics for each pixel, and determining when the appropriate number of dark and illuminated images have been captured based on these sample statistics. We will initialize the procedure by capturing some predetermined number of dark images (i.e. a Y -image stack) and illuminated images (i.e. a X -image stack) and then compute four *master frames*,

denoted \bar{Y} , \bar{X} , \hat{Y} , and \hat{X} , from these stacks. Using this nomenclature, the \bar{Y} and \bar{X} master frames denote arrays computed by averaging the Y - and X -image stacks in the temporal dimension while the \hat{Y} and \hat{X} master frames denote arrays computed by evaluating the variance of the Y - and X -image stacks in the temporal dimension. As an example, Figure 3.7 depicts the process of computing a master \hat{X} -frame from a stack of n X -images.

With master frames computed from the two initial image stacks, we will then capture individual Y - and X -images and use these to continuously update the master frames until a specified criteria is met to halt data capture. Due to the large number of images that will be captured in this experiment, updating the master frames by recomputing the sample statistics from the full image stacks is too computationally expensive to work in practice. As such we will use Welford's algorithm to update the master frames when new image data becomes available. Algorithm 2 presents the procedure `UPDATESTATS()`, which is an adaptation of Welford's algorithm to two-dimensional arrays [26]. This procedure accepts as arguments a new two-dimensional array of data, `newdata`, the current master sum of squares array, $M_{2,n}$, the current master average frame \bar{x}_n , and the number of samples, n , the current master frames are computed from. If no master frames have been initialized we may use the syntax `UPDATESTATS(newdata, 0)` to create them. For all subsequent $n \geq 1$, the syntax `UPDATESTATS(newdata, n, $M_{2,n}$, \bar{x}_n)` takes in the current master arrays and updates them with `newdata` according to Welford's algorithm. We note that all arithmetic operations in this procedure are performed elementwise, where, in particular, the operator \odot denotes the Hadamard product (elementwise multiplication of matrices).

Algorithm 2 Welford's online algorithm for two-dimensional arrays.

```

1: procedure UPDATESTATS(newdata,  $n$ ,  $M_{2,n}$ ,  $\bar{x}_n$ )
2:    $n = n + 1$ ;
3:   if  $n = 1$  then
4:      $\bar{x}_n = \text{newdata}$ ;
5:      $M_{2,n} = \text{zeros}(\text{size}(\text{newdata}))$ ;
6:      $s_n^2 = \text{zeros}(\text{size}(\text{newdata}))$ ;
7:   else
8:      $\bar{x}_n = \bar{x}_{n-1} + \frac{1}{n}(\text{newdata} - \bar{x}_{n-1})$ ;
9:      $M_{2,n} = M_{2,n-1} + (\text{newdata} - \bar{x}_{n-1}) \odot (\text{newdata} - \bar{x}_n)$ ;
10:     $s_n^2 = \frac{1}{n-1} M_{2,n}$ ;
11:  return  $n$ ,  $\bar{x}_n$ ,  $M_{2,n}$ ,  $s_n^2$ 

```

The initial dark and illuminated sample sizes for the data collection algorithm are determined from looking back at the plots for n_1^{opt} and n_2^{opt} in Figure 3.5. Regardless of the parameters chosen, we know that an optimal dark sample size of $n_2 = 1$ occurs for at least one ζ -value and so we set the default initial number of Y -images to be one. This, however, cannot be said for the optimal illuminated sample size n_1 , which always takes on values greater than one. While the optimal illuminated sample size curve is not always strictly increasing, we

will choose its shot noise-limited value $2\text{acv}_0^{-2} + 5$ as a good approximation to the minimum possible value and make this as our required initial number of initial X -images.

Algorithm 3 presents the generic `COLLECTIMAGEDATA(n1Min, Yrule, Xrule, HaltRule)` procedure used for collecting and processing real-time image data in the pixel-level conversion gain estimation experiment. The procedure accepts an initial illuminated sample size, `n1Min`, which will be $2\text{acv}_0^{-2} + 5$ for this experiment, as well as three rules for determining when to halt Y -image collection (`Yrule`), X -image collection (`Xrule`), and the entire routine (`HaltRule`). From Algorithm 3 we observe that the `COLLECTIMAGEDATA()` procedure begins by initializing the master frames and updating the master frames until the initial minimum sample sizes are captured. The procedure then enters a loop whereby the master frames are first updated if their corresponding rule is false. Once the master frames are updated, the estimates of ζ , ν^\dagger , n_1^{opt} , and n_2^{opt} are updated for each pixel group. Lastly, the `Yrule`, `Xrule`, and `HaltRule` are reevaluated to determine if more images are needed and if the procedure can stop. Upon completion, the procedure then returns the final sample sizes n_1 and n_2 , a vector V containing the final group estimates of ν^\dagger , another vector Z containing the final group estimates of ζ , and the four master frames \bar{Y} , \bar{X} , \hat{Y} , and \hat{X} .

For the KAI-0407M pixel-level conversion gain estimation experiment the following three simple rules were chosen:

$$\begin{aligned} \text{Yrule} &= \begin{cases} \text{true,} & \text{if } \hat{n}_2^{\text{opt}} \geq n_2 \text{ for all groups} \\ \text{false,} & \text{otherwise,} \end{cases} \\ \text{Xrule} &= \begin{cases} \text{true,} & \text{if } \hat{n}_1^{\text{opt}} \geq n_1 \text{ for all groups} \\ \text{false,} & \text{otherwise,} \end{cases} \\ \text{HaltRule} &= \begin{cases} \text{true,} & \text{if } (\hat{n}_1^{\text{opt}} \geq n_1 \wedge \hat{n}_2^{\text{opt}} \geq n_2) \text{ for } \geq 95\% \text{ of all groups} \\ \text{false,} & \text{otherwise.} \end{cases} \end{aligned}$$

We see that `Yrule` and `Xrule` direct the algorithm to keep collecting images if the estimated optimal sample sizes are less than the current sample sizes for any of the column groups. Furthermore, `HaltRule` halted the procedure when the current sample sizes exceeded the estimates for at least 95% of the column groups.

3.6.5 Summary of results

The data collection algorithm was executed on the KAI-0407M CCD sensor resulting in dark and illuminated sample sizes of $n_2 = 862$ and $n_1 = 2469$ images, respectively. Figure 3.8 plots the group estimates of ζ and ν^\dagger versus iteration number of the algorithm for fifteen randomly selected columns. We can see that these estimates converge to different values, which confirms our choice of pixel grouping is appropriate. Furthermore, we observe that the variance of these estimates in the final iterations of the algorithm is practically zero showing that

the size (i.e. number of pixels) of the chosen pixel groups was also sufficiently large.

To compute the pixel-level conversion gain array, a.k.a. the *g-map*, we first created a pixel-level ν^\dagger array via

$$V^\dagger = \mathbf{1}_{512 \times 512} \times \text{diag}(V),$$

where $\mathbf{1}_{512 \times 512}$ is a 512×512 array of ones, V is the 512×1 vector of group estimates for ν^\dagger , and $\text{diag}(V)$ is a 512×512 diagonal matrix with diagonal elements equal to elements of V . The master frames \bar{Y} , \bar{X} , \hat{Y} , \hat{X} , along with V^\dagger , and the final sample size values n_1 and n_2 were then imported into a MATHEMATICA. For each set of pixel coordinates (i, j) , $1 \leq i, j \leq 512$, the conversion gain was estimated with

$$(\mathcal{G}_{\nu^\dagger, K})_{ij} = (\bar{X}_{ij} - \bar{Y}_{ij}) \times \mathcal{T}_{V_{ij}^\dagger, K}(\hat{X}_{ij}, \hat{Y}_{ij}, \alpha_1, \alpha_2),$$

where $\mathcal{T}_{\nu^\dagger, K}$ is the K th order asymptotic approximation of $\mathcal{T}_{\nu^\dagger}$ given in (2.6) and $\alpha_i = (n_i - 1)/2$, $i = 1, 2$. Comparing the histograms and sample statistics of $\mathcal{G}_{\nu^\dagger, 1}$ and $\mathcal{G}_{\nu^\dagger, 2}$ showed negligible difference indicating that a $K = 2$ order approximation was sufficient to accurately compute $\mathcal{G}_{\nu^\dagger}$ for each pixel.

Figure 3.9 displays the final *g-map* for the KAI-0407M CCD along with its histogram. First comparing the histogram to the provided normal reference we see it exhibits a positive skewness, which was estimated to be

$$\widehat{\text{Skew}} \mathcal{G}_{\nu^\dagger} = 0.2426.$$

As for the *g-map* itself, we observe what appears to be purely random noise with no noteworthy features or patterns. This behavior is expected since we deliberately inhibited gain nonuniformity by transferring image data from the sensor pixels through a single readout register. Since the fluctuations in the *g-map* for this particular case should be almost entirely due to statistical noise, we can see how effective the data collection algorithm was by comparing the sample absolute coefficient of variation to the target value of $\text{acv}_0 = 0.05$. Computing the sample mean $\hat{\mathbb{E}} \mathcal{G}_{\nu^\dagger}$ and sample variance $\widehat{\text{Var}} \mathcal{G}_{\nu^\dagger}$ of the *g-map* data we found for the sample absolute coefficient of variation

$$\widehat{\text{ACV}} \mathcal{G}_{\nu^\dagger} = \frac{\sqrt{\widehat{\text{Var}} \mathcal{G}_{\nu^\dagger}}}{\hat{\mathbb{E}} \mathcal{G}_{\nu^\dagger}} = 0.0497,$$

which differs from the target value by only 0.7%. This small discrepancy indicates the data collection algorithm was able to adequately control the experiment and halt data capture at the appropriate time.

To see how $\mathcal{G}_{\nu^\dagger}$ compares to the traditional conversion gain estimator we also computed the traditional *g-map* with elements

$$G_{ij} = (\bar{X}_{ij} - \bar{Y}_{ij})(\hat{X}_{ij} - \hat{Y}_{ij})^{-1}.$$

Table 3.5 presents tabulated values for select sample statistics of both maps. While none of these sample statistics are able to compare the bias of each estimator we know that $\text{ARB}\mathcal{G}_{\nu^\dagger} \approx 0.01$. Furthermore, a quick comparison of the histogram for $\hat{X} - \hat{Y}$ against its normal fit shows excellent agreement so that $\text{ARB}G$ can be approximated by [12, c.f. Corollary 3.2]

$$\text{ARB}G = \left| \frac{2(1-\zeta)}{\sqrt{2(\frac{1}{\alpha_1} + \frac{1}{\alpha_2}\zeta^2)}} \mathcal{D} \left(\frac{1-\zeta}{\sqrt{2(\frac{1}{\alpha_1} + \frac{1}{\alpha_2}\zeta^2)}} \right) - 1 \right|. \quad (3.21)$$

Substituting the global estimate

$$Z = \left(\frac{512^2 n_1 - 3}{512^2 n_1 - 1} \right) \frac{\sum_{i=1}^{512} \sum_{y=1}^{512} \hat{Y}_{ij}}{\sum_{i=1}^{512} \sum_{y=1}^{512} \hat{X}_{ij}}$$

for ζ in (3.21) gives $\text{ARB}G \approx 0.0027$ and so we conclude G incurs less relative bias than $\mathcal{G}_{\nu^\dagger}$ ⁷. However, note that this small increase in relative bias affords the estimator $\mathcal{G}_{\nu^\dagger}$ a decrease in sample variance of about 11.4% when compared to that of G .

	$\mathcal{G}_{\nu^\dagger}$	G	Unit
$\hat{\text{E}}(\cdot)$	2.1697	2.1975	e^-/DN
$\widehat{\text{Var}}(\cdot)$	0.0116	0.0131	$(e^-/\text{DN})^2$
$\widehat{\text{ACV}}(\cdot)$	0.0497	0.0521	—

Table 3.5: Comparison of sample statistics for the $\mathcal{G}_{\nu^\dagger}$ - and G -maps.

⁷Technically speaking $\text{ARB}G$ is undefined; however, the expression in (3.21) does give a useful measure of relative bias for G whenever $\text{P}(\hat{X} - \hat{Y} > 0) \approx 1$. Inspection of the \hat{X} and \hat{Y} data for the KAI-0407M CCD reveals all 512^2 values of $\hat{X} - \hat{Y}$ are positive; thus, the comparison of $\text{ARB}\mathcal{G}_{\nu^\dagger}$ and $\text{ARB}G$ is informative.

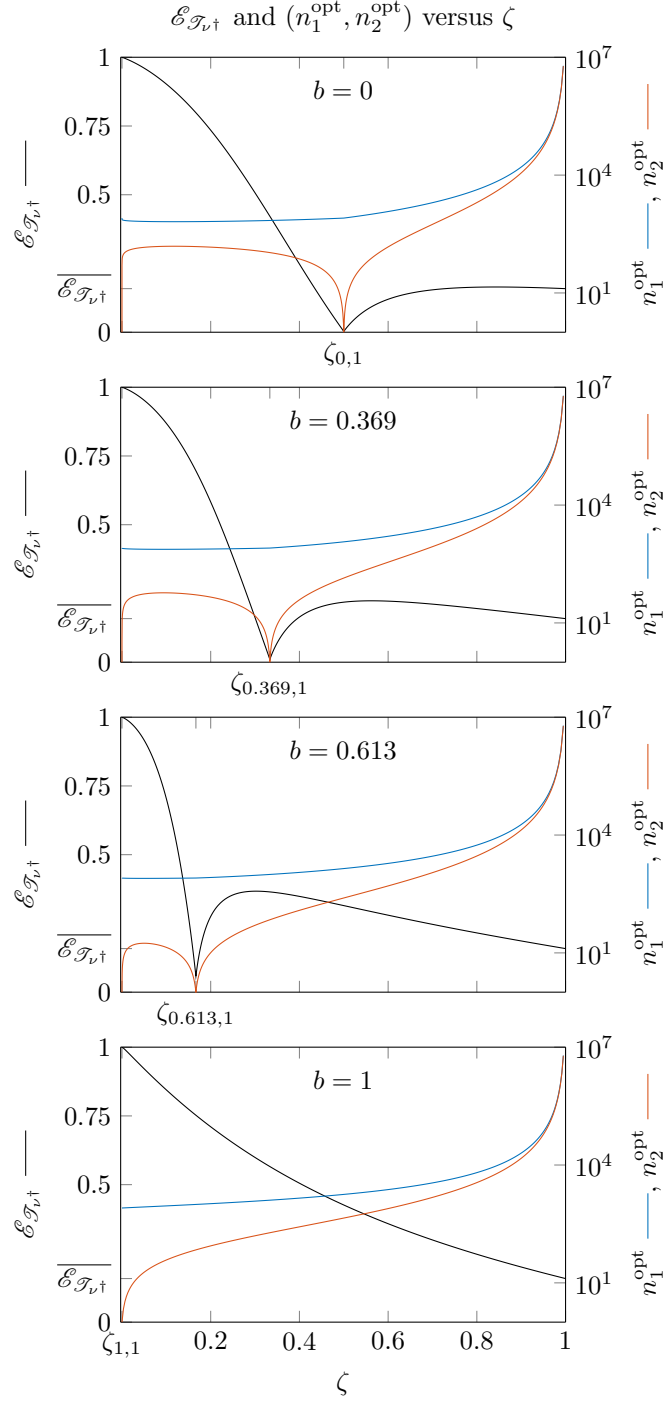


Figure 3.3: $\mathcal{E}_{\mathcal{T}_{\nu^\dagger}}$ and $(n_1^{\text{opt}}, n_2^{\text{opt}})$ versus ζ for $\text{arb}_0 = 0.5$, $\text{acv}_0 = 0.05$, $b = \{0, 0.369, 0.613, 1\}$, and $\sigma_d g = 1e-$. Values of $\zeta_{b,1}$ and $\overline{\mathcal{E}_{\mathcal{T}_{\nu^\dagger}}}$ are also indicated on each plot.

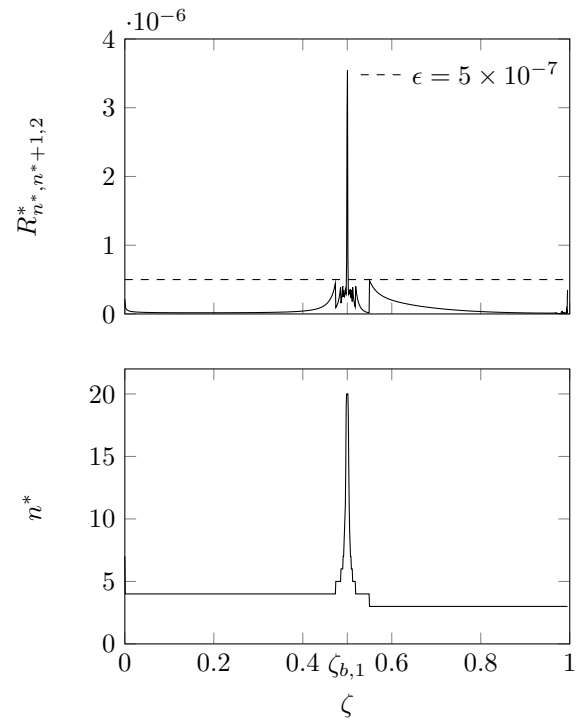


Figure 3.4: $R_{n^*, n^*+1,2}^*$ (top) and n^* (bottom) versus ζ for $\text{arb}_0 = 0.5$, $b = 0$, and $\text{acv}_0 = 0.05$.

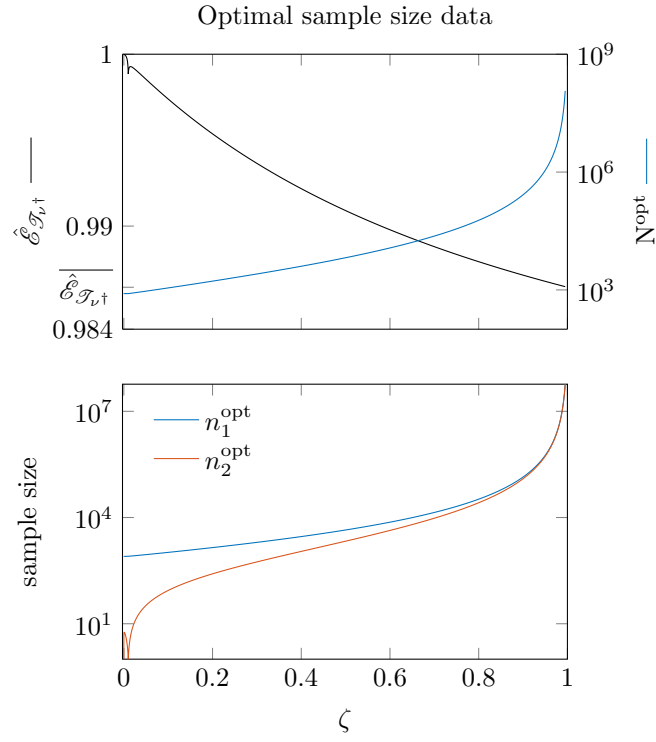


Figure 3.5: $\hat{\mathcal{E}}_{T_{\nu^\dagger}}$ and N^{opt} versus ζ (top) with n_1^{opt} and n_2^{opt} versus ζ (bottom) for $\text{arb}_0 = 0.01$, $\text{acv}_0 = 0.05$, $b = 0$, and $\sigma_{\text{dg}} = \sqrt{39.94}e$.

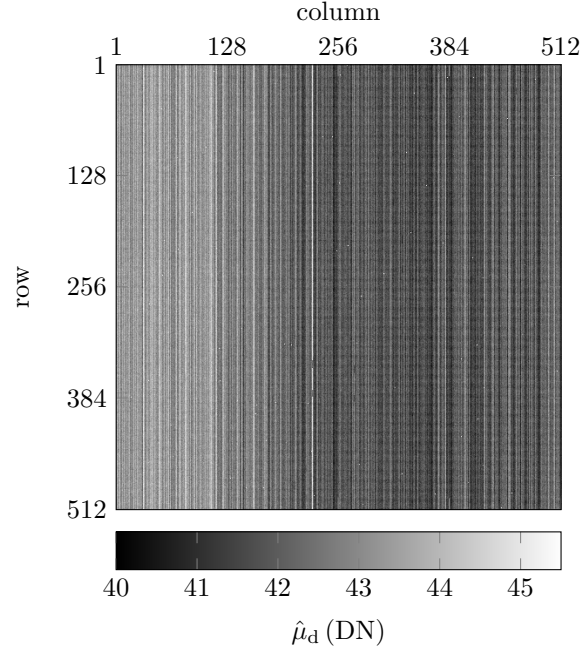


Figure 3.6: Average of dark image stack generated from the KAI-0407M interline transfer CCD showing columnwise nonuniformities in mean dark signal.

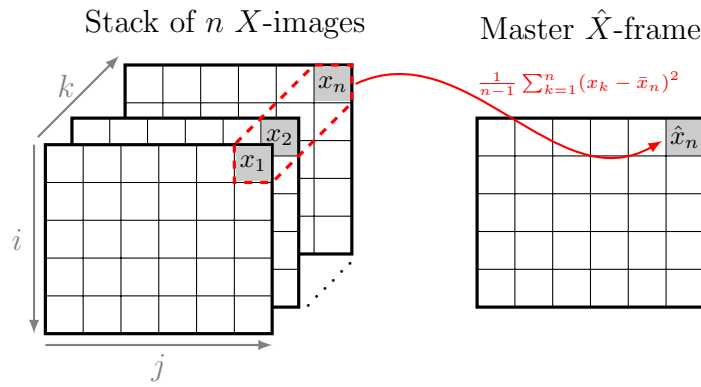


Figure 3.7: Master \hat{X} -frame computed from a stack of n X -images.

Algorithm 3 Data collection procedure.

```

1: procedure COLLECTIMAGEDATA(n1Min, Yrule, Xrule, HaltRule)
2:    $n_2 = 0$ ;
3:   Capture one  $Y$ -image;
4:    $[n_2, \bar{Y}, \hat{Y}, M_2^Y] = \text{UPDATESTATS}(Y, n_2)$ ;
5:    $n_1 = 0$ ;
6:   Capture one  $X$ -image;
7:    $[n_1, \bar{X}, \hat{X}, M_2^X] = \text{UPDATESTATS}(X, n_1)$ ;
8:   while  $n_1 < \mathbf{n1Min}$  do
9:     Capture one  $X$ -image;
10:     $[n_1, \bar{X}, \hat{X}, M_2^X] = \text{UPDATESTATS}(X, n_1, M_2^X, \bar{X})$ ;
11:
12:   Yflag=false;
13:   Xflag=false;
14:   Stop=false;
15:    $N = \#$  of groups;
16:   while Stop=false do
17:     if Yflag=false then
18:       Capture one  $Y$ -image;
19:        $[n_2, \bar{Y}, \hat{Y}, M_2^Y] = \text{UPDATESTATS}(Y, n_2, M_2^Y, \bar{Y})$ ;
20:     if Xflag=false then
21:       Capture one  $X$ -image;
22:        $[n_1, \bar{X}, \hat{X}, M_2^X] = \text{UPDATESTATS}(X, n_1, M_2^X, \bar{X})$ ;
23:     for  $i = 1 : N$  do
24:        $m_i = \#$  of pixels in group  $i$ ;
25:        $Z_i = \frac{m_i n_1 - 3}{m_i n_1 - 1} (\sum_{\text{group } i} \hat{Y}) / (\sum_{\text{group } i} \hat{X})$ ;
26:        $V_i = \nu^{\dagger}(Z_i)$ ;
27:        $(\hat{n}_1^{\text{opt}}, \hat{n}_2^{\text{opt}})_i = (n_1^{\text{opt}}, n_2^{\text{opt}})(Z_i)$ ;
28:     Yflag=Yrule;
29:     Xflag=Xrule;
30:     Stop=HaltRule;
31:   return  $n_2, n_1, V, \bar{Y}, \bar{X}, \hat{Y}, \hat{X}$ 

```

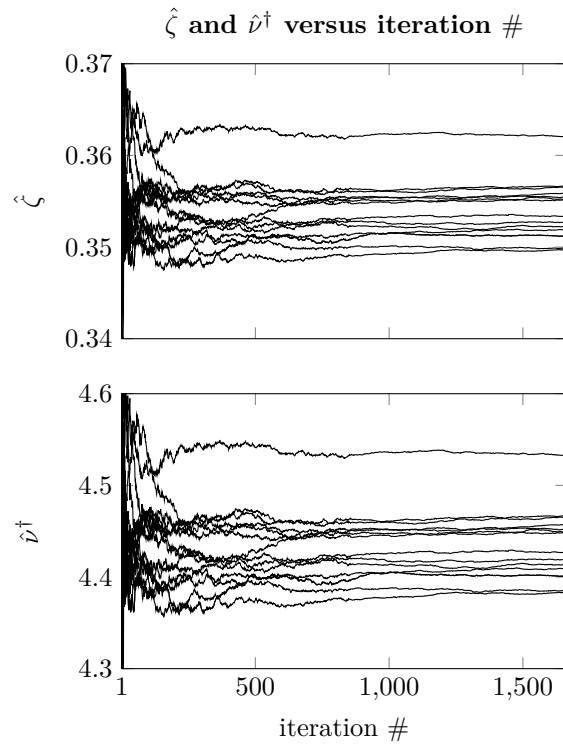


Figure 3.8: Estimates of ζ (top) and ν^\dagger (bottom) versus iteration number for fifteen randomly selected columns.

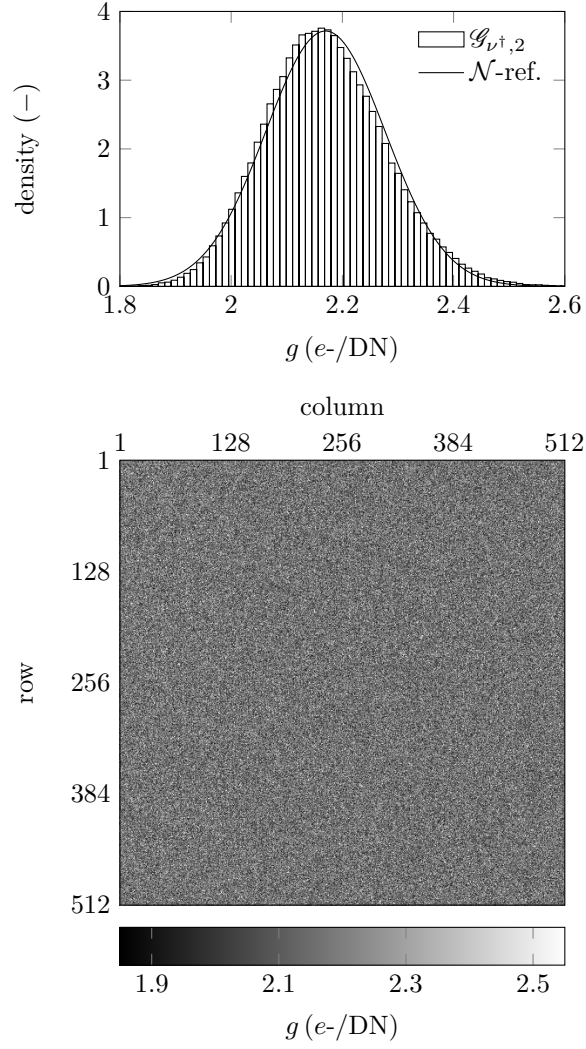


Figure 3.9: Histogram of g -map data with best normal approximation (top) and image plot of the final g -map (bottom).

Chapter 4

Conclusions

In this work we covered a lot of ground in understanding the estimation of the reciprocal difference of normal variances, $\tau = (\sigma_1^2 - \sigma_2^2)^{-1}$, and how this is applicable to the photon transfer method of image sensor characterization.

We began in Theorem 1 by showing that no unbiased, finite-variance estimator of τ existed under the normal model. Appealing to the principle of bias-variance tradeoff a biased yet finite-variance estimator, \mathcal{T}_n , was produced, which estimated the first n terms of the Taylor series for τ . Working with the methods of *Summability Calculus* the domain of \mathcal{T}_n was then extended to include complex-valued n resulting in the generalized estimator \mathcal{T}_ν . Many properties of this generalized estimator were discovered including a reflection formula as well as its first two moments. The absolute relative bias $\text{ARB}\mathcal{T}_\nu$ and absolute coefficient of variation $\text{ACV}\mathcal{T}_\nu$ were also derived along with their exact confidence intervals. An asymptotic expansion of \mathcal{T}_ν for large sample sizes was then given, which played a critical role in applications presented in latter sections.

Equipped with a substantial theoretical foundation, Chapter 3 tackled the problem of applying the results of the preceding analysis to construct a novel estimator, \mathcal{G}_ν , of the photon transfer conversion gain measurement. As a corollary to Theorem 1 it was proven that no unbiased, finite-variance estimator of the conversion gain, g , existed under the normal model of pixel noise. Mirroring the analysis of \mathcal{T}_ν , the first two moments of \mathcal{G}_ν were derived and used to construct expressions for $\text{ARB}\mathcal{G}_\nu$ and $\text{ACV}\mathcal{G}_\nu$. Then, using long standing observations from the literature as a clue, the function \mathcal{E} was introduced as a sort of normalized metric for determining when the dispersion of \mathcal{G}_ν was dominated by the dispersion of \mathcal{T}_ν . It was shown that \mathcal{E} approaches unity in the shot noise limit $\zeta \searrow 1$, which supported the observations in the literature and showed that $\text{ACV}\mathcal{G}_\nu$ could be very well approximated by $\text{ACV}\mathcal{T}_\nu$ given the level of illumination was sufficiently large. These observations were subsequently utilized in a Monte Carlo simulation to demonstrate the process of conversion gain estimation with \mathcal{G}_ν as well as in the computation confidence intervals for $\text{ARB}\mathcal{G}_\nu$ and $\text{ACV}\mathcal{G}_\nu$. A short discussion followed the Monte Carlo experiment,

which introduced the notion of manipulating the parameter ν and sample sizes as to achieved desired values for absolute relative bias and absolute coefficient of variation.

The questions following the Monte Carlo experiment in Section 3.4 served as a springboard into the study of bias control and optimal sample sizes. To control bias, two new estimators $\mathcal{T}_{\nu^\dagger}$ and $\mathcal{G}_{\nu^\dagger}$ were defined, which varied ν^\dagger in such a manner as to force estimator bias to follow a prescribed profile. A definition of optimal sample sizes for was then introduced followed by a study of the optimal sample sizes for $\mathcal{T}_{\nu^\dagger}$ and $\mathcal{G}_{\nu^\dagger}$ in the low illumination limit $\zeta \nearrow 1$. It was demonstrated that as the illumination level decreased, the optimal sample sizes, $(n_1^{\text{opt}}, n_2^{\text{opt}})$, for both estimators were asymptotically equal and proportional to $(1 - \zeta)^{-2}$. Perhaps the most significant finding of this investigation at low illumination came in Corollary 15, which showed that substituting the optimal sample sizes for $\mathcal{T}_{\nu^\dagger}$ into the metric \mathcal{E} produced nonzero values in the limit $\zeta \nearrow 1$. Furthermore, for sufficiently large magnitudes of dark noise, σ_{dg} , this limiting value of \mathcal{E} could be near unity meaning that the optimal sample sizes of $\mathcal{G}_{\nu^\dagger}$ can be very closely approximated to those of $\mathcal{T}_{\nu^\dagger}$ even if the illumination level was near zero.

The fact that the optimal sample sizes of $\mathcal{T}_{\nu^\dagger}$ served as such good approximations to those of $\mathcal{G}_{\nu^\dagger}$ provided the justification needed to perform a detailed investigation of their properties. The investigation began by showing exact solutions for the optimal sample sizes of $\mathcal{T}_{\nu^\dagger}$ could be derived at at two special point of interest in the ζ -domain. For all remaining values of ζ explicit approximations for the optimal sample sizes were found and these approximations were shown to perform very well for a wide range of parameters. To compute the optimal sample sizes, a numerical routine was implemented, which using the explicit approximations as a starting point. A brief analysis of this numerical routine was conducted as to highlight potential weaknesses that could be improved in future work.

With a means for computing optimal sample sizes, Section 3.6 concluded this work with an introduction to *pixel-level* photon transfer conversion gain estimation. The concept of sensor nonuniformity was introduced as a motivation for a pixel-level approach to photon transfer characterization and the challenges of such an approach were discussed. Using a real image sensor a first attempt at pixel-level conversion gain estimation was presented. In particular, a focus was given on how to design a pixel-level conversion gain estimation experiment using the optimal sample size curves and the quantity \mathcal{E} as tools for selecting an appropriate illumination level for collecting data. An algorithm for collecting and halting data capture was discussed and then executed on the chosen image sensor. A summary of the experimental result then ensued, which presented the pixel-level g -map as the primary data product of the experiment. Details of how the g -map was computed as well as analysis of how the data collection algorithm performed were conducted; revealing the algorithms were successful in controlling the experiment and halting data capture at the appropriate time.

The successfulness of the theoretical results presented herein and their application to pixel-level conversion gain estimation subsequently open the door to

developing a much needed comprehensive approach to pixel-level photon transfer characterization.

Chapter 5

Appendices

A Definitions and relations

Definition 17 (Sign Function).

$$\text{sign}(x) := \begin{cases} x/|x|, & x \neq 0 \\ 0, & x = 0. \end{cases}$$

Definition 18 (Indicator Function).

$$\mathbb{1}_A := \begin{cases} 1, & A \text{ is true} \\ 0, & A \text{ is false.} \end{cases}$$

Definition 19 (Gamma Function).

$$\Gamma(z) := \int_0^\infty t^{z-1} e^{-t} dt, \quad \Re z > 0$$

Definition 20 (Beta Function).

$$B(s, z) := \frac{\Gamma(s)\Gamma(z)}{\Gamma(s+z)}$$

Definition 21 (Pochhammer Symbol (rising factorial)).

$$(s)_z := \frac{\Gamma(s+z)}{\Gamma(s)}$$

Definition 22 (Factorial Power (falling factorial)).

$$(s)^{(z)} := \frac{\Gamma(s+1)}{\Gamma(s-z+1)}$$

Relation 3 (Rising and falling factorical connection formula).

$$(s)^{(n)} = (-1)^n (-s)_n, \quad n \in \mathbb{Z}$$

Relation 4 (Falling factorical product representation).

$$(s)_n = \begin{cases} 1, & n = 0 \\ \prod_{k=0}^{n-1} (s + k) & n \in \mathbb{N} \end{cases}$$

Relation 5 (Falling factorical product representation).

$$(s)^{(n)} = \begin{cases} 1, & n = 0 \\ \prod_{k=0}^{n-1} (s - k) & n \in \mathbb{N} \end{cases}$$

Definition 23 (Generating function of Stirling numbers of the 1st-kind $\mathcal{S}_n^{(k)}$).

$$(s)_n := \sum_{k=0}^n (-1)^{n-k} \mathcal{S}_n^{(k)} s^k$$

Definition 24 (Generating function of generalized Nørlund polynomial $B_k^{(\ell)}(z)$).

$$\left(\frac{t}{e^t - 1} \right)^\ell e^{zt} := \sum_{k=0}^{\infty} B_k^{(\ell)}(z) \frac{t^k}{k!}$$

Definition 25 (Nørlund polynomial).

$$B_k^{(\ell)} := B_k^{(\ell)}(0)$$

Definition 26 (Bernoulli polynomial).

$$B_k(z) := B_k^{(1)}(z)$$

Definition 27 (Lerch's Transcendent).

$$\Phi(z, s, \omega) := \sum_{k=0}^{\infty} \frac{z^k}{(k + \omega)^s}$$

Definition 28 (Generalized Hypergeometric Series).

$${}_pF_q \left(\begin{matrix} a_1, \dots, a_p \\ b_1, \dots, b_q \end{matrix}; z \right) := \sum_{k=0}^{\infty} \frac{(a_1)_k \cdots (a_p)_k}{(b_1)_k \cdots (b_q)_k} \frac{z^k}{k!}$$

Definition 29 (Regularized Generalized Hypergeometric Function).

$${}_p\mathbf{F}_q \left(\begin{matrix} a_1, \dots, a_p \\ b_1, \dots, b_q \end{matrix}; z \right) := \frac{1}{\prod_{k=1}^q \Gamma(b_k)} {}_pF_q \left(\begin{matrix} a_1, \dots, a_p \\ b_1, \dots, b_q \end{matrix}; z \right)$$

Definition 30 (Appell F_1 Hypergeometric Series).

$$F_1(a; b, b'; c; s, z) := \sum_{k, \ell=0}^{\infty} \frac{(a)_{k+\ell} (b)_k (b')_{\ell}}{(c)_{k+\ell} k! \ell!} s^k z^{\ell}, \quad \max\{|s|, |z|\} < 1$$

Definition 31 (Appell F_2 Hypergeometric Series).

$$F_2(a; b, b'; c, c'; s, z) := \sum_{k, \ell=0}^{\infty} \frac{(a)_{k+\ell} (b)_k (b')_{\ell}}{(c)_k (c')_{\ell} k! \ell!} s^k z^{\ell}, \quad |s| + |z| < 1$$

Definition 32 (Incomplete Beta Function).

$$B_z(\alpha, \beta) := \Gamma(\alpha) z^{\alpha} \mathbf{F} \left(\alpha, 1 - \beta; \alpha + 1; z \right), \quad -\alpha \notin \mathbb{N}_0$$

Definition 33 (Regularized Incomplete Beta Function).

$$I_z(\alpha, \beta) := \frac{B_z(\alpha, \beta)}{B(\alpha, \beta)}$$

Relation 6. [27, Eq. 07.23.03.0122.01].

$$F(1, \beta; \gamma; s) = (\gamma - 1) s^{1-\gamma} (1 - s)^{-(\beta-\gamma+1)} B_s(\gamma - 1, \beta - \gamma + 1).$$

Relation 7 (Gamma reflection formula).

$$\Gamma(z) \Gamma(1 - z) = \pi \csc \pi z, \quad z \notin \mathbb{Z}$$

Relation 8.

$$(1 - z - n)_n = (-1)^n (z)_n, \quad n \in \mathbb{Z}$$

Proof. Using the gamma reflection formula in Relation 7 one writes

$$(1 - z - n)_n = \frac{\Gamma(1 - z)}{\Gamma(1 - z - n)} = \frac{\csc \pi z}{\csc \pi(z + n)} \frac{\Gamma(z + n)}{\Gamma(z)} = (-1)^n (z)_n$$

□

Relation 9.

$$\frac{1}{(1 - z)_{-n}} = (-1)^n (z)_n, \quad n \in \mathbb{Z}$$

Proof. Using Relation 8 one writes

$$\frac{1}{(1 - z)_{-n}} = \frac{\Gamma(1 - z)}{\Gamma(1 - z - n)} = \frac{\Gamma(1 - z - n + n)}{\Gamma(1 - z - n)} = (1 - z - n)_n = (-1)^n (z)_n$$

□

Relation 10.

$$(z)_n = (z)_m (z + m)_{n-m}$$

Proof.

$$(z)_n = \frac{\Gamma(z+n)}{\Gamma(z)} = \frac{\Gamma(z+m)}{\Gamma(z+m)} \frac{\Gamma(z+m+n-m)}{\Gamma(z)} = (z)_m (z+m)_{n-m}$$

□

Relation 11.

$$\binom{n}{k} = \frac{(-1)^k (-n)_k}{k!}$$

Relation 12. [27, Eq. 07.23.03.0002.01].

$$F\left(\begin{matrix} a, b \\ c \end{matrix}; 1\right) = \frac{\Gamma(c)\Gamma(c-a-b)}{\Gamma(c-a)\Gamma(c-b)}, \quad \Re\{c-a-b\} > 0$$

Relation 13. For $2k = 0, 2, 4, \dots$

$$(1-a-2k)_{2k} = 2^{2k} \left(\frac{a}{2}\right)_k \left(\frac{a+1}{2}\right)_k.$$

Proof. Using the gamma reflection formula in Relation 7 one writes

$$(1-a-2k)_{2k} = \frac{\Gamma(1-a)}{\Gamma(1-a-2k)} = \frac{\csc \pi a}{\csc \pi(a+2k)} \frac{\Gamma(a+2k)}{\Gamma(a)} = \frac{\Gamma(a+2k)}{\Gamma(a)}.$$

Then applying the gamma duplication formula in Relation ?? yields

$$\frac{\Gamma(a+2k)}{\Gamma(a)} = \frac{\Gamma(\frac{a}{2}+k)\Gamma(\frac{a}{2}+k+\frac{1}{2})2^{2k}}{\Gamma(\frac{a}{2})\Gamma(\frac{a}{2}+\frac{1}{2})} = 2^{2k} \left(\frac{a}{2}\right)_k \left(\frac{a+1}{2}\right)_k.$$

□

Relation 14.

$$(a)_{n+k} = (a)_n (a+n)_k.$$

Proof.

$$(a)_{n+k} = \frac{\Gamma(a+n+k)}{\Gamma(a)} = \frac{\Gamma(a+n)}{\Gamma(a)} \frac{\Gamma(a+n+k)}{\Gamma(a+n)} = (a)_n (a+n)_k.$$

□

B Limiting properties of \mathcal{T}_ν as $|\nu| \rightarrow \infty$

One curiosity that remains is what happens to \mathcal{T}_ν and its moments as $|\nu| \rightarrow \infty$. The following theorem presents these results.

Theorem 19. Let $Y_1 \sim \mathcal{G}(\alpha_1, \beta_1)$ and $Y_2 \sim \mathcal{G}(\alpha_2, \beta_2)$ be gamma random variables parameterized in terms of a known shape α_i and unknown rate of the form $\beta_i = \alpha_i/\kappa_i$. Then,

$$\begin{aligned}\mathcal{U} &= \frac{1}{\kappa_1} {}_1F_1\left(\frac{1}{\alpha_2}; \frac{\alpha_2 Y_2}{\kappa_1}\right), \quad \text{with } \kappa_1 > \kappa_2 \text{ and } \kappa_1 \text{ known} \\ \mathcal{V} &= -\frac{1}{\kappa_2} {}_1F_1\left(\frac{1}{\alpha_1}; \frac{\alpha_1 Y_1}{\kappa_2}\right), \quad \text{with } \kappa_1 < \kappa_2 \text{ and } \kappa_2 \text{ known}\end{aligned}$$

are unbiased estimators of $\tau = (\kappa_1 - \kappa_2)^{-1}$.

Proof. Without loss of generality we consider the discrete estimator of Lemma 3 expressed by

$$\mathcal{T}_n = \frac{1}{Y_1} \sum_{k=0}^{n-1} \frac{\alpha_1^{-k-1}}{(\alpha_1)_{-k-1}(\alpha_2)_k} \left(\frac{\alpha_2 Y_2}{Y_1}\right)^k,$$

where we recall that $Y_1 \sim \mathcal{G}(\alpha_1, \alpha_1/\kappa_1)$ and $Y_2 \sim \mathcal{G}(\alpha_2, \alpha_2/\kappa_2)$ are independent. From Theorem 4 we know that $\mathbb{E}\mathcal{T}_n < \infty$ if and only if $n < \alpha_1$; thus, in order for $\mathbb{E}(\lim_{n \rightarrow \infty} \mathcal{T}_n) < \infty$ we require $\alpha_1 \rightarrow \infty$. To evaluate the limit in α_1 note that if $\alpha_1 \in \mathbb{N}$ then in terms of distribution

$$Y_1 = \frac{1}{\alpha_1} \sum_{k=1}^{\alpha_1} Y'_k, \quad Y'_k \sim \mathcal{G}(1, 1/\kappa_1)$$

such that by the strong law of large numbers $Y_1 \xrightarrow{\text{a.s.}} \kappa_1$ as $\alpha_1 \rightarrow \infty$. Furthermore, by [7, Eq. 5.11.13] as $\alpha_1 \rightarrow \infty$ we have $\alpha_1^{-k-1}/(\alpha_1)_{-k-1} \sim 1 + \mathcal{O}\{1/\alpha_1\}$; thus, passing to the limit $\alpha_1 \rightarrow \infty$:

$$\mathcal{T}_n \xrightarrow{\text{a.s.}} \mathcal{U}_n \text{ where } \mathcal{U}_n = \frac{1}{\kappa_1} \sum_{k=0}^{n-1} \frac{1}{(\alpha_2)_k} \left(\frac{\alpha_2 Y_2}{\kappa_1}\right)^k.$$

As a consequence of taking $\alpha_1 \rightarrow \infty$ there is no longer any restriction on how large n can be. Taking the limit $n \rightarrow \infty$ in the previous result subsequently yields

$$\lim_{n \rightarrow \infty} \mathcal{U}_n = \frac{1}{\kappa_1} \sum_{k=0}^{\infty} \frac{(1)_k}{(\alpha_2)_k k!} \left(\frac{\alpha_2 Y_2}{\kappa_1}\right)^k,$$

which is the estimator \mathcal{U} . In addition to κ_1 being known if we assume $\kappa_1 > \kappa_2$ then one can easily confirm

$$\mathbb{E}\mathcal{U} = \lim_{n \rightarrow \infty} \mathbb{E}\mathcal{T}_n = \frac{1}{\kappa_1 - \kappa_2},$$

which completes the proof for the estimator \mathcal{U} . To obtain the corresponding proof for the estimator \mathcal{V} one can use the reflection formula in Theorem 5 to write

$$\lim_{n \rightarrow -\infty} \mathcal{T}_n(Y_1, Y_2, \alpha_1, \alpha_2) = - \lim_{n \rightarrow \infty} \mathcal{T}_n(Y_2, Y_1, \alpha_2, \alpha_1),$$

where we require $\alpha_2 \rightarrow \infty$, i.e. κ_2 known, and $\kappa_1 < \kappa_2$ in order for the limiting expected value to converge to the desired quantity. \square

Remark 4. The estimator \mathcal{U} is the solution to the integral equation (2.1) when κ_1 is known, that is, it satisfies

$$\mathcal{L}\{y_2^{\alpha_2-1}\mathcal{U}(y_2)\}(\beta_2) = \frac{\Gamma(\alpha_2)\beta_2^{-\alpha_2}}{\kappa_1 - \alpha_2/\beta_2}.$$

Likewise,

$$\mathcal{L}\{y_1^{\alpha_1-1}\mathcal{V}(y_1)\}(\beta_1) = \frac{\Gamma(\alpha_1)\beta_1^{-\alpha_1}}{\alpha_1/\beta_1 - \kappa_2}.$$

These results agree with [19, Eq. 5.4.9].

Lemma 39.

$$\text{Var}\mathcal{U} = \frac{1}{(\kappa_1 - \kappa_2)^2} \left(F\left(\frac{1, 1}{\alpha_2}; \frac{\kappa_2^2}{(\kappa_1 - \kappa_2)^2}\right) - 1 \right)$$

if $\kappa_1 > 2\kappa_2$ and infinite otherwise. Likewise,

$$\text{Var}\mathcal{V} = \frac{1}{(\kappa_1 - \kappa_2)^2} \left(F\left(\frac{1, 1}{\alpha_1}; \frac{\kappa_1^2}{(\kappa_1 - \kappa_2)^2}\right) - 1 \right)$$

if $\kappa_2 > 2\kappa_1$ and infinite otherwise.

Proof. We will present the proof for $\text{Var}\mathcal{U}$ with the proof for $\text{Var}\mathcal{V}$ being essentially the same. We begin by evaluating $\lim_{n, \alpha_1 \rightarrow \infty} \mathbb{E}\mathcal{T}_n^2$ from the expression in Lemma 20. According to [7, Eq. 15.12.2] we have the asymptotic relation

$$F\left(\frac{k+1, \ell+1}{\alpha_1}; 1\right) \sim 1 + \mathcal{O}\{1/\alpha_1\}, \quad \alpha_1 \rightarrow \infty.$$

Thus, upon taking the appropriate limits and writing ${}_2F_1(-k, -\ell; \alpha_1; 1)$ in terms of Pochhammer symbols one has

$$\mathbb{E}\mathcal{U}^2 = \frac{1}{\kappa_1^2} \sum_{k, \ell=0}^{\infty} \frac{(\alpha_2)_{k+\ell}(1)_k(1)_\ell}{(\alpha_2)_k(\alpha_2)_\ell k! \ell!} \zeta^k \zeta^\ell. \quad (5.1)$$

where we again use the shorthand $\zeta = \kappa_2/\kappa_1$. According to Definition 31, this double series can be expressed in terms of Appell's second hypergeometric function and is absolutely convergent if $\zeta < 1/2 \implies \kappa_1 > 2\kappa_2$. To simplify this result we apply the reduction formula in [7, Eq. 16.16.3] to find

$$\begin{aligned} \mathbb{E}\mathcal{U}^2 &= \frac{1}{\kappa_1^2} F_2(\alpha_2; 1, 1; \alpha_2, \alpha_2; \zeta, \zeta) \\ &= \frac{1}{\kappa_1^2} (1 - \zeta)^{-1} F_1(1; \alpha_2 - 1, 1; \alpha_2; \zeta, \zeta(1 - \zeta)^{-1}), \end{aligned}$$

where $F_1(\cdot)$ is Appell's first hypergeometric function as defined in Definition 30. Taking advantage of the symmetry $F_1(a; b, b'; c; s, z) = F_1(a; b', b; c; z, s)$ and applying the reduction formula [7, Eq. 15.12.2] then yields

$$\mathbb{E}\mathcal{U}^2 = \frac{1}{\kappa_1^2} (1 - \zeta)^{-2} F\left(\frac{1, 1}{\alpha_2}; \frac{\zeta^2}{(1 - \zeta)^2}\right).$$

Subtracting $(\mathbb{E}\mathcal{U})^2$ and simplifying yields the desired result. \square

Remark 5. The divergence of $\text{Var}\mathcal{U}$ for $\kappa_1 < 2\kappa_2$ is not just a consequence of the double series representation (5.1). Indeed, using the integral definition of $\text{E}\mathcal{U}^2$ and $\zeta = \kappa_2/\kappa_1$ one may deduce with a simple substitution

$$\text{E}\mathcal{U}^2 \propto \int_0^\infty [{}_1F_1(1; \alpha_2; t)]^2 t^{\alpha_2-1} e^{-t/\zeta} dt.$$

But according to [7, Eq. 13.7.1], as $t \rightarrow \infty$

$$[{}_1F_1(1; \alpha_2; t)]^2 t^{\alpha_2-1} e^{-t/\zeta} \sim \Gamma^2(\alpha_2) t^{1-\alpha_2} e^{(2-1/\zeta)t},$$

which diverges for $\zeta^{-1} < 2$, i.e. $\kappa_1 < 2\kappa_2$. At the boundary $\kappa_1 = 2\kappa_2$ we use Relation 12 to further note that

$$\text{E}\mathcal{U}^2 = \begin{cases} 4\kappa_1^{-2}(\alpha_2 - 1)/(\alpha_2 - 2), & \alpha_2 > 2 \\ \infty, & \alpha_2 \leq 2. \end{cases}$$

Proof of Theorem 1. Assume \mathcal{T} exists and let $\zeta = \kappa_2/\kappa_1$ with $\zeta < 1$. Then by the law of total variance we have

$$\text{Var}\mathcal{T}(Y_1, Y_2) = \text{E}(\text{Var}(\mathcal{T}(Y_1, Y_2)|Y_2)) + \text{Var}g(\kappa_1, Y_2),$$

where $g(\kappa_1, Y_2) = \text{E}(\mathcal{T}(Y_1, Y_2)|Y_2)$ and by assumption $\text{E}g(\kappa_1, Y_2) = (\kappa_1 - \kappa_2)^{-1}$. Now, from Lemma 1 we know Y_2 is a complete-sufficient statistic for κ_2 such the Lehmann-Scheffé theorem asserts $g(\kappa_1, Y_2)$ is the unique UMVUE of its expected value when κ_1 is known. But if $g(\kappa_1, Y_2)$ is unique and $\zeta < 1$ then Theorem 19 proves $g(\kappa_1, Y_2) = \mathcal{U}$. Given $\text{E}(\text{Var}(\mathcal{T}(Y_1, Y_2)|Y_2)) \geq 0$ it follows that $\text{Var}\mathcal{U} \leq \text{Var}\mathcal{T}$. Furthermore, Lemma 39 tells us that $\text{Var}\mathcal{U} = \infty$ if $\zeta > 1/2$; thus, it must be that $\text{Var}\mathcal{T} = \infty$ on $1/2 < \zeta < 1$. By a similar argument if $\zeta > 1$ then $\text{Var}\mathcal{V} \leq \text{Var}\mathcal{T}$ with \mathcal{V} also given in Theorem 19. Since $\text{Var}\mathcal{V} = \infty$ for $\zeta < 2$ we can combine the previous result to conclude $\text{Var}\mathcal{T} = \infty$ on $1/2 < \zeta < 2$ which completes the proof. \square

C Proofs of differential operator identities

Here present the proofs associated with the differential operator identities in Lemma 7.

Proof of Lemma 7 (i). Begin by using the Definition 6 to write

$$\Lambda_\omega z^s = \omega z^s + z \partial_z z^s.$$

Then by the chain rule we find

$$\Lambda_\omega z^s = \omega z^s + z(s z^{s-1} + z^s \partial_z) = z^s(\omega + s + z \partial_z) = z^s \Lambda_{\omega+s},$$

which completes the proof. \square

Proof of Lemma 7 (ii). See [10]. \square

Proof of Lemma 7 (iii). Let $P(n) : (z\vartheta)^n = z(\vartheta z)^n z^{-1}$. It is trivial to show that $P(0)$ holds; thus, assuming $P(n)$ we have for $P(n+1)$

$$(z\vartheta)^{n+1} = (z\vartheta)z(\vartheta z)^n z^{-1} = z(\vartheta z)(\vartheta z)^n z^{-1} = z(\vartheta z)^{n+1} z^{-1},$$

thus, $P(n) \implies P(n+1)$. Substituting the result in (ii) for $(\vartheta z)^n$ subsequently produces the desired result. \square

Proof of Lemma 7 (iv). Let $P(n) : \Lambda_\omega^n = z^{-\omega} \vartheta^n z^\omega$ and note that $P(0)$ trivially holds. Assuming $P(n)$ we have for $P(n+1)$

$$\Lambda_\omega^{n+1} = (\omega + z\partial_z)\Lambda_\omega^n = (\omega + z\partial_z)z^{-\omega} \vartheta^n z^\omega = z^{-\omega}(z\partial_z)\vartheta^n z^\omega = z^{-\omega} \vartheta^{n+1} z^\omega,$$

where the second to last equality is due to result (i). Thus, $P(n) \implies P(n+1)$ which completes the proof. \square

Proof of Lemma 7 (v). Let $P(n) : (\vartheta)^{(n)} = \frac{1}{z}(z\vartheta)^n z^{1-n}$. By Definition 7, it immediately follows that $P(0)$ holds. Assuming $P(n)$ we have for $P(n+1)$

$$(\vartheta)^{(n+1)} = (\vartheta)^{(n)}(\vartheta - n) = \frac{1}{z}(z\vartheta)^n z^{1-n} \Lambda_{-n}.$$

Then, making use of (iv) we find

$$(\vartheta)^{(n+1)} = \frac{1}{z}(z\vartheta)^n z^{1-n} z^n \vartheta z^{-n} = \frac{1}{z}(z\vartheta)^{n+1} z^{1-(n+1)}.$$

Therefore, $P(n) \implies P(n+1)$. Substituting the result of (iii) for $(z\vartheta)^n$ then completes the proof. \square

Proof of Lemma 7 (vi). Let $P(n) : (\Lambda_\omega)^{(n)} = z^{-\omega}(\vartheta)^{(n)} z^\omega$. By Definition 7, it immediately follows that $P(0)$ holds. Now use Definition 7 to write

$$(\Lambda_\omega)^{(n+1)} = (\omega - n + \vartheta)(\Lambda_\omega)^{(n)}.$$

Assuming $P(n)$ we have for $P(n+1)$

$$(\Lambda_\omega)^{(n+1)} = (\omega - n + \vartheta)z^{-\omega}(\vartheta)^{(n)} z^\omega = z^{-\omega}(-n + \vartheta)(\vartheta)^{(n)} z^\omega = z^{-\omega}(\vartheta)^{(n+1)} z^\omega,$$

where the second to last equality is due to result (i). Thus, $P(n) \implies P(n+1)$ and upon substituting the result of (v) for $(\vartheta)^{(n)}$ the desired result is obtained. \square

Proof of Lemma 7 (vii). From [7, Eq. 26.8.10] we have

$$\vartheta^n = \sum_{k=0}^n {}_2\mathcal{S}_n^{(k)}(\vartheta)^{(k)}.$$

Substituting the result of (v) for $(\vartheta)^{(k)}$ produces the desired result. \square

D Estimate of truncation error for the ACV \mathcal{T}_ν series expansion

An important ingredient in the computation of confidence intervals in Section 3.4 and optimal sample sizes in Section 3.5.2 is the ability to evaluate $\text{ACV}^2 \mathcal{T}_\nu$ via its series expansion. To evaluate the series expansion we write

$$\text{ACV}^2 \mathcal{T}_\nu = \text{ACV}_n^2 \mathcal{T}_\nu + E_n,$$

where

$$\text{ACV}_n^2 \mathcal{T}_\nu = \sum_{k=1}^n \sum_{\ell=0}^k \frac{\tilde{g}_{k,\ell}^2(z, \nu)}{(\alpha_1)_\ell (\alpha_2)_{k-\ell} \ell! (k-\ell)!}$$

and

$$E_n = \sum_{k=n+1}^{\infty} \sum_{\ell=0}^k \frac{\tilde{g}_{k,\ell}^2(z, \nu)}{(\alpha_1)_\ell (\alpha_2)_{k-\ell} \ell! (k-\ell)!}$$

and then determine the number n such that the error incurred in the approximation $\text{ACV}^2 \mathcal{T}_\nu \approx \text{ACV}_n^2 \mathcal{T}_\nu$ falls within some specified tolerance. Of course, we do not know a closed form for E_n and so whatever procedure used to find n will ultimately require finding a useful upper bound.

Definition 34 (Complementary incomplete Hypergeometric function). *For $\nu \in \mathbb{C}$*

$$F(\alpha, \beta; \gamma; z)_\nu^c := F(\alpha, \beta; \gamma; z) - F(\alpha, \beta; \gamma; z)_\nu,$$

where $F(\alpha, \beta; \gamma; z)_\nu$ is the incomplete hypergeometric function.

Proposition 9. *For $\nu \in \mathbb{C}$*

$$F(\alpha, \beta; \gamma; z)_\nu^c = \frac{(\alpha)_\nu (\beta)_\nu}{(\gamma)_\nu} \frac{z^\nu}{\Gamma(1+\nu)} {}_3F_2 \left(\begin{matrix} 1, \alpha + \nu, \beta + \nu \\ 1 + \nu, \gamma + \nu \end{matrix}; z \right).$$

Likewise, if $\nu = n \in \mathbb{N}_0$

$$F(\alpha, \beta; \gamma; z)_n^c = F(\alpha, \beta; \gamma; z) - \frac{(\alpha)_{n-1} (\beta)_{n-1}}{(\gamma)_{n-1}} \frac{z^{n-1}}{\Gamma(n)} {}_3F_2 \left(\begin{matrix} 1, 1-n, 2-n-\gamma \\ 2-n-\alpha, 2-n-\beta \end{matrix}; \frac{1}{z} \right).$$

Theorem 20. *Let E_n denote the truncation error incurred in approximating $\text{ACV}^2 \mathcal{T}_\nu$ with $\text{ACV}_n^2 \mathcal{T}_\nu$. Then, $E_n \leq E_{n,m}^*$, where*

$$\begin{aligned} E_{n,m}^* &= \sum_{j=0}^{m-1} (\mathbb{E} h_{k'+j, k'})^2 b_j F \left(\begin{matrix} 1+\nu, 1+\nu \\ \alpha_1 \end{matrix}; 1 \right)_{k'}^c \\ &\quad + (\mathbb{E} h_{k''+m, k''} \mathbb{1}_{z \in [0,1]})^2 \left(F \left(\begin{matrix} 1+\nu, 1+\nu \\ \alpha_1 \end{matrix}; 1 \right) F \left(\begin{matrix} 1-\nu, 1-\nu \\ \alpha_2 \end{matrix}; 1 \right) \right)_m^c \\ &\quad - b_m \sum_{k=0}^{k''-1} a_k {}_5F_4 \left(\begin{matrix} -k, 1-k-\alpha_1, 1, 1-\nu+m, 1-\nu+m \\ 1+m, m+\alpha_2, -k-\nu, -k-\nu \end{matrix}; 1 \right), \end{aligned}$$

$k' = \max(0, n+1-j)$, $k'' = \max(0, n+1-m)$, $a_j = (1+\nu)_j^2/((\alpha_1)_j j!)$, $b_j = (1-\nu)_j^2/((\alpha_2)_j j!)$, $F(\alpha, \beta; \gamma; z)_\nu^c$ is the complementary incomplete hypergeometric function of Definition 34, and $\mathbf{E}h_{n,\omega}$ is given in (2.10). Furthermore, $E_{n,m}^* < \infty$ if $\alpha_1 > 2(1+\nu)$ and $\alpha_2 > 2(1-\nu)$ and infinite otherwise.

Proof. We begin by writing

$$E_n = \sum_{k=n+1}^{\infty} \sum_{\ell=0}^k a_\ell b_{k-\ell} (\mathbf{E}h_{k,\ell})^2,$$

where $a_j = (1+\nu)_j^2/((\alpha_1)_j j!)$ and $b_j = (1-\nu)_j^2/((\alpha_2)_j j!)$. The series E_n is absolutely convergent and so we may rearrange its terms as

$$E_n = \sum_{j=0}^{m-1} b_j \sum_{k=k'}^{\infty} a_k (\mathbf{E}h_{k+j,k})^2 + \sum_{k=k''}^{\infty} \sum_{\ell=0}^k a_\ell b_{k-\ell+m} (\mathbf{E}h_{k+m,\ell})^2,$$

where $k' = \max(0, n+1-j)$ and $k'' = \max(0, n+1-m)$. Since all terms are nonnegative we may call on Lemma 18 to obtain the upper bound $E_n \leq E_{n,m}^*$, where

$$E_{n,m}^* = \sum_{j=0}^{m-1} b_j (\mathbf{E}h_{k'+j,k'})^2 \sum_{k=k'}^{\infty} a_k + (\mathbf{E}h_{k''+m,k''} \mathbb{1}_{z \in [0,1]})^2 \sum_{k=k''}^{\infty} \sum_{\ell=0}^k a_\ell b_{k-\ell+m}.$$

Upon inspection,

$$\sum_{k=k'}^{\infty} a_k = F\left(1+\nu, 1+\nu; \alpha_1; 1\right)_{k'}^c,$$

which converges when $\alpha_1 > 2(1+\nu)$. Furthermore,

$$\sum_{k=k''}^{\infty} \sum_{\ell=0}^k a_\ell b_{k-\ell+m} = \sum_{k=0}^{\infty} a_k \sum_{k=m}^{\infty} b_k - \sum_{k=0}^{k''-1} \sum_{\ell=0}^k a_\ell b_{k-\ell+m},$$

where

$$\sum_{k=0}^{\infty} a_k = F\left(1+\nu, 1+\nu; \alpha_1; 1\right),$$

which converges for $\alpha_1 > 2(1+\nu)$ and

$$\sum_{k=m}^{\infty} b_k = F\left(1-\nu, 1-\nu; \alpha_2; 1\right)_m^c,$$

which converges for $\alpha_2 > 2(1-\nu)$. Lastly, with a bit of algebra and working with the properties of the Pochhammer symbol we may use [7, Eq. 16.2.4] to write

$$\sum_{\ell=0}^k a_\ell b_{k-\ell+m} = a_k b_{m+5} F_4\left(\begin{matrix} -k, 1-k-\alpha_1, 1, 1-\nu+m, 1-\nu+m \\ 1+m, m+\alpha_2, -k-\nu, -k-\nu \end{matrix}; 1\right).$$

Bringing all results together gives the desired form for $E_{n,m}^*$. The proof is now complete. \square

Corollary 17. *Let, $p > 0$ and*

$$R_{n,p} = \left| \frac{\text{ACV}_n^p \mathcal{T}_\nu}{\text{ACV}_n^p \mathcal{T}_\nu} - 1 \right|$$

denote the absolute relative error incurred when approximating $\text{ACV}^p \mathcal{T}_\nu$ with $\text{ACV}_n^p \mathcal{T}_\nu$. Then, $R_{n,p} \leq R_{n,m,p}^$ where*

$$R_{n,m,p}^* = \left| \left(1 + \frac{E_{n,m}^*}{\text{ACV}_n^2 \mathcal{T}_\nu} \right)^{-p/2} - 1 \right|$$

and $E_{n,m}^$ is given in Theorem 20. Furthermore, if $\nu > 1$ is constant then for all $z \in Z \subset \mathbb{R}^+$, $R_{n,p}^* \leq R_{n,m,p}^*$ where*

$$R_{n,m,p}^* = \left| \left(1 + \frac{E_{n,m}^*|_{z=\sup Z}}{\text{ACV}_n^2 \mathcal{T}_\nu|_{z=\inf Z}} \right)^{-p/2} - 1 \right| \times 100\%.$$

If instead $\nu < -1$ interchange $\inf Z$ and $\sup Z$.

Proof. The first result follows from writing $\text{ACV}^p \mathcal{T}_\nu = (\text{ACV}_n^2 \mathcal{T}_\nu + E_n)^{p/2}$ and then substituting $E_n \mapsto E_{n,m}^*$ to obtain an upper bound on $R_{n,p}$. For the second result we may use Lemma 19 to claim that $E_{h_{k'+j,k'}}$, $E_{h_{k''+m,k''}}$, and $E_{h_{k''+m,0}}$ are all increasing functions of z for some constant $\nu > 1$ on $z \in \mathbb{R}^+$. Furthermore, since $E_{h_{k''+m,k''}} = E_{h_{k''+m,0}} = (k'' + m + 1)^{-1}$ at $z = 1$ it follows that $E_{h_{k''+m,k''}} \mathbb{1}_{z \in [0,1]}$ must also be increasing in z on $z \in \mathbb{R}^+$. Combinbing these observations with the fact that $E_{n,m}^*$ and $\text{ACV}_n^2 \mathcal{T}_\nu$ are sums of nonnegative terms implies that both of these functions must also be increasing in z on $z \in \mathbb{R}^+$; hence, for all $z \in Z$: $E_n^* \leq E_n^*|_{z=\sup Z}$ and $\text{ACV}_n^{-2} \mathcal{T}_\nu \leq \text{ACV}_n^{-2} \mathcal{T}_\nu|_{z=\inf Z}$, which gives the upper bound on $R_{n,m,p}^*$. Noting the monotonicity of these functions is reversed if $\nu < -1$ gives the complementary bound. \square

E Bounding functions for $|\partial_\beta^n F(\alpha, \alpha; \beta; x)|$

In this section we derive several results that will be used to determine bounding functions for $|\partial_\beta^n F(\alpha, \alpha; \beta; x)|$ on $x \in [0, 1]$ when $\alpha \in \mathbb{R}$ and $\beta \in \mathbb{R}^+$. The main results are found in Theorems 21 and 22.

Before we start deriving the bounding functions we must find a suitable expression for higher order derivatives of the hypergeometric function w.r.t. its bottom parameter. The following Lemma turns out to be key for doing just that.

Lemma 40. *For $a, b > 0$, $n \in \mathbb{N}_0$, and $X \sim \text{Beta}(a, b)$*

$$(a)_b \partial_a^n (a)_b^{-1} = \mathbb{E} \log^n X.$$

Proof. Denoting $P(n) : (a)_b \partial_a^n (a)_b^{-1} = \mathbb{E} \log^n X$ we immediately conclude that $P(0)$ holds. Assuming $P(n)$ we find

$$\begin{aligned} P(n) \implies \partial_a^{n+1} (a)_b^{-1} &= \partial_a (a)_b^{-1} \mathbb{E} \log^n X \\ &= \partial_a \int_0^1 (\log^n t) \frac{t^{a-1} (1-t)^{b-1}}{\Gamma(b)} dt \\ &= \int_0^1 (\log^{n+1} t) \frac{t^{a-1} (1-t)^{b-1}}{\Gamma(b)} dt \\ &= (a)_b^{-1} \mathbb{E} \log^{n+1} X. \end{aligned}$$

Thus, $P(n) \implies P(n+1)$ and the proof is complete. \square

Using this probabilistic interpretation for derivatives of the Pochhammer symbol now facilitates a simple integral representation for $\partial_\gamma^n F(\alpha, \beta; \gamma; x)$ as seen in the following result.

Lemma 41. *For $\gamma > 0$, $|x| < 1$, and $n \in \mathbb{N}_0$*

$$\partial_\gamma^n F(\alpha, \beta; \gamma; x) = \int_0^1 \log^n(1-t) (1-t)^{\gamma-1} \partial_t F(\alpha, \beta; 1; xt) dt + \mathbb{1}_{n=0}$$

Proof. From Lemma 40 we write

$$\partial_\gamma^n F(\alpha, \beta; \gamma; x) = \sum_{k=1}^{\infty} \frac{(\alpha)_k (\beta)_k}{(\gamma)_k} \frac{x^k}{k!} \mathbb{E} \log^n X + \mathbb{1}_{n=0}, \quad X \sim \text{Beta}(\gamma, k).$$

Now writing the expected value in integral form subsequently gives

$$\partial_\gamma^n F(\alpha, \beta; \gamma; x) = \lim_{m \rightarrow \infty} \int_0^1 (\log^n t) t^{\gamma-1} \sum_{k=1}^m \frac{(\alpha)_k (\beta)_k}{\Gamma(k)} \frac{x^k}{k!} (1-t)^{k-1} dt + \mathbb{1}_{n=0}.$$

Since $|x| < 1$ the magnitude of the integrand is bounded above by $C(-\log t)^n t^{\gamma-1}$ for some $C > 0$, which is integrable for all $n \in \mathbb{N}_0$ and $\gamma > 0$. Consequently, we have by argument of dominated convergence

$$\partial_\gamma^n F(\alpha, \beta; \gamma; x) = - \int_0^1 (\log^n t) t^{\gamma-1} \partial_t F(\alpha, \beta; 1; x(1-t)) dt + \mathbb{1}_{n=0},$$

which upon substituting $t \mapsto 1-t$ gives the desired form. The proof is now complete. \square

Upon inspection of the integral representation in Lemma 40, one bounding function immediately stands out.

Theorem 21. *Let $\alpha \in \mathbb{R}$, $\beta > 0$, $x \in [0, 1]$, and $n \in \mathbb{N}_0$. Then for any $d > 1$*

$$|\partial_\beta^n F(\alpha, \alpha; \beta; x)| < e^{-n} \left(\frac{dn}{\beta} \right)^n (F(\alpha, \alpha; (1-d^{-1})\beta; x) - 1) + \mathbb{1}_{n=0},$$

where for the case $n = 0$ we define $0^0 := 1$.

Proof. For brevity denote $\beta' = (1 - d^{-1})\beta$. Then by Lemma 41 we have

$$|\partial_\beta^n F(\alpha, \alpha; \beta; x)| = \int_0^1 (1-t)^{\beta/d} (-\log(1-t))^n (1-t)^{\beta'-1} \partial_t F(\alpha, \alpha; 1; xt) dt + \mathbb{1}_{n=0}.$$

Now, $0 \leq (1-t)^{\beta/d} (-\log(1-t))^n \leq e^{-n} (dn/\beta)^n$; thus, with the help of [11, Eq. 7.512.12] if $d > 0$ then $\beta' > 0$ and we have

$$|\partial_\beta^n F(\alpha, \alpha; \beta; x)| < e^{-n} \left(\frac{dn}{\beta} \right)^n \frac{\alpha^2 x}{\beta'} {}_3F_2 \left(\begin{matrix} 1, \alpha + 1, \alpha + 1 \\ 2, \beta' + 1 \end{matrix}; x \right) + \mathbb{1}_{n=0}.$$

The contiguous relation in [27, Eq. 07.27.17.0012.01] then reduces this result to its final form. The proof is now complete. \square

Our ultimate goal in this effort is to find bounding function for the purposes of studying the convergence of higher order derivatives of $\text{ACV}^2 \mathcal{T}_\nu$ w.r.t. α_1 and α_2 . However, observe that a key feature of the bounding function given in Theorem 21 is a reduction of the bottom parameter by a multiplicative factor of $(1 - d^{-1})$, $d > 1$. Using this bounding function for studying higher order derivatives of $\text{ACV}^2 \mathcal{T}_\nu$ would effectively reduce α_1 and α_2 by this same factor and thus would alter the convergence properties of the integral representing the higher order derivatives of $\text{ACV}^2 \mathcal{T}_\nu$. As a consequence, we would not determine the full range of possible values for α_1 and α_2 and must turn to finding a more suitable bounding function. We proceed with two more preliminary results and then onto Theorem 22 which gives us the result were looking for.

Lemma 42.

$$\int (1-t)^{s-1} (1-xt)^{-s} dt = -\frac{1}{s} (1-t)^s (1-xt)^{-s} F \left(\begin{matrix} 1, s \\ 1+s \end{matrix}; x \frac{1-t}{1-xt} \right) + C.$$

Proof. Let I denote the integral in question. Substituting $s = (1-t)/(1-xt)$ yields

$$I = - \int (1-xs)^{-1} s^{c-1} ds = - \int_0^s (1-xz)^{-1} z^{c-1} dz.$$

Another substitution of $z = sw$ subsequently allows us to write the resulting integral in the form of the integral representation for the hypergeometric function in Relation 1. The proof is now complete. \square

Lemma 43 ([2, Lem. 2.3]). *For $\alpha, \beta \in \mathbb{R}^+$ and $x \in [0, 1]$*

$$F(\alpha, \beta; \alpha + \beta; x) \leq 1 - \frac{1}{B(\alpha, \beta)} \log(1-x).$$

We now present the

Theorem 22. *For $\alpha \in \mathbb{R}$, $\beta \in \mathbb{R}^+$, $x \in [0, 1]$, and $n \in \mathbb{N}_0$:*

$$|\partial_\beta^n F(\alpha, \alpha; \beta; x)| \leq v_n(\alpha, \beta, x),$$

where

$$v_n(\alpha, \beta, x) = \begin{cases} \frac{n!}{B(|\alpha|, |\alpha|)} \frac{1}{(\beta - 2\alpha \mathbb{1}_{\alpha > 0})^{n+1}} + \mathbb{1}_{n=0}, & \beta > 2\alpha \\ \frac{n!}{B(\alpha, \alpha)} \left(\frac{1}{2\alpha} - \log(1-x) \right)^{n+1} + \mathbb{1}_{n=0}, & \beta = 2\alpha \\ \frac{n!}{B(\alpha, \alpha)} (1-x)^{\beta-2\alpha} \left(\frac{1}{\beta} - \log(1-x) \right)^{n+1} + \mathbb{1}_{n=0}, & \beta < 2\alpha. \end{cases}$$

Proof. We begin with the integral representation of Lemma 41 and write

$$|\partial_\beta^n F(\alpha, \alpha; \beta; x)| \leq \alpha^2 (-1)^n \int_0^1 \log^n(1-t) (1-t)^{\beta-1} F(\alpha+1, \alpha+1; 2; xt) dt + \mathbb{1}_{n=0}.$$

Each case will now be proven from this integral representation.

(1) $\beta > 2\alpha$.

Proof. The case $\beta > 2\alpha$ must itself be broken down into three subcases: $\alpha < 0$, $\alpha = 0$, and $\alpha > 0$. If $\alpha < 0$ then we have from Lemma 23 that

$$F(\alpha+1, \alpha+1; 2; xt) \leq \frac{1}{\alpha^2 B(-\alpha, -\alpha)};$$

hence,

$$\begin{aligned} |\partial_\beta^n F(\alpha, \alpha; \beta; x)| &\leq \frac{(-1)^n}{B(-\alpha, -\alpha)} \int_0^1 \log^n(1-t) (1-t)^{\beta-1} dt + \mathbb{1}_{n=0} \\ &= \frac{n!}{B(-\alpha, -\alpha)} \frac{1}{\beta^{n+1}} + \mathbb{1}_{n=0}. \end{aligned}$$

For $\alpha = 0$ we have the trivial calculation

$$|\partial_\beta^n F(0, 0; \beta; x)| = \mathbb{1}_{n=0}.$$

Now if $\alpha > 0$ we again call on Lemma 23 to deduce

$$F(\alpha+1, \alpha+1; 2; xt) = (1-xt)^{-2\alpha} F(1-\alpha, 1-\alpha; 2; xt) \leq \frac{(1-t)^{-2\alpha}}{\alpha^2 B(\alpha, \alpha)}.$$

It follows that

$$\begin{aligned} |\partial_\beta^n F(\alpha, \alpha; \beta; x)| &\leq \frac{(-1)^n}{B(\alpha, \alpha)} \int_0^1 \log^n(1-t) (1-t)^{\beta-2\alpha-1} dt + \mathbb{1}_{n=0} \\ &= \frac{n!}{B(\alpha, \alpha)} \frac{1}{(\beta-2\alpha)^{n+1}} + \mathbb{1}_{n=0}. \end{aligned}$$

Combining these three results yields the desired form for the case $\beta > 2\alpha$. ■

(2) $\beta \leq 2\alpha$.

Proof. First observe that $\beta > 0 \wedge \beta \leq 2\alpha \implies \alpha > 0$ and so we have from Lemma 23

$$F(\alpha + 1, \alpha + 1; 2; xt) \leq \frac{(1 - xt)^{-2\alpha}}{\alpha^2 B(\alpha, \alpha)} \leq \frac{(1 - x)^{\beta - 2\alpha} (1 - xt)^{-\beta}}{\alpha^2 B(\alpha, \alpha)}$$

and

$$|\partial_\beta^n F(\alpha, \alpha; \beta; x)| \leq \frac{(1 - x)^{\beta - 2\alpha}}{B(\alpha, \alpha)} I_n + \mathbb{1}_{n=0},$$

where

$$I_n = \int_0^1 (-1)^n \log^n(1 - t) (1 - t)^{\beta - 1} (1 - xt)^{-\beta} dt.$$

Performing integration by parts with $u = (-1)^n \log^n(1 - t)$ and $dv = (1 - t)^{\beta - 1} (1 - xt)^{-\beta} dt$ we use Lemma 42 to write

$$\begin{aligned} I_n &= -\frac{(-1)^n}{\beta} \log^n(1 - t) (1 - t)^\beta (1 - xt)^{-\beta} F\left(\frac{1, \beta}{1 + \beta}; x \frac{1 - t}{1 - xt}\right) \Big|_{t=0}^1 \\ &+ \frac{n}{\beta} \int_0^1 (-1)^{n-1} \log^{n-1}(1 - t) (1 - t)^{\beta - 1} (1 - xt)^{-\beta} F\left(\frac{1, \beta}{1 + \beta}; x \frac{1 - t}{1 - xt}\right) dt. \end{aligned}$$

Evaluating the limit term gives

$$uv|_{t=0}^1 = \begin{cases} \frac{1}{\beta} F(1, \beta; 1 + \beta; x), & n = 0 \\ 0, & n \in \mathbb{N} \end{cases} \quad (5.2)$$

with the latter case being due to $\log^n(1 - t) (1 - t)^\beta \rightarrow 0$ in both limits. Furthermore, calling in Lemma 43 we find

$$F\left(\frac{1, \beta}{1 + \beta}; x \frac{1 - t}{1 - xt}\right) \leq 1 - \beta \log\left(1 - \frac{x(1 - t)}{1 - xt}\right) \leq 1 - \beta \log(1 - x)$$

Hence, $I_n \leq \frac{n}{\beta} (1 - \beta \log(1 - x)) I_{n-1}$ and

$$I_n \leq \frac{n!}{\beta^n} (1 - \beta \log(1 - x))^n I_0.$$

Note that I_0 is given by the $n = 0$ case of (5.2) and $I_0 \leq \frac{1}{\beta} (1 - \beta \log(1 - x))$. These observations lead us to conclude

$$|\partial_\beta^n F(\alpha, \alpha; \beta; x)| \leq \frac{(1 - x)^{\beta - 2\alpha}}{B(\alpha, \alpha)} \frac{n!}{\beta^{n+1}} (1 - \beta \log(1 - x))^{n+1} + \mathbb{1}_{n=0},$$

which is the final result for the $\beta < 2\alpha$ case. Substituting $\beta \mapsto 2\alpha$ into the r.h.s. of the inequality then gives the desired result for the remaining case of $\beta = 2\alpha$. The proof is now complete. \blacksquare

□

Bibliography

- [1] Ibrahim M. Alabdulmohsin. *Summability Calculus: A Comprehensive Theory of Fractional Finite Sums*. Springer, 1 edition, 2018.
- [2] G. D. Anderson, R. W. Barnard, K. C. Richards, M. K. Vamanamurthy, and M. Vuorinen. Inequalities for zero-balanced hypergeometric functions. *Transactions of the American Mathematical Society*, 347(5):1713–1723, 1995.
- [3] B. P. Beecken and E. R. Fossum. Determination of the conversion gain and the accuracy of its measurement for detector elements and arrays. *Appl. Opt.*, 35(19):3471–3477, Jul 1996.
- [4] S. E. Bohndiek, A. Blue, A. T. Clark, M. L. Prydderch, R. Turchetta, G. J. Royle, and R. D. Speller. Comparison of methods for estimating the conversion gain of cmos active pixel sensors. *IEEE Sensors Journal*, 8(10):1734–1744, Oct 2008.
- [5] L. Carlitz. Note on Nörlund’s polynomial $B_n^{(z)}$. *Proc. Amer. Math. Soc.*, 11:452–455, 1960.
- [6] G. Casella and R.L. Berger. *Statistical Inference*. Duxbury advanced series in statistics and decision sciences. Thomson Learning, 2 edition, 2002.
- [7] NIST Digital Library of Mathematical Functions. <http://dlmf.nist.gov/>, Release 1.0.23 of 2019-06-15. F. W. J. Olver, A. B. Olde Daalhuis, D. W. Lozier, B. I. Schneider, R. F. Boisvert, C. W. Clark, B. R. Miller and B. V. Saunders, eds.
- [8] EMVA standard 1288: Standard for Characterization of Image Sensors and Cameras. Standard, European Machine Vision Association, Barcelona, Spain, December 2016.
- [9] S.R. Finch and G.C. Rota. *Mathematical Constants*. Encyclopedia of Mathematics and its Applications. Cambridge University Press, 2003.
- [10] Norbert Fleury and Alexander Turbiner. Polynomial relations in the heisenberg algebra. *Journal of Mathematical Physics*, 35(11):6144–6149, 1994.

- [11] Izrail S Gradshteyn and Iosif M Ryzhik. *Table of Integrals, Series, and Products*. Academic Press, 8 edition, 2014.
- [12] Aaron Hendrickson. The inverse gamma-difference distribution and its first moment in the cauchy principal value sense. *Statistics and Its Interface*, 12(3):467–478, Jun 2019.
- [13] Aaron J. Hendrickson. Centralized inverse-Fano distribution for controlling conversion gain measurement accuracy of detector elements. *J. Opt. Soc. Am. A*, 34(8):1411–1423, Aug 2017.
- [14] Adel K. Ibrahim. Contiguous relations for ${}_2F_1$ hypergeometric series. *Journal of the Egyptian Mathematical Society*, 20(2):72–78, 2012.
- [15] James Janesick, James T. Andrews, and Tom Elliott. Fundamental performance differences between CMOS and CCD imagers: Part 1. In David A. Dorn and Andrew D. Holland, editors, *High Energy, Optical, and Infrared Detectors for Astronomy II*, volume 6276, pages 208–226. International Society for Optics and Photonics, SPIE, 2006.
- [16] James R. Janesick. *Photon transfer: $DN \rightarrow \lambda$* . SPIE, 2007.
- [17] Guo-Dong Liu and Hari M. Srivastava. Explicit formulas for the Nörlund polynomials $B_n^{(x)}$ and $b_n^{(x)}$. *Computers & Mathematics with Applications*, 51:1377–1384, 2006.
- [18] Masud Mansuripur and Pin Han. Thermodynamics of radiation pressure and photon momentum. In Kishan Dholakia and Gabriel C. Spalding, editors, *Optical Trapping and Optical Micromanipulation XIV*, volume 10347, pages 196–215. International Society for Optics and Photonics, SPIE, 2017.
- [19] California Institute of Technology. Bateman Manuscript Project, H. Bateman, A. Erdélyi, and United States. Office of Naval Research. *Tables of Integral Transforms: Based, in Part, on Notes Left by Harry Bateman*. Number v. 1 in Tables of Integral Transforms: Based, in Part, on Notes Left by Harry Bateman. McGraw-Hill, 1954.
- [20] ON Semiconductors. *KAI-04070: 2048 (H) × 2048 (V) Interline CCD Image Sensor*, July 2015. Rev. 3.
- [21] Bedabrata Pain and Bruce R. Hancock. Accurate estimation of conversion gain and quantum efficiency in cmos imagers. In *Sensors and Camera Systems for Scientific, Industrial, and Digital Photography Applications IV*, pages 94–103, 2003.
- [22] Walter W. Piegorsch and George Casella. The existence of the first negative moment. *The American Statistician*, 39(1):60–62, 1985.
- [23] W. Rudin. *Principles of Mathematical Analysis*. International series in pure and applied mathematics. McGraw-Hill, 3 edition, 1976.

- [24] D. A. Starkey and E. R. Fossum. Determining conversion gain and read noise using a photon-counting histogram method for deep sub-electron read noise image sensors. *IEEE Journal of the Electron Devices Society*, 4(3):129–135, May 2016.
- [25] F. G. Tricomi and A. Erdélyi. The asymptotic expansion of a ratio of gamma functions. *Pacific J. Math.*, 1(1):133–142, 1951.
- [26] B. P. Welford. Note on a Method for Calculating Corrected Sums of Squares and Products. *Technometrics*, 4(3):419–420, 1962.
- [27] Inc. Wolfram Research. The wolfram functions site. Visited on 09/24/19.